

Dissertation zur Erlangung des Doktorgrades
der Fakultät für Chemie und Pharmazie
der Ludwig-Maximilians-Universität München

Neural stem cells in development and cancer

Markus Waldhuber
aus
Leoben

München
2008

Erklärung

Diese Dissertation wurde im Sinne von § 13 Abs. 3 der Promotionsordnung vom 29. Januar 1998 von Herrn Prof. Dr. Ralf-Peter Jansen betreut.

Ehrenwörtliche Versicherung

Diese Dissertation wurde selbstständig, ohne unerlaubte Hilfe erarbeitet.

München, am

.....

Markus Waldhuber

Dissertation eingereicht am: 23.06.2008

1. Begutachter: Prof. Dr. Ralf Peter Jansen

2. Begutachter: Prof. Dr. Klaus Förstemann

Tag der mündlichen Prüfung: 29.07.2008

"Discovery consists of seeing what everybody has seen and
thinking what nobody has thought."
Albert Szent-Györgyi (1893-1992)

Meinen Eltern und Anna

Acknowledgements

I would like to gratefully acknowledge the enthusiastic supervision of Dr. Claudia Petritsch during this work. I thank her for offering such an interesting subject, for constant support and encouragement and for providing a great scientific environment during my doctoral thesis.

Thanks to Prof. Dr. Ralf-Peter Jansen for his help at every opportunity, for being my “doctor father” and evaluating this work as well as to Prof. Dr. Klaus Förstemann, Prof. Dr. Roland Beckmann, Prof. Dr. Martin Biel, Dr. Angelika Böttger and Dr. Dietmar Martin, the members of my PhD committee.

Sincere thanks are given to all people involved in this work, for providing reagents and helpful advice. Therefore I want to thank Ingrid Fetka, Anders Persson, William Weiss, Graeme Hodgson, Matthias Kieslinger and Geri Dobрева. Special thanks to Prof. Dr. Gabriele Bergers for giving me the opportunity to do some of my experimental work in her laboratory at University of California San Francisco.

Thanks are also addressed to all (former) members of the laboratory, Diana, Ingrid, Birgit, Stefan, Tati, Tijana for their help, the friendly atmosphere and nice coffee talks. It has been a great pleasure to work with all of you! Vroni, we finally made it!

In addition, I would like to thank the members of the Neurosurgery Department at UCSF for the warm welcome, help and support during my time abroad. Patty, Chrystelle, Kan, Jim, Bina, Scott, Anita, Katharine, Gilson, Kristen, Eduard - I really miss you guys!

Again, a very special thank belongs to Margit for proofreading this thesis, her endless patience and encouragement when it was most required - where do we end up next?

Sincere thanks are given to Anneliese and Fritz Haller, my parents in law, for providing a roof over my head when I came back from San Francisco and, of course, for all those delicious Leberkäsemmeln, Weißwürste and other Bavarian specialities.

Is that everyone?

I wish to thank my parents, Ingrid and Ferdinand Waldhuber for their love, confidence and support at all times. You provided a stable and stimulating environment for my personal and intellectual development.

Most importantly, I would like to thank Anna for her constant support, faithful love and optimism in “good times and in bad times”. I don’t know what my life would be without you.

To them, I dedicate this thesis

Preface

I started my PhD thesis in the group of Dr. Claudia Petritsch at the Genecenter Munich working on asymmetric cell division and cell fate determination of neuronal stem cell-like neuroblasts. In the first part of this thesis, I will focus on the molecular details of asymmetric Miranda localization during neuroblast mitosis.

In the middle of my thesis I joined my supervisor, who moved to San Francisco to start a new position in the laboratory of Dr. Gabriele Bergers in the Department of Neurosurgery at UCSF. My move was motivated by my growing interest in stem cell biology and the connection of defective stem cell division and cancer which I was investigating in a murine mouse model of oligodendroglioma. Results from this project will be discussed in part 2 of the present thesis.

Neural stem cells in development and cancer

Summary

Neural stem cells are defined by their unique ability to undergo self-renewal divisions. By dividing asymmetrically, a stem cell simultaneously produces a daughter cell that retains stem cell identity, whereas the other starts to differentiate and contributes to a continuous supply of neural cell types.

Drosophila neuroblasts provide an excellent model system to study asymmetric stem cell divisions. The first part of this thesis will concentrate on the important adaptor protein Miranda which ensures the asymmetric segregation of cell fate determinants to the differentiating ganglion mother cell during neuroblast mitosis.

The dynamic apical-then-basal localization pattern and the requirement for both Myosin II and Myosin VI suggested that Miranda is actively transported to the basal pole as a myosin cargo. However, immunofluorescence studies combined with time-lapse confocal microscopy and FRAP analyses revealed that Miranda reaches the basal cortex by passive diffusion throughout the cell rather than by long range myosin-directed transport. Instead, myosins play an indirect role in asymmetric Miranda localization. The formation of active Myosin II filaments in early prophase results in the exclusion of Miranda from the apical cortex. In the cytoplasm, Miranda diffuses three-dimensionally through the cell and becomes restricted to the basal half of the metaphase neuroblast by Myosin VI to facilitate its interaction with a putative basal cortical anchor.

There is growing evidence that deregulation of the self-renewing process of stem cells may be an early event in tumorigenesis and that many cancers contain a small population of so called cancer stem cells which are responsible for maintenance and growth of tumors.

The second part of the thesis will report on the isolation of cells with stem-like features from a murine mouse model of oligodendroglioma with activated EGFR signaling and loss of the tumor suppressor p53 in the postnatal stem cell lineage. Although oligodendroglioma-derived progenitor cells share many similarities with normal neural stem cells, they have increased self-renewing and proliferation capacities and in addition, undergo aberrant differentiation. They are multipotential, however, when induced to differentiate they preferentially generate cells of the oligodendrocytic lineage recapitulating the properties of the tumor they originate from. Brain cancer derived stem-like cells generate new tumors following intracranial injections that faithfully reproduce the phenotype of the parental tumor qualifying them as cancer stem cells.

Interestingly, neural stem cells isolated from tumor prone mice long before oligodendroglioma occurrence show similar, but less severe alterations in their self-renewing and differentiation capacities. Importantly, they never form orthotopic tumors and thus were referred to as premalignant stem cells. The overproduction of oligodendrocytic cells is caused by a defect in asymmetric cell division that is very likely accompanied with genetic instabilities and epigenetic alterations. This results strengthen the hypothesis that early defects in neural stem cells, together with additional genetic alterations lead to the progression to a more malignant stem cell type which is responsible for tumor growth and maintenance.

Zusammenfassung

Neurale Stammzellen in der Entwicklung und Tumorentstehung

Neurale Stammzellen sind undifferenzierte Vorgängerzellen, die sich durch asymmetrische Zellteilung unbegrenzt vermehren und gleichzeitig in die verschiedenen Zelltypen des zentralen Nervensystems differenzieren können.

Miranda ist ein wichtiges Adapterprotein in *Drosophila* Neuroblasten und stellt sicher, dass während der Zellteilung bestimmte Faktoren selektiv in nur eine Tochterzelle gelangen und dort Linienentscheidungen beeinflussen. Die dynamische apikale und später basale Lokalisierung von Miranda sowie die Beteiligung von Myosin II und Myosin VI lässt darauf schließen, dass Miranda aktiv und Myosin-abhängig an den basalen Kortex transportiert wird. Live Imaging und FRAP Studien, die im ersten Teil dieser Doktorarbeit behandelt werden, deuten jedoch darauf hin, dass Miranda den basalen Pol des Neuroblasten eher durch passive Diffusion als durch aktiven Transport erreicht. Myosine spielen dennoch eine wichtige Rolle bei diesem Vorgang: Die Bildung aktiver Myosin II Filamente zu Beginn der Zellteilung führt zur Abstoßung von Miranda vom apikalen Kortex. Daraufhin diffundiert Miranda frei im Cytoplasma und wird schließlich von Myosin VI im basalen Bereich des Neuroblasten gebunden wodurch die Interaktion mit einem bisher unbekanntem kortikalen Ankerprotein erleichtert wird.

Seit einigen Jahren häufen sich die Hinweise, dass genetisch veränderte Stammzellen bei der Tumorentwicklung eine wichtige Rolle spielen und bei einigen Krebsarten wurden bereits so genannte Krebsstammzellen identifiziert. Der zweite Teil dieser Dissertation beschreibt die Isolierung und Charakterisierung von Zellen mit stammzellähnlichen Eigenschaften aus Oligodendrogliomen. In dem verwendeten Mausmodell führt die Expression einer onkogenen Form des EGF-Rezeptors, sowie der Verlust von p53 in postnatalen neuralen Stammzellen zur Entstehung von Oligodendrogliomen. Nach Transplantation der isolierten Krebsstammzellen in Gehirngewebe anderer Versuchstiere entstehen erneut Tumore, die dem Erscheinungsbild des ursprünglichen Tumors entsprechen.

Im Vergleich zu normalen neuralen Stammzellen besitzen Krebsstammzellen ein erhöhtes Potential zur Selbsterneuerung und unterscheiden sich auch in ihrem Differenzierungsmuster. Obwohl die aus Gehirntumoren gewonnenen Krebsstammzellen multipotent sind und alle drei Zelltypen des Nervensystems bilden, entwickeln sie sich dennoch bevorzugt in Oligodendrozyten, die auch den Großteil der Zellen im Tumor ausmachen. Interessanterweise kann man ein ähnliches, wenn auch wenig stark ausgeprägtes Verhalten bei neuralen Stammzellen beobachten, die Mäusen zu einem Zeitpunkt entnommen werden, an dem noch kein Tumorwachstum feststellbar ist. Da diese Zellen jedoch noch nicht tumorigen sind, werden sie als prä-maligne Stammzellen bezeichnet.

Defekte der asymmetrischen Zellteilung verbunden mit genetischen Veränderungen von neuralen Stammzellen sind wahrscheinliche Ursachen für die Überproduktion von Oligodendrozyten. Diese Ergebnisse stärken die so genannte Krebsstammzelltheorie: Mutationen führen dazu, dass Selbsterneuerungsprozesse einer Stammzelle, die normalerweise einer strikten Kontrolle unterliegen, dereguliert werden. Es kommt zu einer unkontrollierten Teilung von Stammzellen, der Ansammlung zusätzlicher Mutationen und schließlich zur Entstehung von malignen Krebsstammzellen, die für das Wachstum von Tumoren verantwortlich sind.

Table of Contents

| | | |
|----------|--|-----------|
| 1 | Introduction | 1 |
| 1.1 | Stem cells | 1 |
| 1.2 | Mechanism of asymmetric stem cell division | 1 |
| 1.3 | The apparatus regulating asymmetric cell division in <i>Drosophila</i> | 3 |
| 1.3.1 | The apical complex: a central regulator of cell polarity, spindle positioning and asymmetric segregation of cell fate determinants | 3 |
| 1.3.2 | Segregating cell fate determinants specify daughter cell fate | 4 |
| 1.3.3 | Asymmetric localization of cell fate determinants | 5 |
| 1.3.4 | Cell cycle genes regulate ACD and act as tumor suppressors | 6 |
| 1.4 | Adult neural stem cells | 8 |
| 1.4.1 | Architecture of germinal zones | 9 |
| 1.5 | Asymmetric cell division in the mammalian brain | 11 |
| 1.5.1 | Neurogenesis in the murine brain | 11 |
| 1.5.2 | Conservation of ACD in mammalian stem cells | 12 |
| 1.6 | Asymmetric cell division and cancer | 14 |
| 1.6.1 | The cancer stem cell theory | 15 |
| 1.6.2 | Origin of brain tumor cells | 15 |
| 2 | Aim of this work | 18 |
| 2.1 | Asymmetric localization of Miranda during neuroblast division | 18 |
| 2.2 | The origin of brain cancer stem cells | 19 |
| 3 | Thesis Part 1 - Asymmetric localization of Miranda during neuroblast division | 20 |
| 3.1 | Results | 20 |
| 3.1.1 | Miranda forms a basal crescent independent of basal translation or localized protein degradation | 20 |
| 3.1.2 | Miranda accumulates in the cytoplasm prior to formation of a basal crescent | 23 |
| 3.1.3 | PON protein moves along the cortex to form a basal crescent | 26 |
| 3.1.4 | Miranda diffuses freely in the cytoplasm but shows spatially-limited and slower movement at the cortex | 28 |
| 3.1.5 | Myosin II and Myosin VI act at distinctive steps in the same pathway to localize Miranda | 30 |
| 3.2 | Discussion | 32 |
| 3.2.1 | Miranda is asymmetrically localized by protein movement throughout the cell prior to basal crescent formation | 32 |
| 3.2.2 | Adaptor proteins take different routes to the basal cortex | 34 |
| 3.2.3 | Myosin II and Myosin VI interact in one pathway to shuttle Miranda between cortex and cytoplasm | 35 |
| 3.2.4 | A model for Miranda localization | 36 |
| 4 | Thesis Part 2 - The origin of brain cancer stem cells | 38 |
| 4.1 | Results | 38 |
| 4.1.1 | Isolation and characterization of cancer stem cells from high grade oligodendroglioma | 38 |
| 4.1.2 | Tumor-derived cells undergo self-renewal and are multipotential | 39 |
| 4.1.3 | Oligodendroglioma derived cancer stem cells are tumorigenic | 41 |
| 4.1.4 | Spontaneous and orthotopic tumors show similar marker expression | 44 |
| 4.1.5 | Isolation and characterization of premalignant stem cells from S100 β - <i>verbB</i> , p53 ^{+/-} mice | 45 |

| | | |
|------------|---|------------|
| 4.1.6 | Stem cells isolated from premalignant S100 β - <i>verbB</i> , p53 ^{+/-} mice and from S100 β - <i>verbB</i> , p53 ^{-/-} tumorspheres show self-renewal defects..... | 47 |
| 4.1.7 | Differentiation defects in oligodendrogloma derived cancer stem cells and premalignant stem cells | 48 |
| 4.1.8 | Neural stem cells from S100 β - <i>verbB</i> , p53 ^{-/-} but not S100 β - <i>verbB</i> , p53 ^{+/-} are tumorigenic..... | 56 |
| 4.1.9 | Deregulation of EGFR signaling but not loss of p53 influences cell fate decisions..... | 57 |
| 4.1.10 | Pre-malignant stem cells and cancer stem cells encounter a defect in asymmetric cell division..... | 61 |
| 4.1.11 | Epigenetic changes lead to the progression of pre-malignant to cancer stem cells..... | 65 |
| 4.2 | Discussion | 68 |
| 4.2.1 | Tumor-derived cells share common characteristics of neural stem cells | 68 |
| 4.2.2 | Oligodendrogloma derived cancer stem cells are tumorigenic and phenocopy the parental tumor in transplantation experiments..... | 69 |
| 4.2.3 | Stem cells undergo changes before tumor occurrence - progression of neural stem cells to pre-malignant and cancer stem cells | 72 |
| 4.2.4 | Differentiation defects in transgenic stem cells..... | 73 |
| 4.2.5 | Defects in asymmetric cell division and epigenetic changes influence stem cell differentiation..... | 76 |
| 5 | Material and Methods..... | 82 |
| 5.1 | Animals..... | 82 |
| 5.1.1 | Transgenic mice..... | 82 |
| 5.1.2 | <i>Drosophila</i> strains | 82 |
| 5.2 | Tissue culture | 83 |
| 5.2.1 | Adult neurosphere culture | 83 |
| 5.2.2 | Isolation of cancer stem cells from oligodendrogloma | 83 |
| 5.2.3 | Passaging of neuro- and tumorspheres..... | 83 |
| 5.2.4 | Sphere forming- and cell proliferation assays..... | 84 |
| 5.2.5 | Differentiation of neurosphere cultures..... | 84 |
| 5.2.6 | Cell pair assays..... | 84 |
| 5.2.7 | Transfection of miRNAs into neural stem cells | 84 |
| 5.3 | Immunostaining and histology | 85 |
| 5.3.1 | Immunofluorescence on <i>Drosophila</i> embryos | 85 |
| 5.3.2 | Whole-mount in situ hybridization of <i>Drosophila</i> embryos..... | 85 |
| 5.3.3 | Immunocytochemistry | 86 |
| 5.3.4 | Immunohistochemistry | 86 |
| 5.3.5 | Haematoxylin and Eosin staining..... | 86 |
| 5.3.6 | Tunel staining..... | 86 |
| 5.4 | Live Imaging..... | 87 |
| 5.4.1 | Fluorescence recovery after photobleaching (FRAP)..... | 87 |
| 5.5 | RNA interference and drug treatment of <i>Drosophila</i> embryos..... | 87 |
| 5.5.1 | Myosin VI RNA interference..... | 87 |
| 5.5.2 | Injection of Rho kinase inhibitor to impair Myosin II activity | 88 |
| 5.5.3 | Downregulation of proteasome activity..... | 88 |
| 5.6 | Stereotactic injections and serial transplantation of cancer stem cells | 88 |
| 5.7 | SDS Page and immunoblotting..... | 88 |
| 6 | References..... | 91 |
| 7 | Abbreviations | 103 |
| 8 | Curriculum vitae..... | 105 |

1 Introduction

1.1 Stem cells

Stem cells are commonly defined as immature, unspecialized cells that are capable of perpetuating themselves as stem cells and of undergoing differentiation into more specialized types of cells (Weissman, 2000a; Gage, 2000; Till & McCulloch, 1961).

Stem cells are most active during embryonic development and give rise to all tissues in the body. Embryonic stem cells (ES cells) were first isolated from mouse embryos in 1981 (Evans & Kaufmann, 1981; Martin, 1981). Animal embryos were the only source for research on ES cells until 1998, when a group led by James Thomson at the University of Wisconsin-Madison announced the first successful isolation of human embryonic stem cells (Thomson et al., 1998).

Adult stem cells are undifferentiated cells found throughout the body after embryonic development. In general, adult stem cells are lineage-restricted (multipotential) and only differentiate into specialized cell types of the tissue or organ they originate from (e.g. adult neural stem cells only differentiate into neurons, astrocytes and oligodendrocytes). Their function in a living organism is to maintain and repair tissue and organs they are residing in. Because of these features, adult stem cells have received much attention during recent years as attractive tools for regenerative medicine (Weissman, 2000b).

Adult stem cells are rare and generally small in number but have been identified in many organs and tissues. They are believed to reside in special areas of the tissue, the stem cell niche, often quiescently for a long period of time, until they become activated following disease or injury. The adult tissues demonstrated to contain stem cells include brain (Singh et al, 2004; Galli et al, 2004; Singh et al, 2003; Ignatova et al, 2002; Hemmati et al, 2003), bone marrow (Mazurier et al, 2003; Jiang et al, 2002), peripheral blood (Kessinger & Sharp, 2003), adipose tissue (Rodríguez et al, 2006; Gimble & Guilak, 2003; Zuk et al, 2002), skin (Toma et al, 2001; Oshima et al, 2001; Taylor et al, 2000), liver (Horb et al, 2003), pancreas (Gmyr et al, 2000), skeletal muscle (Asakura et al, 2002), corneal limb (Meller et al, 2002), mammary gland (Dontu et al, 2003; Alvi et al, 2003) and heart (Beltrami et al, 2001).

1.2 Mechanism of asymmetric stem cell division

Stem cells possess the unique ability to self-renew and simultaneously generate more differentiated progeny (Morrison & Kimble, 2006). One strategy by which stem cells can accomplish this is asymmetric cell division (ACD) (Betschinger & Knoblich, 2004; Clevers, 2005; Doe & Bowerman, 2001; Yamashita et al, 2005).

Work mostly done in *Drosophila* has suggested two different mechanisms by which ACD can be achieved (Horvitz & Herskowitz, 1992): The extrinsic mechanism involves placement of daughter cells relative to external cues in a stem cell niche, defined as a microenvironment that promotes stem cell maintenance (Li & Xie, 2005). During stem cell division, the mitotic spindle is oriented perpendicular to the niche surface ensuring that only one daughter cell can maintain contact with the stem cell niche and retains stem cell identity. The other daughter cell is placed away from the niche, loses access to extrinsic signals and begins to differentiate. The *Drosophila* germline stem cell provides a classic example of an asymmetric division that is controlled by an extrinsic mechanism (Yamashita et al, 2005).

Alternatively, intrinsic mechanisms include assembly of polarity factors and the subsequent asymmetric localization of so called cell fate determinants during mitosis so that they are only inherited by one of the daughter cells (Yu et al, 2006; Betschinger & Knoblich, 2004). A typical example of ACD controlled by an intrinsic mechanism is provided by the *Caenorhabditis elegans* zygote. Here, asymmetrically localized PAR proteins govern both mitotic spindle orientation and asymmetric segregation of cell fate determinants (Gönczy & Rose, 2007). *Drosophila* neuroblast (NB) division is controlled by a closely related mechanism (Wodarz, 2005; Doe & Bowerman, 2001).

The apparatus regulating ACD is conserved from *Drosophila* neuroblasts to mammalian neural stem cells. Although neuroblasts have restricted self-renewal capacities and therefore are not classical stem cells, they provide a useful model that will help to understand the complexity of mammalian stem cell biology.

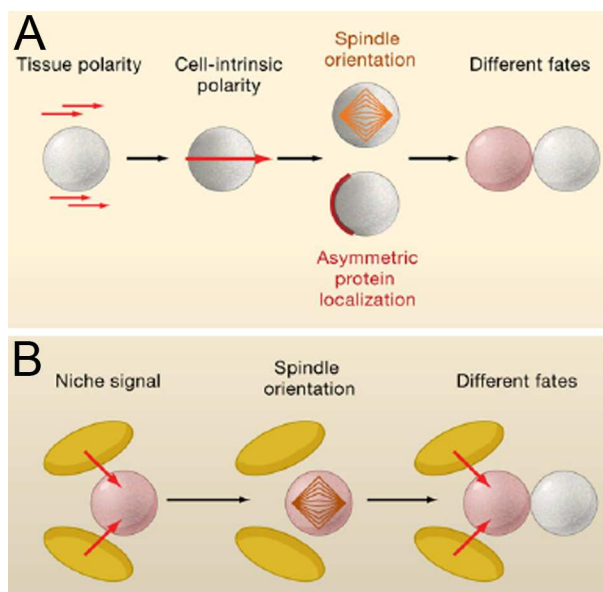


Figure 1: Self-renewal of stem cells can be achieved by intrinsic and extrinsic regulation. (A) Intrinsic mechanisms include the establishment of an axis of polarity which is used to localize cell fate determinants asymmetrically in mitosis. Orientation of the mitotic spindle along this axis ensures that cell fate regulators are exclusively segregated into only one daughter cell. (B) Stem cells may depend on signals coming from the surrounding stem cell niche. Regulated orientation of the mitotic spindle retains only one daughter in the stem cell niche such that only this cell has access to extrinsic signals necessary for maintaining stem cell identity. From: Knoblich, 2008.

1.3 The apparatus regulating asymmetric cell division in *Drosophila*

Drosophila neuroblasts divide in an asymmetric fashion to generate a larger cell that retains neuroblast properties (self-renewal) and a smaller ganglion mother cell (GMC) (Lee et al, 2006b). Whereas neuroblasts undergo multiple rounds of stem-like divisions, the GMC only divides once more to generate two differentiating neurons.

Embryonic neuroblasts give rise to the relatively simple nervous system of the larva. They are specified within a monolayered epithelium called the ventral neuroectoderm from where they delaminate to undergo asymmetric cell division along the apical-basal axis (Justice et al, 2003).

1.3.1 The apical complex: a central regulator of cell polarity, spindle positioning and asymmetric segregation of cell fate determinants

Before mitosis, a protein complex consisting of Par-3, Par-6 and atypical protein kinase C (aPKC) assembles on the apical side of the cell. This complex is not thought to influence cell fate directly, instead it regulates the transport of cell fate determinants to the opposite basal pole of the cell (Goldstein & Macara, 2007; Suzuki & Ohno, 2006; Betschinger & Knoblich, 2004). Par-6 is a small protein containing a PDZ domain through which it interacts with aPKC and a CRIB domain which is critical for the localization to the cell cortex (Atwood et al, 2007; Petronczki & Knoblich, 2001). Par-3 also contains PDZ domains and can interact with aPKC (Wodarz et al, 1999; Schober et al, 1999; Kuchinke et al, 1999). The Par protein complex has a conserved function in establishing cell polarity and providing positional information (Ohno, 2001).

The cytoskeletal protein Lethal (2) giant larvae (Lgl) is a key substrate of aPKC (Plant et al, 2003; Yamanaka et al, 2003; Betschinger et al, 2003a). Although Lgl is required for restricting the Par complex to the apical domain it is not concentrated apically but localized uniformly cortical instead. Phosphorylation is supposed to inhibit Lgl on the apical pole and restricts Lgl-activity to the basal side of the neuroblast. Because Lgl seems to be important to recruit cell fate determinants to the cell cortex, this model could explain their asymmetric localization in neuroblasts (Betschinger et al, 2003a; Peng et al, 2000; Ohshiro et al, 2000).

For successful asymmetric segregation of cell fate determinants, the orientation of the mitotic spindle needs to be coordinated with their asymmetric localization. Neuroblasts delaminate from the neuroepithelium and divide perpendicularly to the epithelial plane by rotating their bipolar spindle 90° along their apical/basal axis (Kaltschmidt & Brand, 2002; Kaltschmidt et al, 2000).

A central role for the coordination of spindle positioning has been demonstrated for a protein called Inscuteable (Kraut et al, 1996). Inscuteable localizes apically by binding to Par-3 and recruits an additional protein called Pins (Parmentier et al, 2002; Schaefer et al, 2000; Yu et al, 2000) into the apical complex which in turn binds to the heterotrimeric G protein subunit G α i. This leads to a conformational change of Pins and facilitates binding of an additional protein called Mud (Izumi et al, 2006), the *Drosophila* homolog of the microtubule and dynein binding protein NuMA. Although the precise mechanism is not totally understood, it is believed that the apical concentration of Mud provides a binding site for astral microtubules which attract one of the spindle poles to orient the mitotic spindle.

1.3.2 Segregating cell fate determinants specify daughter cell fate

Unequal segregation of several proteins into only one cell during neuroblast mitosis leads to a different fate of the two neuroblast daughter cells. Due to their ability to specify daughter cell fate, these proteins are referred to as cell fate determinants.

Upon neuroblast division, a basal protein complex is inherited exclusively by the ganglion mother cell (Wodarz & Huttner, 2003; Knoblich, 1998; Jan & Jan, 1998).

The basal protein complex consists of the cell fate determinants Numb (Rhyu et al, 1994), Prospero (Doe et al, 1991) and *prospero* RNA (Broadus et al, 1998), the adaptor proteins Miranda (Shen et al, 1997) and Partner of Numb (PON) (Lu et al, 1998), and the RNA binding protein Staufen (Li et al, 1997).

Numb is an evolutionary conserved cell fate-determining factor and plays a pivotal role in the development of *Drosophila* and the nervous systems of other vertebrates (Cayouette & Raff, 2002; Shen et al, 2002; Wakamatsu et al, 1999; Zhong et al, 1996a). Numb is membrane associated and acts as a tissue-specific repressor of the Notch pathway (Le Borgne et al, 2005; Schweisguth, 2004).

Like Numb, the transcription factor Prospero segregates asymmetrically in neuroblasts. Shortly after neuroblast mitosis it translocates into the nucleus of the GMC where it acts both as a transcriptional activator or repressor (Karcavich, 2005; Doe et al, 1991). When Prospero is mutated in embryonic neuroblasts, the GMC undergoes multiple rounds of divisions and continues to express neuroblast markers (Choksi et al, 2006).

Only recently, the protein Brat has been identified as another important regulator of stem cell renewal (Betschinger et al, 2006b; Bello et al, 2006; Lee et al., 2006c). Brat was previously shown to act as an inhibitor of ribosome biogenesis and cell growth (Frank et al, 2002). Thus it is speculated that Brat might inhibit cell growth in the GMC to prevent self-renewal and induce differentiation.

The asymmetric segregation of the cell fate determinants Prospero, Brat and Numb is mediated by two adaptor proteins called Miranda and Partner of Numb (PON). Miranda associates with the transcription factor Prospero and the growth regulator Brat and is essential for their asymmetric localization into only one daughter cell (Lee et al., 2006c; Schuldt et al, 1998; Matsuzaki et al, 1998; Shen et al, 1998; Shen et al, 1997; Ikeshima-Kataoka et al, 1997). Miranda also binds to the RNA binding protein Staufeu (Broadus et al, 1998) which transports *prospero* RNA to the GMC.

Miranda localizes asymmetrically in metaphase and segregates exclusively into one of the daughter cells during neuroblast division. In Miranda mutants, Prospero, Brat and Staufeu are mislocalized uniformly to the cytoplasm and inherited equally by both daughter cells highlighting the obligatory role of Miranda for proper asymmetric neuroblast division (Matsuzaki et al, 1998; Slack et al, 2007).

Similar to Miranda, PON, the adaptor protein for Numb, localizes to a basal crescent in metaphase and is inherited by the smaller GMC. However, it is not strictly required for Numb localization as Numb eventually localizes asymmetrically in PON mutants. However, Numb localization is delayed in metaphase which finally leads to defects in self-renewal. This suggests that PON assists the asymmetric localization of Numb but is not necessarily required at later stages of cell division (Wang et al, 2006).

1.3.3 Asymmetric localization of cell fate determinants

Miranda localization requires both Myosin VI (Petritsch et al, 2003) and Myosin II (Barros et al, 2003). In mutant embryos with reduced Myosin VI activity, Miranda does not form a basal crescent but is mislocalized to the cytoplasm (Petritsch et al, 2003). Unlike all other characterized myosins, Myosin VI moves processively towards the minus end of actin filaments taking large steps but can also function as an actin-based anchor (Sweeney & Houdusse, 2007). Myosin VI protein is abundantly expressed in neuroblasts, where it transiently accumulates in the basal half of the metaphase cell and partially co-localizes with Miranda (Petritsch et al, 2003). In addition, Myosin VI forms a complex with Miranda and Prospero in *Drosophila* embryonic extracts and shows direct physical interaction with Miranda *in vitro* (Petritsch et al, 2003). These observations suggested that Miranda might be actively transported to the basal cortex by Myosin VI. However, this proposed model for actin-myosin dependent transport of cell fate determinants is incompatible with more recent photobleaching experiments which failed to detect any directional transport of segregating determinants (Erben et al, 2008; Mayer et al, 2005).

Miranda also shows physical interaction with Zipper, the heavy chain of Myosin II (Petritsch et al, 2003). Myosin II is a plus end-directed motor which forms bipolar filaments as a

heterohexamer (Bresnick, 1999). Earlier data have suggested that Zipper antagonizes basal crescent formation by negatively interacting with Lgl (Peng et al, 2000; Ohshiro et al., 2000). The zygotic *zipper* mutant has intact asymmetric cell division most likely due to maternal contribution of wild type Zipper. More recently, it has been shown that Myosin II is activated through phosphorylation by Rho kinase and can be selectively inhibited by Rho kinase inhibitor (Barros et al, 2003). Inhibition of Myosin II results in mislocalization of Miranda uniformly around the cortex. Myosin II itself localizes asymmetrically to the apical pole at prophase and subsequently moves along the cortex to accumulate at the cleavage furrow (Barros et al, 2003; Strand et al, 1994). Myosin II interacts with the tumor suppressor Lgl to localize Miranda. Myosin II can only become activated after Lgl is phosphorylated and inactivated by aPKC at the apical cortex (Betschinger et al, 2003b). Thus it has been proposed that active Myosin II filaments on the apical pole exclude Miranda from the cortex rather than transport it from the apical to the basal cortex (Barros et al, 2003).

As previously determined by time-lapse confocal microscopy, PON protein is recruited from the cytoplasm to the cortex at interphase in neuroblasts and moves two-dimensionally along the cortex to a basal cortical crescent (Lu et al, 1999). FRAP analysis of PON in sensory organ precursor cells of *Drosophila* pupae suggested that PON becomes rapidly recruited from juxta-cortical areas to form a basal cortical crescent by binding to a high-affinity binding partner. PON localization depends on aPKC activity and the phosphorylation status of Lgl (Mayer et al, 2005) and is sensitive to 2,3-butanedione monoxime (BDM), an inhibitor of myosin ATPase activity (Lu et al, 1999). These data suggest that PON like Miranda requires myosin motor activity for basal localization. Since Miranda and PON both localize to a basal crescent in metaphase in a myosin-dependent fashion, it is possible that they engage similar molecules such as the cortical Myosin II to reach their destination. However, a requirement of Myosin II for PON localization has not been studied yet.

1.3.4 Cell cycle genes regulate ACD and act as tumor suppressors

There is increasing evidence that cell cycle regulators can control various aspects of asymmetric cell division such as the decision of self-renewal versus differentiation (Chia et al, 2008).

Neuroblast polarity is already set up in interphase, however, cell fate determinants only localize during mitosis which suggests a tight coordination with cell-cycle progression. In general, entry into mitosis is triggered by activation of Cdc2. The first indication that cell cycle regulators might also control ACD came from a study on a dominant negative allele of Cdc2, *cdc2^{E51Q}* (Tio et al, 2001). When the activity of Cdc2 was attenuated, neuroblasts failed to

asymmetrically localize components of both the apical and basal complex resulting in a conversion from asymmetric to symmetric cell divisions.

In contrast to Cdc2, the kinases Aurora A, Aurora B and Polo are only required for a subset of mitotic events including the spindle checkpoint, centrosome maturation and cytokinesis (Barr et al, 2004; Meraldi et al, 2004). Loss of function mutations in either gene have been described to cause defects in centrosome maturation, delay and/or arrest at metaphase and defects during cytokinesis (Carmena et al, 1998; Glover et al, 1995; Llamazares et al, 1992). Surprisingly, it was recently shown that mutations in Aurora A or Polo cause massive overgrowth in the brain (Wang et al, 2007; Lee et al, 2006a) qualifying these kinases as tumor suppressor proteins.

In addition, recent findings suggest that the anaphase-promoting complex/cyclosome (APC/C) is specifically required for asymmetric localization of Miranda and its cargo proteins Prospero, Brat and Staufen (Slack et al, 2007). The APC/C functions as an E3 ubiquitin ligase that normally targets proteins for degradation via the 26S proteasome (Peters, 2006), including mitotic cyclins and inhibitors of chromosome separation as well as regulators of DNA replication, centrosome duplication and mitotic spindle assembly (Leismann & Lehner, 2003; Zur & Brandeis, 2001; Sigrist et al, 1995).

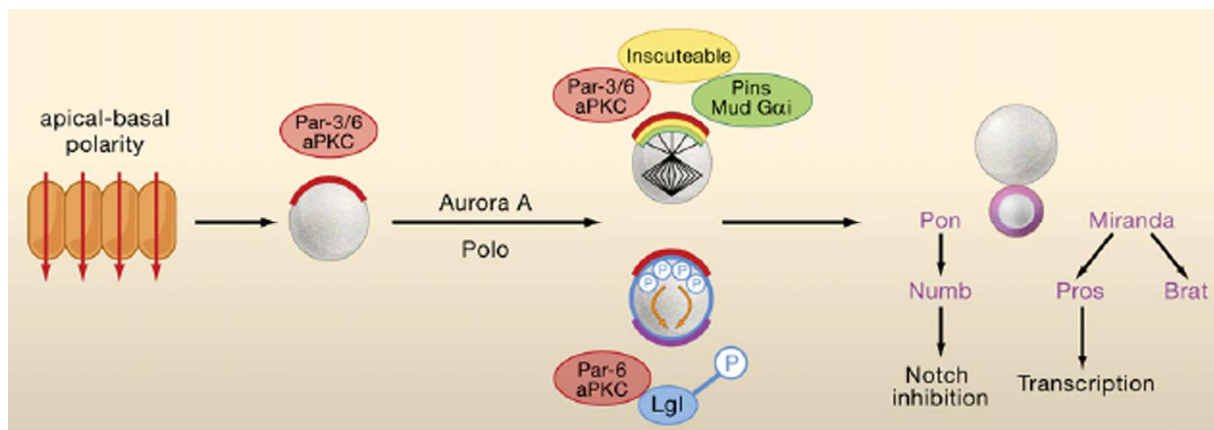


Figure 2: Summary of *Drosophila* neuroblast asymmetric division. The asymmetric segregation of cell fate determinants into the smaller ganglion mother cell (GMC) requires the correct localization of protein complexes to the apical cell cortex. Epithelial apical basal polarity is used to establish the Par complex consisting of Par-3, Par-6 and aPKC (red crescent). Upon entry into mitosis, activation of the kinases Aurora-A and Polo results in the orientation of the mitotic spindle perpendicular to the epithelial plane by the microtubule binding protein Mud, which is recruited apically by Pins and the G protein Gai (green). Inscuteable associates with Gai and links this protein complex with the Par complex. aPKC is believed to inactivate Lgl by phosphorylation and results, most likely due to apical exclusion, in the localization of cell fate determinants (purple) to the basal cortex. The basal proteins exist in two protein complexes: one complex contains the adaptor protein Miranda which transports the translational repressor Brat, the transcription factor Prospero and the RNA binding protein Staufen together with *prospero* mRNA. The second complex consists of Partner of Numb and its binding partner Numb, which represses Notch signaling in the GMC. From: Knoblich, 2008.

1.4 Adult neural stem cells

Until recently, neurogenesis in the mammalian central nervous system (CNS) was believed to be accomplished briefly after birth (Rakic, 1985). Although studies in the 1960s reported that neurogenesis occurs in discrete areas of the rodent brain (Altman, 1970; Altman & Das, 1966a; Altman, 1963), it was many years later that newly developed techniques to identify dividing cell in the CNS contributed to confirm that neurogenesis occurs in the adult mammalian brain (Kuhn et al, 1996; Seki & Arai, 1993; Luskin, 1993), including humans (Eriksson et al, 1998). The discovery of neural stem cells (NSC) was of outstanding interest, indicating that cell replenishment was possible within the brain, something previously considered impossible.

Adult NSC are cells of the adult nervous system that can self-renew and differentiate into all types of neural cells, including neurons, astrocytes and oligodendrocytes (Gage, 2000). As the functional components of the nervous system, neurons are responsible for information processing, whereas astrocytes and oligodendrocytes (collectively known as glia) have supporting roles.

Neurogenesis primarily occurs in two areas of the adult mammalian brain: the subgranular zone (SGZ) of the dentate gyrus in the hippocampus (Gage et al, 1998) and the subventricular zone (SVZ) of the lateral ventricles (Lois & Alvarez-Buylla, 1994) (Figure 3). Neurons born in the SVZ migrate over a great distance through the rostral migratory stream and differentiate into interneurons in the olfactory bulb (Kornack & Rakic, 2001; Lois & Alvarez-Buylla, 1994; Corotto et al, 1993). Newly generated neurons in the adult SGZ migrate into the granule cell layer of the dentate gyrus and become dentate granule cells (van Praag et al, 2002; Markakis & Gage, 1999; Kornack & Rakic, 1999).

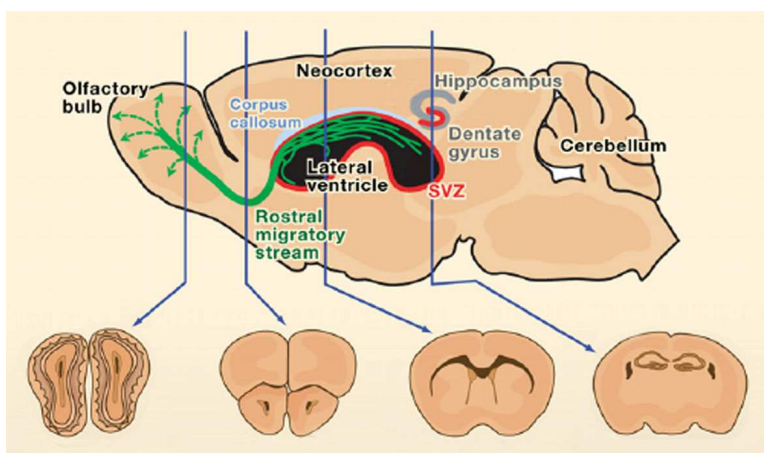


Figure 3: Neurogenesis in the adult mammalian brain. Sagittal and coronal views of a mouse brain in areas where neurogenesis occurs. Germinal zones are indicated in red: the subgranular zone (SGZ) of the hippocampal dentate gyros an the subventricular zone (SVZ) of the lateral ventricles. Neurons generated in the SVZ migrate through the rostral migratory stream (green) and are incorporated into the olfactory bulb. Adapted from: Zhao et al., 2008

Adult neurogenesis is modulated by various environmental stimuli and pathophysiological conditions and affects the proliferation of neural stem cells, differentiation and fate determination of progenitor cells. Learning, environmental enrichment and various forms of exercise enhance neurogenesis in the adult hippocampus (Brown et al, 2003; Ra et al, 2002; Gould et al, 1999) whereas social isolation, stress and sleep deprivation decrease hippocampal neurogenesis (Guzman-Marin et al, 2005; Malberg & Duman, 2003; Lu et al, 2003). New neuronal cells have also been reported to be generated at the sites of injury or degeneration, where they are able to replace some of the lost nerve cells (Zhao et al, 2008; Jessberger et al, 2007).

1.4.1 Architecture of germinal zones

The subventricular zone (SVZ), a thin layer that lines the lateral ventricles of the brain, contains most dividing cells in the adult mammalian brain (Lois & Alvarez-Buylla, 1993; Altman & Das, 1966b). The SVZ contains three types of progenitor cells: slowly dividing astrocyte-like neural stem cells known as type-B cells which give rise to actively dividing type-C transit amplifying cells. These in turn give rise to immature neuroblasts, called type-A cells, which subsequently migrate through the rostral migratory chain to the olfactory bulb and differentiate into interneurons (Doetsch et al, 1997; Doetsch & Alvarez-Buylla, 1996; Lois & Alvarez-Buylla, 1994). Evidence for the existence of astrocytes with stem-cell properties in the SVZ came from experiments using the antimetabolic drug cytosin- β -D-arabinofuranoside (Ara-C). Infusion of Ara-C into the brain for 6 days completely abolished neuroblasts and transit amplifying type-C cells but did not affect all type-B astrocytes. Indeed, after this treatment, astrocytes started to divide and regenerated the SVZ within 10 days (Doetsch et al, 1999). More recently, it has been demonstrated that progenitors of the SVZ are also capable of generating oligodendrocytes in addition to olfactory interneurons (Menn et al, 2006).

The SVZ also contains blood vessels, microglia, and cells are also in contact with multiciliated ependymal cells that line the lateral ventricle (Mercier et al, 2002). This architecture allows for extensive cell-cell interaction and the propagation from the cerebrospinal fluid in the ventricle, the surrounding extracellular matrix and blood vessels. It is hypothesized that such a microenvironment, known as the neurogenic stem cell niche, may provide specific factors that are permissive for neural progenitor cells (Morrison & Spradling, 2008; Ramírez-Castillejo et al, 2006; Alvarez-Buylla & Lim, 2004).

Two types of progenitors can be identified in the subgranular zone of the hippocampal dentate gyrus: Type 1 hippocampal progenitors have a radial process spanning the entire granule layer (Steiner et al, 2006; Fukuda et al, 2003; Seri et al, 2001). The SGZ also

contains horizontally oriented progenitors that lack a radial process (Seri et al, 2001; Filippov et al, 2003). Unlike the cells of the SVZ, progeny of SGZ cells, called type-D cells, do not migrate a long distance through the brain but differentiate within the granule cell layer to form new granule neurons (Seri et al, 2001).

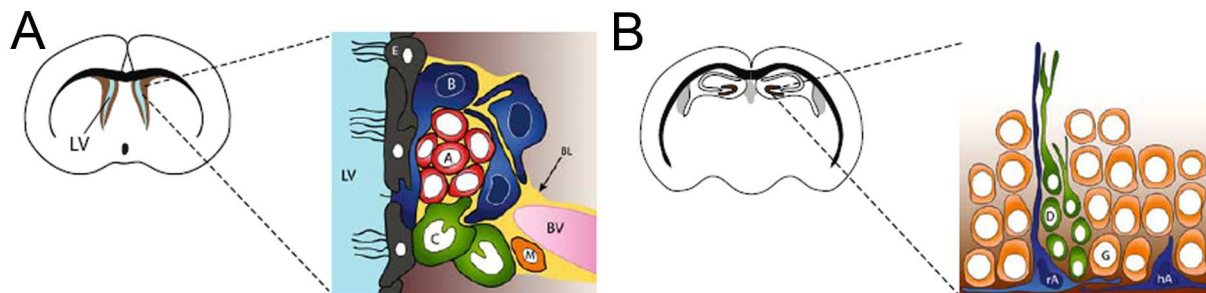


Figure 4: Architecture of germinal zones in the adult murine brain. (A) The position of the subventricular zone at the lateral wall of the lateral ventricle (LV) is indicated in the coronal brain section. (Inset in A) Detailed view of the lateral ventricle wall. The SVZ contains type-B neural stem cells, transit amplifying type-C cells and neuroblasts, also called type-A cells. The cells of the SVZ have extensive contact with the basal lamina (BL) microglia (M) and ependymal cells (E) that line the lateral ventricle (LV) and also lie near blood vessels (BV). (B) The subgranular zone is located within the dentate gyrus of the hippocampus. (Inset in B). The SGZ contains radial progenitor cells with long processes that span through the granular layer (rA) and horizontal progenitors (hA). Their progeny, the type-D cells, develop apical processes that become dendrites of new granule neurons. Adapted from Ihrie et al., 2006

In 1992, Reynolds and Weiss reported the first isolation and *in vitro* characterization of NSC from the adult murine brain (Reynolds & Weiss, 1992). The investigators isolated a population of undifferentiated cells that differentiated into the main cell types of the nervous system, neurons, astrocytes and oligodendrocytes. In the presence of epidermal growth factor in the medium, they formed floating clusters of cells, also called neurospheres. This approach represents a serum-free selective culture system in which most differentiating or differentiated cells are rapidly abolished. In contrast, neural stem cells respond to mitogens, divide to form neurospheres that can be dissociated and re-plated to generate secondary neurospheres (Reynolds & Rietze, 2005). These progenitor cells expressed Nestin, an intermediate filament that has been characterized as a marker for neuroepithelial and CNS stem cells during development and thus is also considered as a marker for adult neural progenitor cells (Reynolds & Weiss, 1992; Lendahl et al, 1990; Frederiksen & McKay, 1988). Later, a population of cells with similar properties was isolated from the adult rat hippocampus (Gage et al, 1995). These cells were grown as monolayers in defined medium containing basic fibroblast growth factor (bFGF) and *in vitro* studies identified self-renewing and multipotential NSC within this population (Gritti et al, 1996; Palmer et al, 1997).

Since then, neural progenitor cells with characteristic features of stem cells have been isolated and characterized from various areas of the adult CNS and various species, including humans (Taupin, 2007).

Neural stem cells can be passaged and expanded indefinitely with little change in their growth or differentiation characteristics (Gritti et al, 1996; Reynolds & Weiss, 1992) indicating that neural stem cells possess the fundamental stem-cell criteria of self-renewal and multipotency.

1.5 Asymmetric cell division in the mammalian brain

Asymmetric cell division is also a hallmark of mammalian stem cells. However, the mechanism by which asymmetry is generated is less understood. Adult stem cells have long cycling-times or are completely quiescent, making the analysis of ACD in these cells enormously complicated. Thus, a lot of our current knowledge about ACD in mammals comes from studies of more rapidly dividing embryonic progenitor cells, and the developing brain is one of the most investigated model systems.

1.5.1 Neurogenesis in the murine brain

The murine brain develops from a neuroepithelium which invaginates from an area called the neural plate (Götz & Huttner, 2005). Early in development, neural plate cells display all features of a polarized epithelium but soon express the neural stem cell marker Nestin. Later, they show characteristic features of glia cells and from this time on are referred to as radial glial cells (RGC). RGC are elongated cells with their cell body in the ventricular zone (the most apical part of the epithelium) of the developing brain and long processes which span the entire neuroepithelium. Thus, they have long been considered as support cells for the brain (Rakic, 1981). RGC were thought to be glial cells not only because they are the immediate precursors of astrocytes (Voigt, 1989; Schmechel & Rakic, 1979) but also because they express markers of astroglial cells and share morphological and ultrastructural characteristics. However, recent evidence suggest RGC to be the progenitors of neurons in the mammalian neocortex (Miyata et al, 2001; Noctor et al, 2001; Malatesta et al, 2000; Tamamaki et al, 2001).

Most neurons are generated from the asymmetric division of radial glial cells (Noctor et al, 2004) and migrate along the processes of RGC to the more basal side of the neuroepithelium where their differentiation occurs. The majority of RCS divisions are stem cell-like and produce another RGC and one neuron, however, sometimes either two proliferating RCS or differentiating neurons are generated (Noctor et al, 2001; Miyata et al, 2001).

1.5.2 Conservation of ACD in mammalian stem cells

Unlike neuroepithelial cells, radial glia can divide either parallel or perpendicular to the epithelial surface and several studies have provided evidence for a correlation between spindle orientation and the asymmetry of radial glia division (Haydar et al, 2003; Chenn & McConnell, 1995). However, a precise correlation of cleavage plane orientation and asymmetric outcome of the division is still unclear as more recent experiments determined a strong predominance of vertical divisions at all stages of neurogenesis. As a consequence, the number of horizontal divisions is too low to explain the high amount of asymmetric cell divisions of neural progenitor cells (Konno et al, 2008; Stricker et al, 2006).

Similar to *Drosophila*, spindle orientation is regulated by heterotrimeric G proteins and their binding partners Inscuteable and AGS-3, the mammalian Pins homolog (Konno et al, 2008; Sanada & Tsai, 2005; Zigman et al, 2005). Inhibition of these molecules alters the ratio of asymmetric versus symmetric cell divisions and results in the generation of higher numbers of neurons. However, a recent study claims that spindle orientation does not effect neuronal production rate (Konno et al, 2008).

Many other molecules regulating asymmetric cell division of *Drosophila* neuroblasts are also conserved in mammalian stem cells. Par proteins, such as Par-3 (Izumi et al, 1998) and Par-6 (Joberty et al, 2000), together with the aPKC homologs PKC ζ and PKC α form an apical complex and are inherited by the stem cell daughter (Manabe et al, 2002). The Par complex regulates polarity via phosphorylation of the Lgl homolog Lgl-1 (Plant et al, 2003; Joberty et al, 2000).

The mammalian Numb homologs mNumb and Numbl (Numbl) were the first segregating cell fate determinants to be discovered in mammalian progenitor cells. Both proteins inhibit Notch signalling and are essential for brain development (Petersen et al, 2002). Mammalian Notch1 promotes stem cell fate of radial glial cells and astrocytes (Gaiano et al, 2000) but inhibits oligodendrogenesis (Gaiano & Fishell, 2002). Whereas Numbl is a cytoplasmic protein, mNumb is apically localized in the developing neocortex (Zhong et al, 1996b). This localization has led to the hypothesis that mNumb might be asymmetrically inherited during horizontal divisions and thus be responsible for the asymmetric outcome. Deletion of mNumb and Numbl in progenitor cells leads to the depletion of progenitor cells and stops neurogenesis, supporting a role as segregating determinant. However, the contribution of Numbl is not clear as it does not localize asymmetrically. In addition, deletion of mNumb at later stages of development using an conditional knock out leads to overproliferation of neural progenitors and is contradictory to earlier results (Li et al, 2003). Surprisingly, loss of mNumb does not affect stem cell maintenance in the adult brain where neural stem cells also divide in a asymmetric fashion (Kuo et al, 2006). Instead, ependymal cells in the stem cell

niche are affected and thus, loss of mNumb has only an indirect effect on stem cell proliferation. A recent study demonstrated that the actual function of mNumb during brain development might be the maintenance of adherens junctions in radial glial cells (Rasin et al, 2007). mNumb was shown to localize to the apical endfeet of interphase radial glial cells that surround mitotic progenitors - something that so far was thought to be an apical crescent in actively dividing progenitors. In contrast, within the dividing cell, the apical domain is actually very narrow and mNumb has shown to be localized mainly basolateral concentrated at vesicles near adherens junctions. In the absence of mNumb adherens junctions are lost and it is thus suggested that mNumb might not be a segregating determinant on mouse neural progenitors but more likely, regulates epithelial polarity (Rasin et al, 2007).

The Prospero homolog Prox-1 is a potential tumor suppressor and is expressed in the brain but seems not to be segregated asymmetrically (Dyer et al, 2003). Similar, Staufen has a conserved role in RNA transport but does not seem to be involved in ACD of mammalian neural progenitor cells (Knoblich, 2008). The Brat homologs TRIM2, TRIM3 and TRIM32 are highly expressed but their role as segregating determinants remains to be determined (Knoblich, 2008).

However, it is also possible that proteins not implicated in the regulation of *Drosophila* neuroblast divisions have important roles in the mammalian ACD apparatus. Intriguingly, the epidermal growth factor receptor (EGFR) has been shown to be asymmetrically segregated in dividing neural progenitors (Sun et al, 2005). In culture, the daughter cell that inherits EGFR responds differently to EGF and expresses different markers, suggesting that asymmetric EGFR distribution might bias cell fate decisions.

In addition, divisions of neural progenitors are morphologically asymmetric. Compared to other epithelial cells, the apical domain of radial glia cells is very narrow due to their elongated shape (Rasin et al, 2007; Götz & Huttner, 2005). As a consequence, the apical domain can be asymmetrically inherited in all divisions in which the cleavage furrow is not perfectly vertically oriented. This might also explain why the amount of asymmetric divisions is much higher as estimated from the number of clearly horizontal divisions (Kosodo et al, 2004; Noctor et al, 2001).

Together, the precise mechanism by which mammalian neural progenitors can self-renew and generate cell diversity is currently unclear. It is also not known whether components of the ACD-apparatus are conserved between *Drosophila* and vertebrates. Whereas some proteins are functionally conserved (e.g. proteins of the Par complex) and obligatory for proper ACD, others seem to be elusive or regulate ACD only indirectly (e.g. Numb, Staufen, Prox-1). Moreover, whether cell fates are generated by unequal inheritance of segregating determinants is unclear (Fuja et al., 2004).

1.6 Asymmetric cell division and cancer

Cancers are composed of heterogeneous cell populations including highly proliferative immature precursors and more differentiated cells (Tang et al, 2007; Guo et al, 2006). It has recently become clear that many tumors are maintained by a small fraction of so called cancer stem cells (CSC) that give rise to all the cells present in the tumor (Reya et al, 2001). This raises the possibility that defects in stem cell lineages might be among the earliest lesions that lead to tumor formation. Indeed, several findings point to dysfunctional ACD as a key factor in cancer development.

1) *Drosophila* neuroblasts have recently emerged as a model system to study the transition from a normal stem cell to a tumor stem cell (Caussinus & Gonzalez, 2005). Upon mutation of genes involved in asymmetric cell division, neuroblasts hyperproliferate and acquire massive chromosomal abnormalities and genetic changes. Interestingly, injection of larval brain tissue mutant for any of the components that control neuroblast asymmetric cell division (i.e. Miranda, Prospero, Numb, Lgl, Brat, Pins) into the abdomen of adult flies leads to overproliferation of the transplanted neuroblasts and the formation of metastasizing tumors (Beaucher et al, 2007; Caussinus & Gonzalez, 2005). These implanted cells appear to be immortal and can be serially transplanted over long periods of time.

It has been proposed, that these tumors arise from a common mechanism, the disruption of neuroblast asymmetry and the production of excess self-renewing cells. Supporting this hypothesis, more recent studies have shown that all segregating cell fate determinants (Prospero, Numb and Brat) as well as their adaptor molecules Miranda and Pon can act as tumor suppressors (Bello et al, 2006; Choksi et al, 2006; Lee et al, 2006a; Wang et al, 2006; Betschinger et al, 2006a).

2) The human Lgl homolog Hugel-1 is frequently deleted in solid human cancers such as melanoma, breast and pancreatic cancer (Kuphal et al, 2006; Schimanski et al, 2005).

3) Atypical PKC ζ is an oncogene in human non-small cell lung cancer (Fields & Regala, 2007; Regala et al, 2005).

4) Mice deficient in mNumb/Numbl or Lgl-1 show severe abnormalities during brain development resulting in hyperplasia and rosette-like structures that resemble medulloblastoma, a human neuron-ectodermal tumor (Klezovitch et al, 2004; Li et al, 2003).

5) EGFR is asymmetrically segregated in some mammalian neural progenitor cells (Sun et al, 2005) and EGFR amplification, overexpression and mutations are frequently detected in many human tumors, including carcinoma and glioblastoma (Sibilia et al, 2007).

Together, these studies suggest a causal link between defects in asymmetric cell division and tumorigenesis.

1.6.1 The cancer stem cell theory

Tumors have long been known to consist of a heterogeneous population of cells (Tang et al, 2007; Guo et al, 2006). While the great majority of cells that form the tumor are destined to differentiate, albeit aberrantly, only a small population possesses extensive self-renewing capacity to regenerate the tumor and sustain its growth when injected into immune-compromised mice (Tang et al, 2007). These rare cells are named cancer stem cells (CSCs), after normal stem cells, as both have similar abilities to self-renew and to give rise to heterogeneous differentiated cell types (Reya et al, 2001).

Two models of cancer growth can explain tumor development: Traditionally, in the stochastic model, it was assumed that all tumor cells can form new tumors and therefore are equally tumorigenic (Reya et al, 2001). In contrast, the cancer stem cell theory proposes that tumors are driven and maintained by a minority of transformed stem/precursor cells and unregulated cell growth is due to a disruption in the regulatory mechanism in stem cell renewal (Clarke et al, 2006; Passegué et al, 2003).

The existence of cancer stem cells has been hypothesized for many decades, but it was not until 1997 that they were isolated from patients with acute myeloid leukemia (Bonnet & Dick, 1997). Subsequently, CSCs have been isolated from breast (Al-Hajj et al, 2003) and brain cancers (Singh et al, 2004; Galli et al, 2004; Singh et al, 2003; Hemmati et al, 2003; Ignatova et al, 2002).

In addition, these studies raised the strong possibility that CSCs might derive from mutations in normal stem cells that reside within the respective tissue. Alternatively, differentiated tumor cells may acquire the characteristics of stem cells.

1.6.2 Origin of brain tumor cells

The most common form of primary brain tumors are gliomas, i.e. tumors of glial origin (Russell & Rubinstein, 1989). The most malignant, glioblastoma multiforme (GBM), is characterized by resistance to chemo- and radiotherapy and by a short median survival (Stupp et al, 2005). Moreover, gliomas are highly infiltrative and their ability to invade normal brain structures limit the efficacy of complete surgical resection (Holland, 2000).

The first evidence for the existence of cells with stem-like characteristic in brain tumors was reported by Steindler and colleagues in 2003 who successfully isolated neurosphere-forming precursors from post-surgery specimens of human GBMs (Ignatova et al, 2002). Upon growth factor withdrawal, most tumor-derived spheres gave rise to cells with glial and neuronal morphology and marker expression. Tumor-derived spheres could be serially passaged, and secondary spheres again have been demonstrated to be multipotential.

Later, cancer stem cells have been reported to be isolated from other brain tumors, including gliomas, astrocytoma, medulloblastoma and ependymomas (Nakano & Kornblum, 2006).

These studies clearly showed that brain tumors contain transformed, undifferentiated neural precursors that possess characteristics of true stem cells, i.e. long-term self-renewal and multipotency. However, it was not proven whether they have cancer-initiating properties as would be expected of brain cancer stem cells.

This was demonstrated later independently by two groups. In the first study, neurospheres cultured from GBMs could give rise to tumors in immune-compromised mice with characteristics resembling those of the parental tumor (Galli et al, 2004). It has been demonstrated that neurosphere-forming cells expressed CD133 (Singh et al, 2004; Singh et al, 2003), a cell surface marker previously shown to be expressed on human neural stem cells (Uchida et al, 2001). Using this cell-surface marker for immunopurification, it was possible to enrich cancer stem cells from human medulloblastoma and GBMs (Singh et al, 2004). This group demonstrated that as few as 100 CD133-positive cells can form tumors in immune-compromised mice. Tumors recapitulated the original cell heterogeneity and CD133-positive cells could be serially transplanted, providing a more definite proof of the existence of self-renewing and cancer-initiating stem-like cells in brain tumors. In contrast, CD133-negative cells failed to generate tumors, even when injected in much larger numbers (Singh et al, 2004), again highlighting that only a minority of cells within a tumor is responsible for its maintenance and growth. Furthermore, additional studies suggested that CD133-positive tumor cells are more radioresistant than the CD133-negative fraction, implying that they may be responsible for disease recurrence after therapy (Bao et al, 2006a; Bao et al, 2006b).

However, it is still unknown how CSCs are generated and whether they are derived from the transformation of neural stem cells found in the adult brain.

Neurogenesis persists throughout adulthood within discrete brain regions as the dentate gyrus of the hippocampus or the subventricular zone of the lateral ventricles (Lois & Alvarez-Buylla, 1994; Gage et al, 1998). Germinal regions such as the SVZ have long been proposed as possible sources of gliomas (Globus & Kuhlenbeck, 1944; Lewis, 1968) and many gliomas develop near these regions. Exposure to oncogenic viruses or administration of carcinogens results in the preferential tumor formation in germinal zones as opposed to non-proliferative regions of the brains as the peripheral cortex (Sanai et al, 2005; Hopewell & Wright, 1969). Furthermore, it has been shown that tumors found in distinct areas of the brain originate in the SVZ and subsequently migrate to their final destination (Vick et al, 1977). The observation that the site of tumor-origin is often distinct from the site where the tumor eventually develops might be explained by the hypothesis that a defect stem cell, e.g. a type-B stem cell in the SVZ, by dividing asymmetrically generates another cancer stem cell

that remains in the germinal niche whereas the daughter cell, most likely a progenitor cell, migrates away to give rise to the tumor mass (Berger et al, 2004).

Transiently dividing progenitors only have a short lifetime, and therefore, mutagenic events might not have the opportunity to accumulate in transit amplifying cells and their terminally differentiated progeny. In contrast, stem cells persist the whole lifetime of an organism and have the potential to self-renew and proliferate making them a preferential target for tumorigenesis (Huntly & Gilliland, 2005). However, transit amplifying cells, the immediate descendants of adult stem cells, inherit these mutations and therefore might play an indirect role in tumor initiation. The role of these cells is further supported by the finding that in the adult subventricular zone these progenitors express EGFR (Doetsch et al, 2002), a receptor that is altered in more than 50% of human gliomas (Sibilia et al, 2007) and its constitutive activation can cause glioma formation in the CNS (Bachoo et al, 2002).

2 Aim of this work

2.1 Asymmetric localization of Miranda during neuroblast division

A central question in stem cell research is how stem cells achieve asymmetric cell divisions to replicate themselves while generating more committed daughter cells.

Drosophila neuroblasts provide one of the best understood models to study asymmetric cell division which is based on the unequal segregation of intrinsic cell fate determinants. Over the past decades, many components of the machinery that regulate the asymmetric division of neuroblasts have been identified and their functions elucidated (Chia et al, 2008; Knoblich, 2008). However, the precise mechanism how cell fate determinants localize asymmetrically in mitosis is unknown and remains to be determined.

Immunofluorescence staining on fixed tissue detected Miranda in an apical crescent as well as in the cytoplasm prior to formation of a basal metaphase crescent (Barros et al, 2003; Petritsch et al, 2003; Fuerstenberg et al, 1999; Shen et al, 1997; Ikeshima-Kataoka et al, 1997). These data suggest a dynamic, stepwise pattern for Miranda localization, but the exact mode and temporal sequence of Miranda localization during neuroblast division has not been studied in live embryos yet.

Miranda localization requires both Myosin VI and Myosin II. However, it was unknown at what stage of Miranda localization these myosins act and whether they cooperate in the same pathway to localize Miranda. In addition, although Miranda and the second adaptor protein PON are both localized to an overlapping basal cortical crescent in metaphase, it is still unknown whether they are localized by similar mechanisms.

The molecular details of asymmetric Miranda localization are the central question of the first part of this thesis and will be addressed by combining immunofluorescence studies with time-lapse confocal microscopy on embryos expressing Miranda-GFP.

The exact mechanism of Myosin VI and Myosin II directed basal protein localization is not yet fully understood and will be studied in living embryos that exert reduced Myosin VI and Myosin II activity.

2.2 The origin of brain cancer stem cells

There is growing evidence that many cancers contain a small population of so called cancer stem cells which are responsible for maintenance and growth of tumors and explain the cellular heterogeneity in most cancers.

The origin of brain cancers has not been determined yet and is a highly controversial topic (Sakariassen et al, 2007). Brain cancer stem cells might be generated from adult neural stem cells and a defect in asymmetric cell division might be the initiating step in the progressive advancement of their pathological state. These aberrant stem cells are referred to as premalignant stem cells (PSC) and it is believed that they evade normal cell cycle control and/or differentiation. PSC are not necessarily tumorigenic themselves but because defects in ACD predispose stem cells to genetic instability, PSC are prone to acquire additional mutations such as the amplification of oncogenes or loss of tumor suppressors. Accumulation of additional mutations will lead to the formation of a pathological stem cell pool, the cancer stem cells, giving rise to tumor cells.

Oligodendroglioma are diffusely infiltrating brain tumors which mainly consist of immature oligodendrocytes and oligodendrocyte progenitors (Ligon et al, 2006). EGFR amplification and loss of the tumor suppressor(s) *ink4a/arf* and *p53*, respectively, are mutations frequently found in human oligodendroglioma (Weiss et al, 2003). Only recently, a potential stem cell population has been identified in human oligodendroglioma (Calabrese et al, 2007). However, its tumorigenic potential has not been evaluated yet.

Here, I study the origin of cancer stem cells in a transgenic mouse model with activated EGFR signaling in postnatal stem cell lineage (Weiss et al, 2003). Mice expressing an oncogenic version of the EGFR (*verbB*) in neural stem cells and their progeny from the *S100 β* promoter develop low-grade oligodendroglioma. Loss of *p53* leads to the development of high-grade oligodendroglioma in both *S100 β -verbB, p53^{+/-}* and *S100 β -verbB, p53^{-/-}* mice. Because tumor development in animals heterozygous for *p53* is significantly delayed, this model provides a unique opportunity to study the potential stepwise progression of neural stem cells to premalignant and finally cancer stem cells.

3 Thesis Part 1 - Asymmetric localization of Miranda during neuroblast division

3.1 Results

It has been shown that adaptor proteins like Miranda or PON play a pivotal role in asymmetric cell division as they ensure the asymmetric segregation of cell fate determinants to the GMC. Immunohistochemical analysis of fixed embryonic tissue revealed that Miranda exerts dynamic localization during asymmetric cell division of neuroblasts and previous data detected Miranda in an apical cortical crescent prior to formation of a basal crescent. However, the exact timing of the formation of the apical Miranda crescent remained controversial as several reports stated that Miranda is apical at interphase and/or at prophase (Fuerstenberg et al, 1999; Matsuzaki et al, 1998; Shen et al, 1998), whereas others reported that Miranda localizes to the cytoplasm at interphase (Ikeshima-Kataoka et al, 1997).

3.1.1 Miranda forms a basal crescent independent of basal translation or localized protein degradation

To correlate Miranda localization with distinct steps during the cell cycle, I stained fixed *Drosophila* embryos for Miranda, γ -tubulin to label the centrosome, and aPKC to mark the apical crescent. Centrosomes duplicate on either the apical or basal side of the cell and migrate laterally to become positioned at opposite poles along the apical/basal axis at pro/metaphase (Kaltschmidt et al, 2000). At early and late stages of prophase, when centrosomes were migrating laterally, Miranda localized mainly to the cytoplasm and the cortex but not the nucleus (Figure 5A,B). At pro/metaphase, when centrosomes moved towards opposite poles and the nuclear membrane breaks down, Miranda filled the entire cytoplasm including nuclear regions (Figure 5C). Later at metaphase, Miranda disappeared from the cytoplasm and formed a basal crescent, which was segregated exclusively to the GMC at telophase (Figure 5D,E). In contrast, aPKC remained apically localized during mitosis.

Previous data indicate that Miranda might be actively transported to the basal side of the neuroblast by the action of myosins. Alternatively, Miranda localization could be explained by localized translation of Miranda protein at the basal pole and its localized degradation at the apical pole at metaphase.

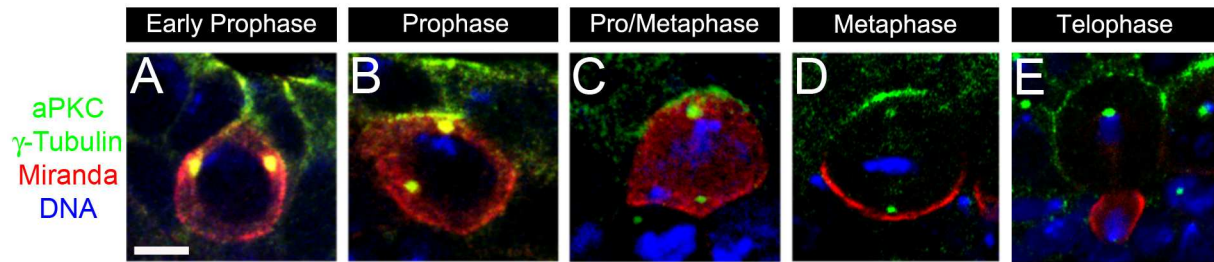


Figure 5: Miranda protein localization at defined steps during neuroblast mitosis. At early prophase (A) and prophase (B), centrosomes (visualized by γ -Tubulin, green dots) moved laterally, aPKC (green) accumulated at the apical cortex and Miranda protein (red) predominantly localized to the cytoplasm and the cortex. At pro/metaphase (C), centrosomes were positioned at opposite poles along the apical/basal axis, aPKC was apical and Miranda protein filled the entire cell including nuclear regions. At metaphase (D), centrosomes remained aligned along the apical/basal axis, aPKC was apical and Miranda is entirely localized to a basal cortical crescent. At telophase (E), Miranda was exclusively inherited by the GMC while aPKC remained in the neuroblast. Apical is up in all figures. Scale bar represents 5 μ m.

If *de novo* protein synthesis contributes to asymmetric Miranda localization, *miranda* mRNA should be detected at the basal pole. To investigate whether *miranda* mRNA overlapped with Miranda protein in a basal crescent at metaphase, I performed fluorescent *in situ* hybridization and visualized Miranda protein by immunohistochemistry (Figure 6). In agreement with earlier data, *miranda* mRNA accumulated around the apical pole and partially colocalized with cytoplasmic Miranda protein at prophase (Schuldt et al, 1998) (Figure 6A). *miranda* mRNA remained apical at meta- and anaphase and was exclusively inherited by the neuroblast daughter, whereas Miranda protein localized to a basal metaphase crescent and segregated to the GMC (Figure 6B-D). Thus, Miranda protein and *miranda* mRNA localize exclusively at the time when Miranda protein becomes basally localized. Moreover, the absence of *miranda* mRNA at the basal side of the dividing neuroblast argues against localized translation as a means to generate asymmetry of the Miranda protein.

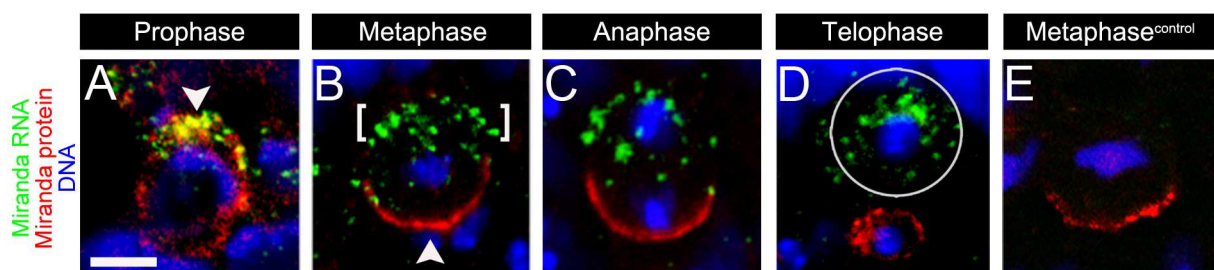


Figure 6: Miranda protein and *miranda* mRNA show distinct localization during neuroblast division. (A) *miranda* mRNA (green) was apically enriched at prophase and partially co-localized with Miranda protein (red, white arrowhead). (B) At metaphase, *miranda* mRNA (white brackets) remained apical and never co-localized with Miranda protein (white arrowhead). At anaphase (C) and telophase (D), *miranda* mRNA remained in the neuroblast whereas Miranda protein was in the GMC. No signal for Miranda mRNA could be detected using a sense RNA probe as a control (Metaphase^{control}). The neuroblast at telophase is marked by a white circle. Scale bar represents 5 μ m.

In order to become basally enriched in metaphase, Miranda protein may be selectively degraded by the 26S proteasome at the apical side of dividing neuroblasts. Miranda contains four potential destruction boxes (Shen et al, 1997), which in other proteins mediates cell cycle-dependent degradation by the proteasome. This suggests that Miranda too could be locally degraded by the 26S proteasome in areas outside the basal metaphase crescent.

Mutations in the 26S proteasome affect cell fate decisions in the sensory organ precursor lineage of the developing pupae presumably because the Notch receptor is targeted for degradation (Schweisguth, 1999). To investigate a potential role of 26S proteasome-dependent degradation for basal Miranda localization, I initially studied embryos carrying a dominant temperature sensitive mutation in the $\beta 2$ proteasome subunit gene *DTS5* or embryos expressing the *DTS5* mutant in neuroblasts (Schweisguth, 1999). However, at this stage of development, proteasome activity was not strongly affected (data not shown) and thus I used the potent proteasome inhibitor MG132 to impair proteasome activity (Muro et al, 2002).

Embryos were treated with the proteasome inhibitor MG132 for 15 or 30 minutes and Miranda protein was detected by immunohistochemistry. Almost all metaphase neuroblasts showed normal, basal localization of Miranda protein after MG132-treatment for 15 minutes (100%; $n=167$) and 30 minutes ($98.5 \pm 2.1\%$; $n=153$) (Figure 7D). During metaphase, cyclin A is degraded by the 26S proteasome (Tio et al, 2001), and in the absence of proteasome activity, cyclin A persists and cells arrest at metaphase (Sigrist et al, 1995). To control for successful inhibition of the proteasome, I detected cyclin A in addition to Miranda and determined the ratio of neuroblasts at metaphase versus ana-/telophase (Figure 7C). After 30 minutes of MG132-treatment, cyclin A protein persisted in $75.3 \pm 11.5\%$ of metaphase neuroblasts (Figure 7B; $n=153$). In contrast, cyclin A was detected in $29.0 \pm 5.3\%$ of metaphase neuroblasts in untreated embryos ($n=205$) and in $34.0 \pm 1.8\%$ of control embryos incubated with DMSO as control ($n=178$). Coinciding with defective cyclin A degradation, the number of neuroblasts in metaphase increased from $51.0 \pm 10.0\%$ in untreated and $51.8 \pm 7.8\%$ in control embryos to $84.6 \pm 5.7\%$ after 30 minutes with MG132. Cyclin A was still properly degraded after 15 minutes treatment with MG132 ($28.3 \pm 4.7\%$; $n=167$) or DMSO ($30.4 \pm 6.5\%$; $n=119$) and in addition, the number of metaphase neuroblasts was not significantly altered ($47.9 \pm 4.4\%$ and $42.7 \pm 11.5\%$, respectively). Together, these data showed that short-term inhibition of proteasome activity did not disrupt the basal localization of Miranda.

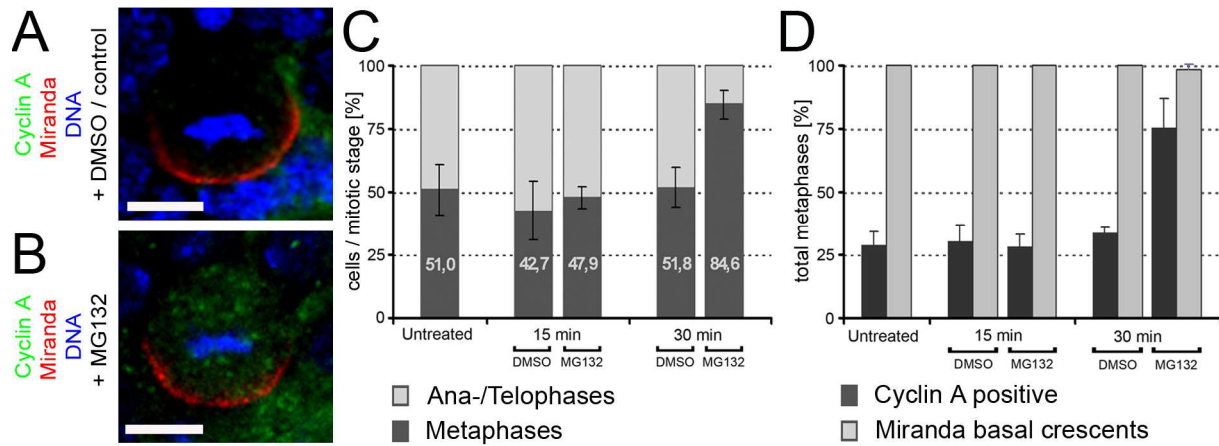


Figure 7: Inhibition of the proteasome prevents cyclin A degradation at metaphase and progression to anaphase but does not affect Miranda localization. Miranda protein (red) still formed a basal metaphase crescent in neuroblasts of embryos treated with DMSO as control (A) or MG132 (B). Cyclin A (green) was degraded in the majority of metaphase neuroblasts of control embryos (A) but persisted in metaphase neuroblasts of MG132-treated embryos (B). Quantification of metaphase versus ana/telophase neuroblasts (C) and Miranda metaphase crescents versus metaphases with persistent cyclin A (D) revealed that 30 min but not 15 min with MG132 inhibited progression of metaphase neuroblasts to anaphase and efficient degradation of cyclin A. Miranda protein localized to a basal crescent in the majority of MG132-treated neuroblasts. Scale bare represents 5 μ m.

In summary, the localization of Miranda does not depend on localized translation of *miranda* mRNA at the basal cortex nor Miranda protein degradation at areas outside the basal crescent. More likely, a pre-existing pool of Miranda protein is dynamically moved from the apical cortex throughout the entire cell to the basal cortex.

3.1.2 Miranda accumulates in the cytoplasm prior to formation of a basal crescent

By using immunohistochemical analysis on fixed tissue one is limited to observe Miranda localization in a single neuroblast and at a single time point. Therefore, a live-imaging approach was established to investigate the dynamics of Miranda localization in more detail. Note that live-imaging experiments were done together with Veronika Erben, a former colleague in the lab, and results from this study were recently published (Erben et al, 2008).

A full length Miranda-GFP construct was expressed in living embryos using the UAS-Gal4 system (Brand & Perrimon, 1993) and its localization in neuroblasts was followed by time-lapse confocal microscopy. The UAS-Gal4 system relies on 2 fly strains, an activator line expressing the transcription factor Gal-4 controlled by a specific promotor and an effector line containing the Gal-4 binding upstream activator sequence (UAS) linked to the gene of interest. Thus, crossing these lines allows the selective expression of any cloned gene in a time and spatial manner.

In analogy with immunohistochemical data, Miranda localized uniformly to the cytoplasm and the cortex sparing the nucleus in most neuroblasts at early prophase (Figure 8A). Presumably around the time of nuclear envelope breakdown, Miranda accumulated throughout the entire cytoplasm including the nuclear region and gradually formed a basal crescent at metaphase. Upon cytokinesis, Miranda is entirely inherited by the smaller, basal ganglion mother cell in neuroblast divisions (Figure 8A).

To ensure that the ubiquitous cytoplasmic localization of Miranda was not caused by artificial saturation of the localization machinery as a result of the ectopic expression of Miranda-GFP, various Gal4-driver strains of different strengths were used. I found very similar protein localization patterns, including the cytoplasmic localization of Miranda at pro/metaphase when Miranda-GFP was expressed under the control of neuralized-Gal4 (Figure 8A), a strong neuroblast- and neuroepithelial-specific driver, V32A-Gal4 (Figure 8B), driving maternal gene expression or scabrous-Gal4 (Figure 8C), a weaker neuroblast- and neuroepithelial-specific driver.

In addition, I investigated the localization of Miranda-GFP by immunohistochemistry (Figure 8D,F,G) and compared it to endogenous Miranda protein. Miranda-GFP localization patterns from two lines generated by our lab (Figure 8D,F) and a preexisting line (Figure 8G) (Ohshiro et al, 2000) were determined. All three lines showed overlapping localization of Miranda-GFP with total Miranda protein and thus were used interchangeably in live imaging experiments giving very similar Miranda-GFP localization patterns although the signal intensity varied.

In Western blot analysis of embryos expressing Miranda-GFP under the control of Gal4 a single band of 130 kDa was recognized by a GFP antibody which was not detectable in controls carrying only the Miranda-GFP transgene or only the Gal4 driver (Figure 8H). In addition, Miranda-GFP was expressed at lower levels than endogenous Miranda protein detected by a Miranda specific antibody.

Finally, the functional behavior of Miranda-GFP was evaluated by studying Miranda-GFP localization in embryos expressing a constitutively active form of Lgl (Lgl^{3A}) which has been shown to disrupt Miranda localization (Betschinger et al, 2003b). Intriguingly, cytoplasmic localization of Miranda was completely abolished when coexpressed with Lgl^{3A} and Miranda-GFP localized to the cortex throughout neuroblast mitosis and finally segregated symmetrically to both daughter cells (Figure 8F).

Taken together, these data suggest that Miranda-GFP does not saturate the localization machinery but rather faithfully recapitulates the localization of endogenous Miranda protein in live embryos.

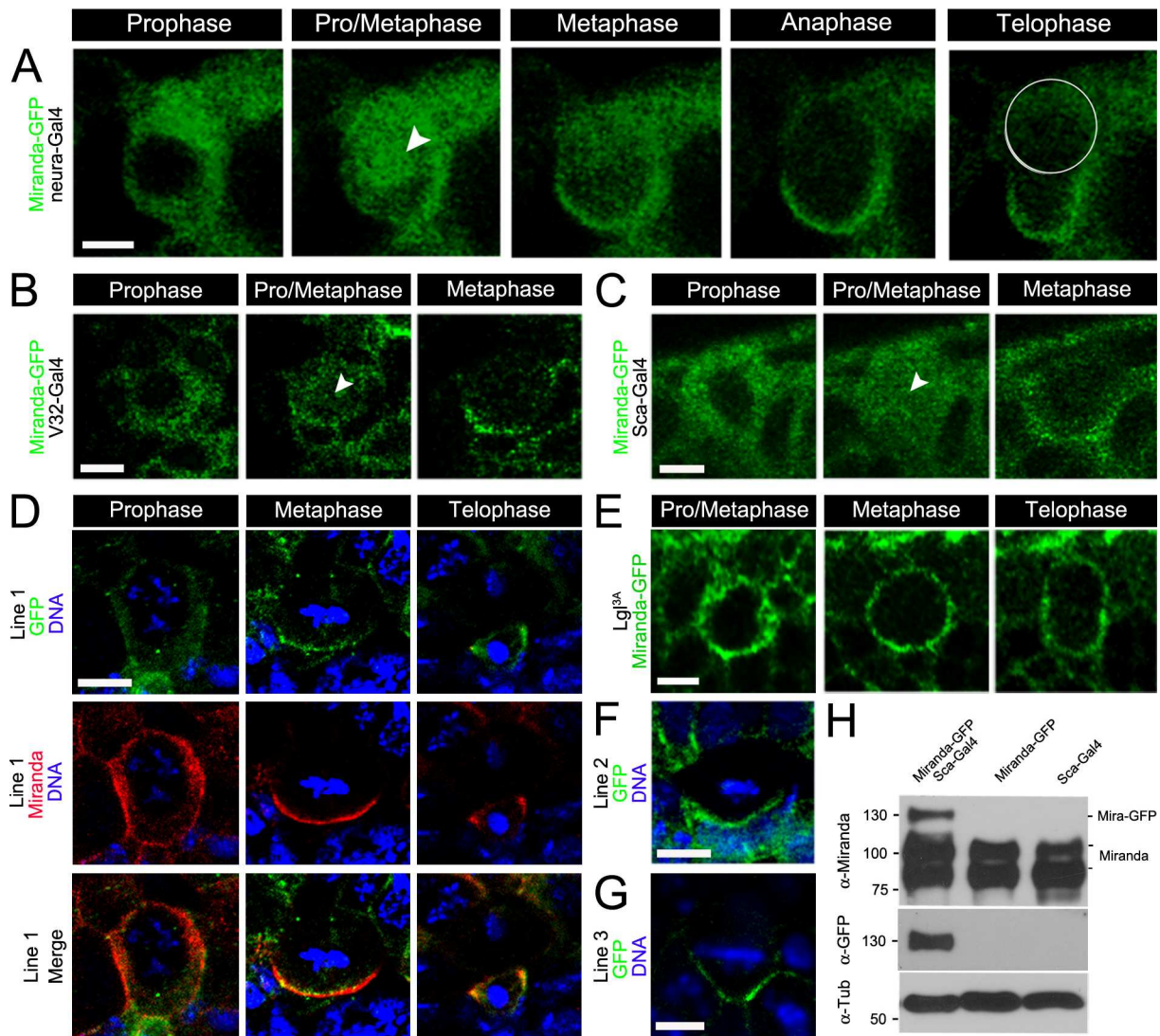
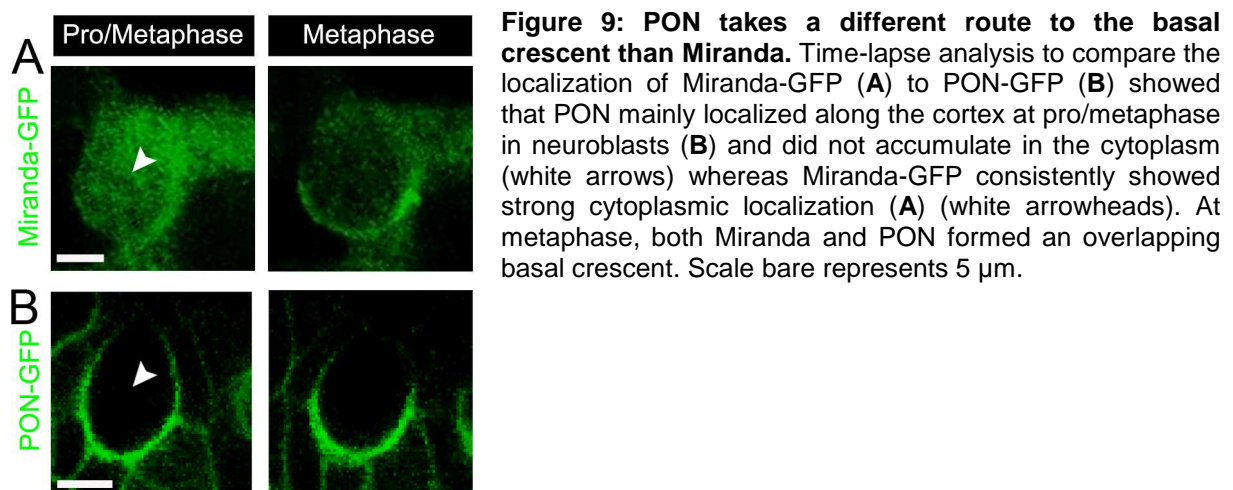


Figure 8: Miranda localization in neuroblasts is a dynamic, multistep process. Neuroblasts (NB) undergoing mitosis in embryos expressing Miranda-GFP under control of *neuralized-Gal4* (*neura-Gal4*) were examined by time-lapse confocal microscopy. (A) In the majority of neuroblasts Miranda-GFP (green) localized uniformly to the cytoplasm and the cortex but not to an apical crescent at prophase. At pro/metaphase cytoplasmic Miranda-GFP accumulated throughout the entire cytoplasm including nuclear regions (white arrowhead). At metaphase, the basal cortical crescent formed and Miranda-GFP gradually disappeared from the remaining areas of the cell. Miranda-GFP was inherited exclusively by the GMC at telophase (white circle). Miranda-GFP showed a very similar cytoplasm-to-basal cortex localization pattern when expressed under the control of *V32-Gal4* (B) and *scabrous-Gal4* (*sca-Gal4*) (C). Cytoplasmic Miranda accumulation is indicated by white arrows. (D) In fixed embryos, the location of Miranda-GFP (green) was indistinguishable from that of total Miranda (red), in the cytoplasm at prophase and at the basal crescent at metaphase. (E) In embryos expressing a constitutively active form of Lgl, *UAS-Lgl^{3A}*, Miranda-GFP was found uniformly around the cortex and cytoplasmic localization was abolished. (F,G) Miranda-GFP localized to a tight metaphase crescent overlapping with total Miranda in two additional transgenic lines. (H) Immunoblotting using a Miranda antibody (top panel) and a GFP antibody (middle panel) revealed that ectopically expressed Miranda-GFP represented by the 130 kDa band is specifically expressed in *UAS-Miranda-GFP/Sca-Gal4* embryos but not in *UAS-Miranda-GFP* or *Sca-Gal4* embryos (controls). Miranda-GFP levels were low compared with total Miranda protein running at 75-100 kDa. Tubulin was used as a loading control (bottom panel). Scale bar represents 5 μ m.

3.1.3 PON protein moves along the cortex to form a basal crescent

As reported previously, PON is cleared from the cytoplasm at interphase and primarily localized to the cortex throughout cell division of neuroblasts (Lu et al, 1999). A pre-existing PON-GFP line (Lu et al, 1999) was used for time-lapse confocal microscopy to compare its dynamic localization during neuroblast division with that of Miranda-GFP.

PON-GFP moved basolaterally essentially along the cortex and gradually accumulated at the basal side to form the metaphase crescent. Interestingly, Pon-GFP never displayed the strong cytoplasmic localization observed with Miranda-GFP at prophase and pro/metaphase (Figure 9). This data demonstrates that although Miranda and PON colocalize to a metaphase crescent they use different routes to translocate to the basal side.



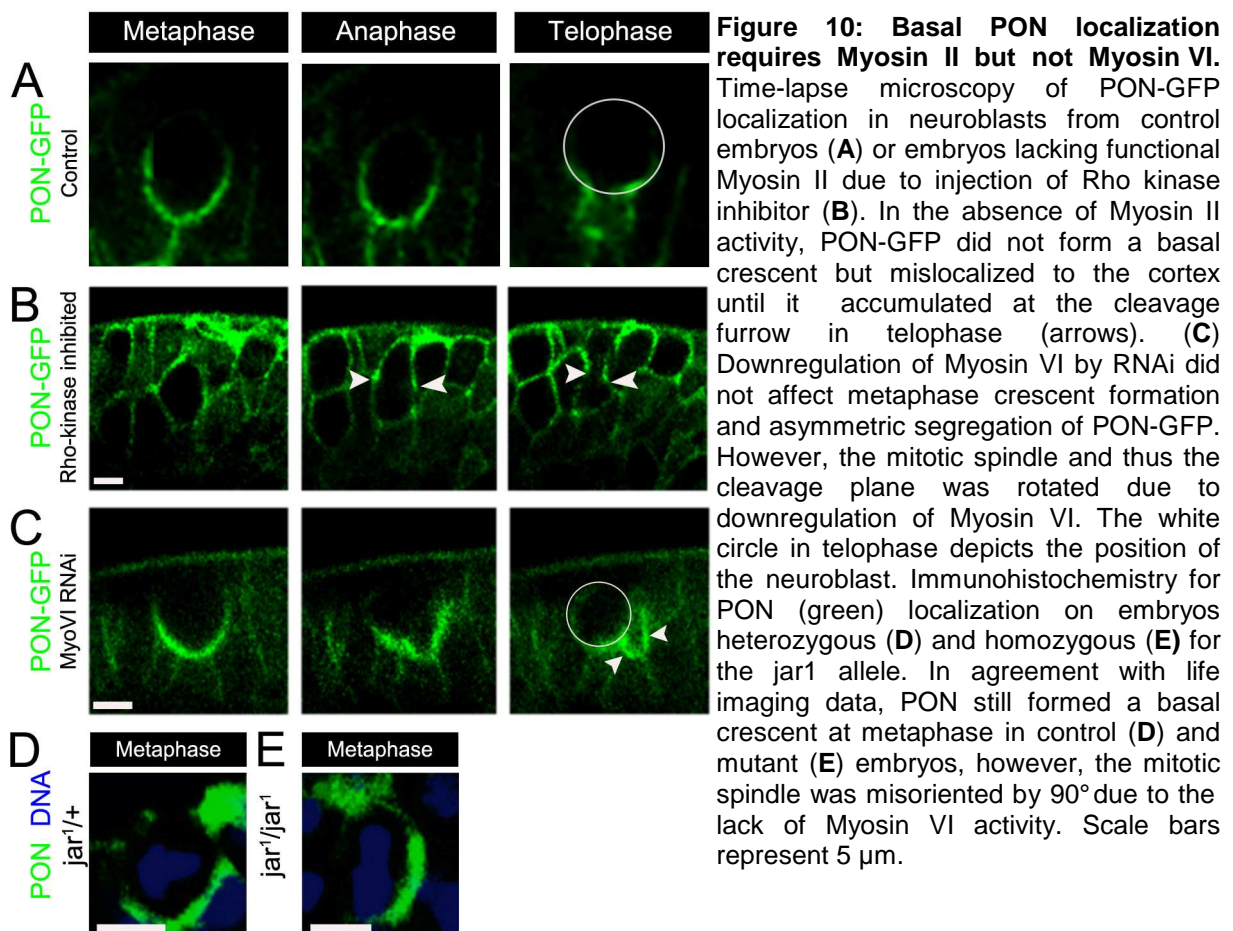
It has been shown that asymmetric localization of PON is sensitive to butanedione-2-monoxime, a well-studied inhibitor of muscle Myosin II. However, its efficacy towards other, non-muscle myosins remains controversial (Ostap, 2002) and thus, it is not known yet whether additional myosin motors regulate PON localization.

In order to selectively test the requirement of Myosin II for PON localization, the Rho kinase inhibitor Y-27632 was injected into PON-GFP-expressing embryos which were then examined by live imaging. When Myosin II activity was impaired, PON-GFP localized uniformly around the cortex at pro- and metaphase and later accumulated at the cleavage furrow (Figure 10B, white arrowheads). In contrast, in control embryos PON-GFP is inherited asymmetrically by the GMC (Figure 10A) similar to Miranda-GFP (Figure 9B). Thus, Myosin II might indeed be required for proper localization of PON to a basal crescent, presumably by cortical exclusion of PON from the apical pole in prophase.

The pointed end-directed myosin motor Myosin VI has been shown earlier to be required for basal Miranda localization (Petritsch et al, 2003). Myosin VI predominantly localizes to the

cytoplasm which suggests that it does not directly transport PON to the basal side of the cell. To test for an indirect role of Myosin VI for PON localization, I injected double stranded RNA complementary to parts of Myosin VI in embryos expressing PON-GFP to downregulate Myosin VI activity (Figure 10C). In embryos lacking zygotic Myosin VI, the mitotic spindle is misoriented resulting in a rotation of the division plane by 45-90° (Petritsch et al, 2003). As shown by time-lapse confocal microscopy, although the division plane was rotated, PON-GFP still formed a basal crescent in metaphase which was positioned lateral to the epithelial surface presumably due to a general loss of proper apical-basal polarity (Figure 10C). In addition, immunohistochemistry on a zygotic mutant allele of Myosin VI (*jar*¹) (Petritsch et al, 2003) revealed that PON was localized to a metaphase crescent in both the heterozygous (*jar*^{1/+}) (Figure 10D) and homozygous (*jar*^{1/jar}¹) (Figure 10E) Myosin VI mutants although the mitotic spindle was misoriented in the null mutation.

Thus, in contrast to its function in localizing Miranda, Myosin VI is not required for the asymmetric localization of PON in a cortical metaphase crescent.



3.1.4 Miranda diffuses freely in the cytoplasm but shows spatially-limited and slower movement at the cortex

Miranda protein could either freely diffuse or could be actively transported through the cytoplasm to the basal side of the cell (e.g. by myosin motor proteins) prior to forming a metaphase crescent.

To distinguish between a myosin-directed movement and passive diffusion of Miranda, fluorescence recovery after photobleaching (FRAP) of Miranda-GFP was determined. Histone-RFP was coexpressed to visualize DNA condensation and thus the mitotic stages of dividing neuroblasts (Schuh et al, 2007). The motility of Miranda-GFP was calculated after selectively bleaching a region of interest (ROI) within either cytoplasmic regions or the cortical crescent and measuring the recovery of the fluorescent signal by Miranda-GFP molecules moving into the ROI from adjacent areas (see Material and Methods for details).

To investigate FRAP of cytoplasmic Miranda, I attempted to bleach various ROIs at either the apical or basal half of the cell in dividing neuroblasts at pro/metaphase and recorded the recovery of the fluorescent signal by Miranda-GFP (Figure 11A,B). However, it was not possible to significantly reduce the fluorescent signal of cytoplasmic Miranda-GFP by applying the same parameters which reduced the cortical Miranda signal used as a reference (Figure 11E). These results were indicative of rapid movement of Miranda-GFP and suggested that Miranda diffused unrestrictedly throughout the cytoplasm rather than being actively transported. As a control for a freely diffusing protein, FRAP of eGFP was studied and showed very similar characteristics (Figure 11C). The slightly higher recovery rate of Miranda-GFP could be explained by its greater molecular mass and association with other diffusible cargo molecules.

When the entire cytoplasm of neuroblasts at pro/metaphase was bleached, basal Miranda-GFP crescent formation was abolished (Figure 11D) (note that in the previous experiment, only a small area was bleached by point bleaching). This corroborated earlier data showing that the basal crescent is generated by a pre-existing pool of Miranda protein.

It has been suggested that Miranda attaches to a cortical anchor which restricts protein movement within basal areas. To test this hypothesis, FRAP of Miranda-GFP in the basal crescent was analyzed (Figure 11E,F) and compared to its mobility in the cytoplasm (Figure 11A-C,F) and to the cortical mobility of PON-GFP (Figure 11G). The recovery rate of Miranda-GFP at the basal cortex was significantly higher than the recovery of cytoplasmic Miranda-GFP demonstrating that cortical Miranda has a lower mobility and might indeed be anchored at the basal cortex. In contrast, half-time of recovery values of Miranda-GFP ($t_{1/2}$ 6.76 ± 0.66 s) and PON ($t_{1/2}$ 6.78 ± 0.43 s) were almost identical. In addition, following FRAP, Miranda-GFP only filled areas within the existing basal crescent as has been demonstrated

for PON (Lu et al, 1999). These data suggest that both Miranda and PON are attached to probably the same as yet unidentified cortical anchor.

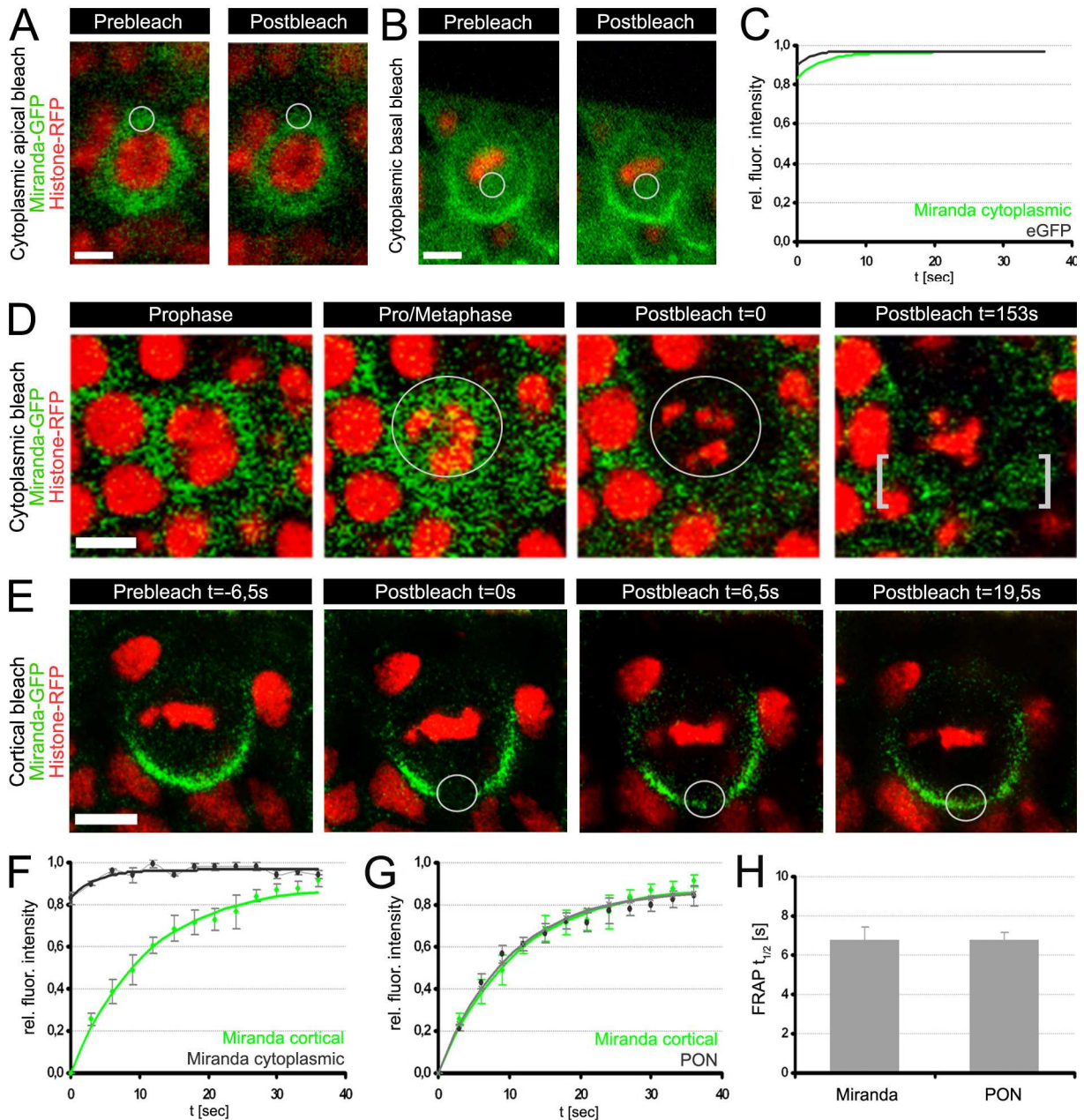


Figure 11: Miranda moves three-dimensionally in the cytoplasm by passive diffusion, but shows a spatially limited and slower movement at the cortex. (A-E) FRAP experiments in living embryos co-expressing Miranda-GFP (green) and Histone-RFP (red). White circles indicate bleached regions. (A,B) Images of prophase neuroblasts before and after bleaching are shown. It was not possible to bleach cytoplasmic Miranda-GFP on the apical (A) or basal (B) side of the cell by using the same parameters used to decrease fluorescence signal from cortical Miranda-GFP (E) indicative of rapid diffusion. (C) Cytoplasmic Miranda-GFP and freely diffusing eGFP showed similar kinetics. (D) The pro/metaphase neuroblast was repeatedly bleached at high laser intensity to remove Miranda-GFP signal from the entire cytoplasm resulting in the absence of a metaphase crescent (white brackets). This suggest that ubiquitously localized Miranda at pro/metaphase was required to form the basal crescent at metaphase. (E) FRAP of Miranda-GFP in the metaphase crescent revealed that cortical Miranda was less motile probably through the interaction with a cortical basal anchor. (F,G,H) Quantification of the recovery rate showed that cortical Miranda moved slower ($t_{1/2}$ 6.76 ± 0.67 s) than did freely diffusing cytoplasmic Miranda ($t_{1/2} < 1.5$ s) but at similar rate to cortical PON-GFP ($t_{1/2}$ 6.78 ± 0.43 s). Scale bars represent 5 μ m.

3.1.5 Myosin II and Myosin VI act at distinctive steps in the same pathway to localize Miranda

Myosin II as well as Myosin VI have been implicated in regulating proper localization of Miranda to a basal crescent (Barros et al, 2003; Petritsch et al, 2003; Peng et al, 2000). The temporal and spatial order of their interaction with Miranda is poorly understood. To address this question Miranda-GFP localization in dividing neuroblast was studied by time lapse confocal imaging in the absence of Myosin II and Myosin VI, respectively.

Miranda localization was monitored after Myosin II activity was impaired by injection of the Rho kinase inhibitor Y-27632 into living embryos expressing Miranda-GFP and Histone-RFP. Consistent with earlier observations, in control embryos injected with buffer only, Miranda-GFP accumulated in the cytoplasm in late prophase before forming a metaphase crescent and was inherited by the GMC in telophase (Figure 12A). However, in the absence of Myosin II activity, the cytoplasmic localization of Miranda, the formation of a basal crescent and the asymmetric segregation of Miranda were completely abolished (Figure 12B). These results are consistent with earlier data showing mislocalization of Miranda around the cortex in mutants lacking the regulatory light chain of Myosin II (spaghetti squash) (Barros et al, 2003) and suggest that Myosin II is required at prophase to translocate Miranda to the cytoplasm.

To study the function of Myosin VI at defined stages of Miranda localization, I downregulated Myosin VI activity by RNAi (Figure 12B). In embryos injected with dsRNA complimentary to Myosin VI (Petritsch et al, 2003), Miranda-GFP was completely mislocalized to the cytoplasm during all phases of neuroblast mitosis, never formed a basal crescent and thus was segregated symmetrically to both daughter cells. Myosin VI has been demonstrated to partially colocalize with Miranda, mainly in the cytoplasm (Petritsch et al, 2003). Together, these data indicate that Myosin VI is essential for cortical localization of cytoplasmic Miranda at pro/metaphase.

Myosin II and Myosin VI may either act sequentially in the same pathway or in parallel pathways at distinct steps to localize Miranda. Analyzing a potential interaction of Myosin II and Myosin VI has been hampered by the overall abnormal morphology of the double mutant for the Myosin VI and the Myosin II heavy chain (Petritsch et al., 2003). As an alternative approach, I injected both the Rho kinase inhibitor to inhibit Myosin II and *myosin VI* dsRNA into live embryos and monitored Miranda movement by time-lapse confocal microscopy. Miranda was uniformly mislocalized to the cortex whereas the cytoplasmic phase was completely eliminated (Figure 12D). Miranda mislocalization in the absence of both myosins closely resembled the localization pattern of Miranda seen in embryos with reduced Myosin II activity alone (Figure 12B) rather than an additive or a Myosin VI loss-of-function phenotype.

Taken together, Myosin II might exclude Miranda from the apical cortex at early prophase. Miranda then translocates to the cytoplasm and diffuses throughout the cell at pro/metaphase. At the basal side of the cell, Miranda becomes restricted to the cortex by a yet unknown mechanism which is indispensable of Myosin VI.

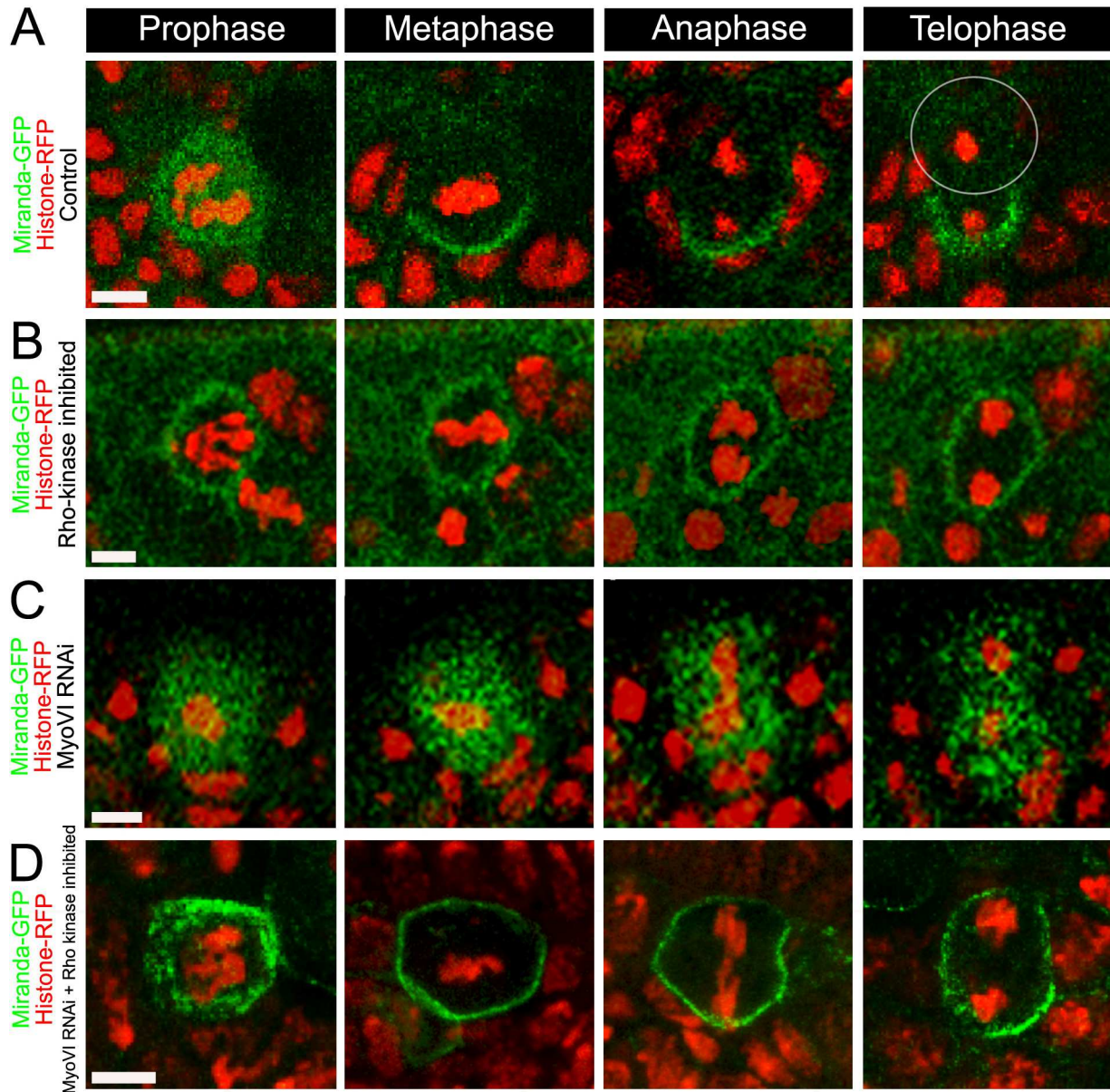


Figure 12: Myosin II and Myosin VI act at distinctive steps in the same pathway to localize Miranda. Live imaging of embryos coexpressing Miranda-GFP (green) and Histone-RFP (red) in control embryos injected with buffer (A), Rho kinase inhibitor to downregulate Myosin II (B), *myosin VI* dsRNA to impair Myosin VI activity (C), or both RKI and *myosin VI* dsRNA (D). In control embryos (A) Miranda protein was cytoplasmic at pro/metaphase, then moved to a basal crescent in metaphase and became asymmetrically inherited by the GMC. (B) In embryos with reduced Myosin II activity, Miranda never accumulated in the cytoplasm at prophase but localized uniformly around the cortex and was therefore symmetrically segregated upon cytokinesis. (C) In contrast, downregulation of Myosin VI by RNAi still allowed Miranda to localize to the cytoplasm at prophase, but prevented formation of the basal crescent at metaphase leading to its symmetric segregation at ana- and telophase. (D) In embryos lacking both Myosin II as well as Myosin VI activity, Miranda localized uniformly around the cortex at prophase, does not form a basal crescent at metaphase and was symmetrically inherited by both daughter cells. The double-mutant phenotype closely resembled the localization pattern of Miranda-GFP observed when Myosin II is inhibited alone (B). Scale bars represent 5 μ m.

3.2 Discussion

Miranda and PON are known to be adaptor proteins for cell fate determinants and indispensable for asymmetric cell division of *Drosophila* neuroblasts (Lu et al, 1998; Shen et al, 1997). Both proteins show dynamic localization, accumulate in a metaphase crescent at the basal side of the cell and are asymmetrically inherited exclusively by the ganglion mother cell. However, here it is shown for the first time that Miranda and PON take different routes to translocate to the basal pole. Whereas Miranda moves dynamically from the apical to the basal side of the cell via the cytoplasm, PON localization occurs exclusively on the cortex.

3.2.1 Miranda is asymmetrically localized by protein movement throughout the cell prior to basal crescent formation

This study showed that the dynamic localization of Miranda is achieved primarily by protein movement rather than by alternative mechanisms such as localized translation of *miranda* mRNA at the basal cortex or localized degradation at areas outside of the metaphase crescent.

To test whether *miranda* mRNA localized to the basal pole prior to Miranda crescent formation and might contribute to its local translation, I performed in situ hybridizations to study the localization of *miranda* mRNA (Figure 6). Both Miranda protein and *miranda* mRNA were apically localized in prophase and partially overlapped. Miranda protein later translocated to the basal pole of the cell and accumulated in a basal crescent before being inherited by the GMC. In contrast, *miranda* mRNA remained apically concentrated throughout the entire cell cycle and thus was inherited exclusively by the neuroblast daughter. Together, *miranda* mRNA localized exclusively to Miranda protein at metaphase and although I can not exclude that undetectable amounts of mRNA are translated at the basal cortex, I propose that they do not significantly contribute to Miranda protein localization. It has been shown earlier that *prospero* mRNA is localized to the basal side due to its association with the Miranda/Staufen complex which is supposed to serve as a back-up pool for Prospero in the GMC (Broadus & Doe, 1998). In contrast, *inscuteable* mRNA becomes apically localized in neuroblasts (Hughes et al, 2004) and supports the stability of the apical protein complex with Pins, Gai and Par proteins. Thus, it will be interesting in the future to determine whether asymmetric *miranda* mRNA localization has similar functions in the neuroblast daughter.

Next, I investigated the importance of the proteasome and localized degradation of Miranda for its localization to the apical cortex. I initially quantified Miranda localization in embryos with impaired proteasome activity due to mutations in the β 2 proteasome subunit gene

(Schweisguth, 1999) and found Miranda to be normally localized. However, cyclin A degradation and progression from metaphase to anaphase as well was unaffected in DTS5 mutants (data not shown) and thus it was not clear whether proteasome activity was indeed impaired at this stage of development. Therefore, I turned to chemical inhibition of the proteasome by short-term treatment with MG132. Cyclin A is necessary for progression through S-phase of the cell cycle and becomes rapidly degraded by the proteasome in metaphase (Tio et al, 2001; Sigrist et al, 1995). Short-term inhibition of embryos with MG132 led to the persistence of cyclin A in metaphase neuroblasts and a metaphase arrest indicative of an efficient inhibition of the proteasome. However, Miranda protein localization to the basal cortex was not disrupted (Figure 7). In a recent study, MARCM clones for *Tbp-1*, a gene encoding a regulatory subunit of the proteasome, showed mislocalization of Miranda in larval neuroblasts (Slack et al, 2007). However, the authors proposed rather an indirect role of the proteasome in Miranda localization as the Miranda protein is only mono- but not polyubiquitinated, which would be a prerequisite for proteasome-dependent proteolysis.

Together, I conclude that neither the translation of *miranda* mRNA at the basal cortex nor localized Miranda protein degradation leads to the formation of a basal crescent.

Live imaging experiments revealed that Miranda-GFP mainly localized to the cytoplasm and the cortex at prophase and accumulated in the cytoplasm at pro/metaphase (Figure 5). Cytoplasmic localization of Miranda in neuroblasts could have a general relevance: In *C. elegans*, the conserved Par proteins direct a polarized cytoplasmic flow to move P granules to the posterior cortex of the zygote (Cheeks et al, 2004). Thus, similar to the *C. elegans* zygotes, *Drosophila* neuroblasts employ a Par protein-dependent cytoplasmic movement to drive the Miranda complex to the basal pole.

However, to rule out that ubiquitous localization and cytoplasmic accumulation of Miranda was not an overexpression artefact caused by saturation of the localization machinery, several control experiments were performed. Miranda-GFP showed very similar localization patterns when expressed under the control of additional Gal-4 driver lines of different strengths (Figure 8A,B,C). Moreover, I found cytoplasmic Miranda in immunostainings and a comparison between Miranda-GFP and total Miranda protein by immunohistochemistry revealed that Miranda-GFP indeed reflects the localization of wild type protein (Figure 8D,F,G). In contrast, in *Lgl*^{3A} mutants, expressing an unphosphorylatable form of Lgl, Miranda-GFP is found uniformly around the cortex and cytoplasmic localization of Miranda-GFP is abolished (Figure 8E). Finally, immunoblotting revealed that Miranda-GFP is expressed at lower levels as endogenous Miranda (Figure 8H). Taken together, these data suggest that Miranda-GFP faithfully recapitulates the localization and function of endogenous Miranda protein in live embryos.

3.2.2 Adaptor proteins take different routes to the basal cortex

Miranda and PON have been demonstrated to interact *in vitro* (Shen et al, 1997) and both accumulate in a metaphase crescent in dividing neuroblasts suggesting that they exist in only one complex and might be recruited to the basal side by the same mechanism. However, asymmetric localization of Miranda in *numb* mutants is indistinguishable from that in wild-type embryos (Shen et al, 1997) and localization of Numb is not affected in Miranda mutants (Ikeshima-Kataoka et al, 1997). Both findings suggest that the interaction of Miranda and Numb is more likely transient and restricted to their colocalization in the metaphase crescent.

Moreover, in agreement with earlier data, PON mainly moves two-dimensionally along the cortex to become restricted to a basal metaphase crescent in embryonic neuroblasts (Figure 9B, Figure 10A) (Lu et al, 1999). In contrast to Miranda-GFP, an accumulation of PON-GFP was never found in the cytoplasm at pro/metaphase.

Myosin II and Myosin VI are both required for asymmetric localization of Miranda (Petritsch et al, 2003). In contrast, PON localization only depends on Myosin II but not on Myosin VI. In embryos with reduced Myosin II activity due to treatment with Rho kinase inhibitor, PON-GFP did not form a basal crescent in metaphase but was mislocalized to the entire cortex and accumulated at the cleavage furrow in telophase (Figure 10B). This suggests that similar to Miranda, PON localization requires fully functional Myosin II. However, downregulation of Myosin VI by RNA interference did not affect crescent formation at metaphase or the asymmetric segregation of PON-GFP at ana- and telophase.

The distinct localization modes of Miranda and PON might reflect their association with different cargo molecules and their intracellular localization. Miranda is required for the localization of transcriptional and translational regulators, such as Prospero and Brat, which presumably act in the cytoplasm and the nucleus. PON, on the other hand, is an adaptor protein for Numb, a negative regulator of the Notch receptor that is primarily localized to the membrane or to cortical actin.

Both PON and Miranda accumulate in a metaphase crescent and as suggested by FRAP analysis, their interaction with the basal cortex appears to be similar. Both proteins associate dynamically with the cortex, as indicated by their relatively short half-time of recovery after photo-bleaching, but are retained within the limits of the basal cortical crescent (Figure 11F-H). These data provide evidence for the presence of a common anchor protein that retains both PON and Miranda at the basal cortex. In a recent study, FRAP analysis of GFP-PON in sensory organ precursors of *Drosophila* pupae suggested that there might be a constant exchange between cortical and cytoplasmic PON (Mayer et al, 2005) further supporting the hypothesis of a cortical anchor.

Taken together, differences have been evidently identified in the localization machinery and the route for the adaptor proteins Miranda and PON in *Drosophila* neuroblasts. Myosin II is required for the asymmetric segregation of both Miranda and PON, whereas Myosin VI seems not to be necessary for PON localization. In addition, the different localization pattern of Miranda and PON strongly support the hypothesis of two differentially regulated basal protein complexes. Further analyses studying the localization of their cargo proteins, such as Prospero and Numb, will be needed to elucidate whether PON and Miranda indeed form two independently localized protein complexes.

3.2.3 Myosin II and Myosin VI interact in one pathway to shuttle Miranda between cortex and cytoplasm

Previous studies reported that Miranda becomes apically enriched at interphase or at prophase and demonstrated a physical interaction of Miranda with Inscuteable, a component of the apical complex (Shen et al, 1998). It was therefore speculated that, after binding to its cargo molecules Prospero and Staufen at the apical cortex, Miranda receives a signal, which triggers the Miranda complex to move towards the basal pole of the neuroblast. Recent data showed that Myosin II is required to exclude Miranda from the apical cortex (Barros et al, 2003; Petritsch et al, 2003) and that Miranda forms a complex with Myosin II in embryonic protein extracts (Petritsch et al, 2003). This might reflect the interaction of the two proteins in interphase and early prophase since at later stages they localize almost exclusively (Barros et al, 2003). At the transition between interphase to prophase, aPKC is recruited to the apical complex (Figure 5) and phosphorylates Lgl, which allows for the activation of Myosin II (Betschinger et al, 2005; Barros et al, 2003) and consequently, the exclusion of Miranda from the cortex. Moreover, the successful integration of Miranda to the basal crescent is dependent on Myosin VI at a subsequent step (Petritsch et al, 2003).

Live imaging experiments in the absence of Myosin II and Myosin VI, respectively, enabled me to elucidate the individual role of each myosin in the apical-to-basal localization of Miranda during neuroblast mitosis. Chemical inhibition of Myosin II by injection of Rho kinase inhibitor into live embryos resulted in the mislocalization of Miranda-GFP uniformly around the cortex (Figure 12B) and the cytoplasmic phase observed in control embryos (Figure 12A) was completely absent. This suggests that Myosin II is required in interphase to restrict Miranda to the apical side of the cell and excludes it from the baso-lateral cortex but also later in prophase to release it to the cytoplasm (Figure 12). Results from live imaging experiments extended earlier data in fixed embryonic tissue demonstrating Miranda mislocalization around the cortex in embryos with impaired Myosin II activity (Barros et al, 2003).

Miranda diffuses rapidly throughout the cytoplasm and in line with earlier data (Petritsch et al., 2003), live imaging analysis demonstrated that Myosin VI is essential for integration of cytoplasmically localized Miranda into the basal crescent at metaphase. Downregulation of Myosin VI by RNAi still allows Miranda to be released to the cytoplasm at prophase, but prevents formation of the basal crescent (Figure 12C). In *Drosophila* neuroblasts, Myosin VI is localized to particles mainly to the cytoplasm which accumulate in the basal half of the metaphase neuroblast coinciding in time and space with basal localization of Miranda (Petritsch et al, 2003). Thus, it would be possible that Myosin VI binds to Miranda in the basal half of the cell and transports it in a short-range to the basal cortex or, alternatively, restricts Miranda in the basal half of the cell to present it to an additional motor protein. However, FRAP analysis of Miranda-GFP suggested that Miranda is diffusing throughout the cytoplasm rather than being actively transported by a myosin motor (Figure 11). Intriguingly, Myosin VI is not only capable to function as a processive motor but also as an anchor *in vitro* (Sweeney & Houdusse, 2007). Consequently, an alternative role of Myosin VI might be to retain the diffusing Miranda and its cargo at the basal side of the cell to facilitate the delivery of the protein complex to a so far unknown anchor. However, currently it cannot be distinguished between these possibilities and it will be necessary in future experiments to study in more detail the interaction of Miranda and Myosin VI by mapping binding domains and determining local and spatial binding affinities between the two molecules probably by fluorescent resonance energy transfer experiments (FRET).

Inhibition of Myosin II as well as Myosin VI activity resulted in Miranda mislocalization uniformly around the cortex at prophase, a lack of basal crescent formation at metaphase and thus symmetrical inheritance of Miranda by both daughter cells. In addition, the cytoplasmic phase of Miranda-GFP was never observed. Evidently, this double-mutant phenotype closely resembles the localization pattern of Miranda-GFP after Myosin II inhibition. These results clearly demonstrate that Myosin II and Myosin VI act at consecutive steps in a single pathway to localize Miranda basally.

3.2.4 A model for Miranda localization

On the basis of the results presented above, I propose the following model how asymmetric localization of Miranda is established in *Drosophila* neuroblasts:

In interphase, aPKC is absent from the apical complex and inactive Myosin II can interact with Miranda which thereby becomes enriched at the apical side of the cell (Figure 13A) and assembles in a complex with its cargo molecules Staufen, Prospero and Brat (not shown). In contrast, PON is ubiquitously cytoplasmic during interphase. In early prophase, Miranda is excluded from the apical cortex due to the formation of Myosin II microfilaments following

phosphorylation of Lgl by aPKC and the subsequent activation of Myosin II. At the same time, PON is recruited to the cortex (Figure 13B). In the cytoplasm, the Miranda complex diffuses three-dimensionally throughout the cell and becomes restricted in the basal half of the metaphase neuroblast by Myosin VI (Figure 13C). By a currently unknown mechanism, Myosin VI either directly transports Miranda to the basal cortex or retains cytoplasmic Miranda to facilitate its interaction with a basal cortical anchor. PON localization occurs mainly over the cortex and PON is pushed into the basal half of the cell by the action of Myosin II to form a metaphase crescent.

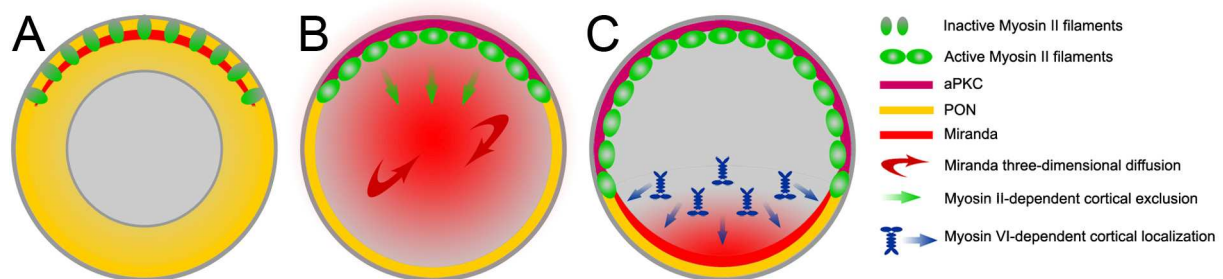


Figure 13: A model for Miranda localization by Myosin II and Myosin VI. (A) Inactive Myosin II forms a crescent during late interphase (individual green ovals) because aPKC is absent and cannot phosphorylate and inactivate Lgl (not shown). Myosin II binds to Miranda (red crescent) and becomes apically enriched whereas PON is still cytoplasmic (yellow area). (B) Very early at prophase, aPKC localizes to the apical side of the cell (purple crescent) and phosphorylates Lgl (not shown) which results in the activation of Myosin II and the formation of microfilaments (connected green ovals). Consequently, Miranda is excluded from the apical cortex and released to diffuse rapidly throughout the entire cytoplasm including the nucleus after nuclear envelope breakdown at pro/metaphase (red area). At that time, PON is recruited to the cortex (yellow circle). (C) Myosin VI (blue) in the basal half of the cell binds to Miranda to either anchor it or to deliver Miranda by short-range transport to a cortical anchor at the basal crescent. By the action of Myosin II PON is 'pushed' along the cortex to form a basal crescent.

While many asymmetrically localized cell fate determinants such as Numb, Prospero and Staufen share mammalian homologues, mammalian proteins resembling Miranda or PON have yet to be found in neural stem cells of the mammalian brain. However, the high degree of conservation and the presence of asymmetric stem cell division suggest that functional homologues might exist and that they are probably localized by similar mechanisms.

4 Thesis Part 2 - The origin of brain cancer stem cells

4.1 Results

Oligodendrogliomas are primary glial brain tumors and are believed to originate from oligodendrocytes or from a glial precursor (Marie et al, 2001).

Here I study the presence of putative cancer stem cells (CSCs) in a transgenic mouse model of oligodendroglioma. Mice expressing an oncogenic version of the EGFR (*verbB*) from the S100 β promoter in neural stem cells and their progeny and lacking both copies of the tumor suppressor p53 develop high grade oligodendroglioma reflecting the pathology of the human disorder (Weiss et al, 2003).

4.1.1 Isolation and characterization of cancer stem cells from high grade oligodendroglioma

Acute isolation of neural stem cells (NSCs) has been difficult as there is no specific marker available to identify adult neural stem cells. Currently, they can be enriched in neurosphere cultures and identified retrospectively. CD133, a hematopoietic stem cell marker, has been proven useful to identify human NSC (Uchida et al, 2001) but also for tumor stem cells from human glioma (Singh et al, 2004). Therefore, I was hoping that prominin-1, the mouse homolog of CD133 could be used to directly isolate stem-like cells from oligodendroglioma. However, antibodies for prominin-1 available at the begin of this study did neither show immunoreactivity with neural stem cells located in the subventricular zone (SVZ) of adult mice nor neurosphere cultures (data not shown) and as a consequence were not valuable for the selection of neural stem cells.

Potential cancer stem cells were isolated from tumor bearing S100 β -*verbB*, p53^{-/-} mice at 8 weeks postnatally. Due to a lack of a specific marker for CSCs in mouse oligodendroglioma I enriched for these cells by culturing them under specific growth conditions. Animals were sacrificed and the tumor mass was dissected out taking care not to include stem cell enriched regions like the SVZ. Enzymatically dissociated tumor cells were seeded in Neurobasal medium supplemented with B27, EGF and bFGF (complete medium) allowing for amplification and maintenance of neural stem cells (Doetsch et al, 1999) and selecting against differentiating/differentiated cells. Under these conditions, tumor derived cells formed free floating clusters within one to two weeks resembling classical neurospheres formed *in vitro* by neural stem cells (Figure 15A). As these spheres originated from tumor cells, they were referred to as tumorspheres.

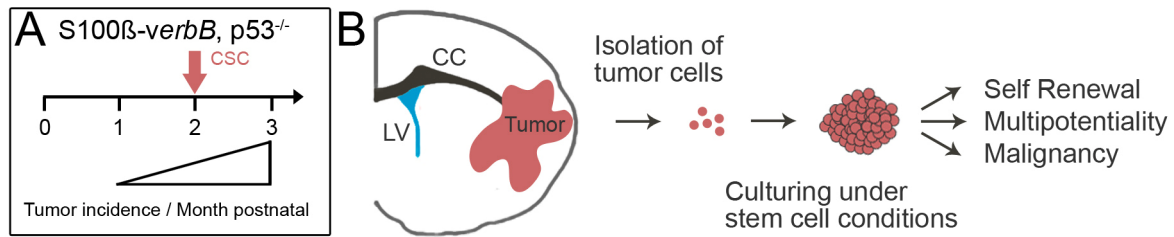


Figure 14: Isolation of cancer stem cells from oligodendroglioma. (A) Illustration of the progression pathway of transgenic *S100β-verbB*, *p53*^{-/-} mice. (B) Schematic representation of an adult mouse brain hemisphere showing a large tumor mass from which tumor cells were isolated and cultured under stem cell conditions. Stem-like properties such as self-renewal capacity, multipotentiality and malignant potential were assessed from tumor-derived cells (B). CC, corpus callosum; LV, lateral ventricle.

However, the sole formation of tumorspheres does not completely prove the presence of cancer stem cells therein. Transit amplifying cells are also known to produce neurospheres in this system and they can even undergo a limited number of passages in culture (Doetsch et al, 2002). Hence I determined whether the cells in primary tumorsphere culture were generated by short-time proliferating, transit amplifying cells or possessed the expected properties of cultured neural cancer stem cells.

To this end, I first assessed their capacity for long-term proliferation, self-renewal, multipotentiality (defined as the ability to generate the three major neural cell types, i.e., neurons, astrocytes and oligodendrocytes) and their tumorigenicity.

4.1.2 Tumor-derived cells undergo self-renewal and are multipotential

Tumorspheres from a primary culture were dissociated into single cells, whereupon a small percentage of these cells generated secondary spheres. CSCs could be serially passaged over a long period of time (> 6 months) with no obvious change of their proliferative properties indicative of their potential for unlimited self-renewal.

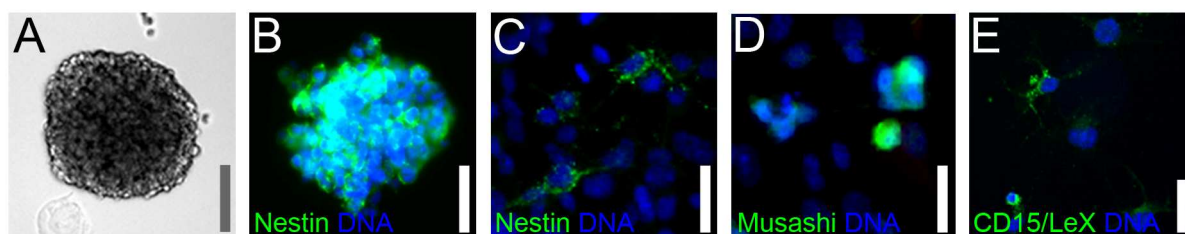


Figure 15: Tumor-derived cells undergo self-renewal and express stem cell and early progenitor markers. (A) Phase contrast image of a tumorsphere cultured from an oligodendroglioma of a *S100β-verbB*, *p53*^{-/-} transgenic mouse. Immunofluorescence images of Nestin protein in cryomicrodissected tumorspheres (B) and primary tumor sections (C). Expression of the neural stem cell marker Musashi (D) and CD15/LeX (E) was determined in tumor-derived cells. DAPI counterstained nuclei are in blue (B-E). Scale bars in (A) 200 μm, in (B) 100 μm, in (C-E) 20 μm.

Next, I tested whether tumor-derived cells expressed markers of neural stem cells. Nestin is an intermediate filament protein expressed in many cells during development, although its expression is often transient and does not persist into adulthood. Maybe the most prominent example of Nestin expression in adult organisms are neural precursors of the subventricular zone (SVZ) (Lendahl et al, 1990). Upon differentiation, Nestin becomes downregulated and replaced by cell-type-specific intermediate filaments like neurofilaments and glial fibrillary acidic protein during neuro- and gliogenesis (Steinert et al, 1999; Dahlstrand et al, 1992). Interestingly, Nestin expression is often reinduced in adulthood during pathological situations, such as in various central nervous system tumors (Rani et al, 2006). Therefore, immunofluorescence stainings were used to detect Nestin-positive neural progenitors in oligodendroglioma and tumor derived cells. Undifferentiated tumorspheres in proliferating medium contained many cells expressing Nestin (Figure 15B). Furthermore, immunohistochemistry on tumor cryostat sections identified a few Nestin positive stem-like precursors in primary oligodendroglioma (Figure 15C). To test for additional markers of neural stem cells, tumorspheres grown in complete medium were enzymatically dissociated, cells spun down on poly-L-lysine coated microscope slides using a cytopspin apparatus (StatSpin CytoFuge2), fixed and subjected to immunocytochemistry. I found high levels of Musashi-1 (Figure 15D), another putative marker of neural stem cells (Sakakibara et al, 2002) and in addition, CD15/LeX, a marker for self-renewing stem cells/transit amplifying cells (Figure 15E) (Capela & Temple, 2002) could be detected. In contrast, under proliferative conditions, tumorspheres contained relatively few cells expressing the neuronal marker β -III-tubulin and the astrocyte marker GFAP (data not shown).

Multipotentiality is defined as the ability of stem cells to differentiate into various cell types. To determine if the cells which gave rise to tumorspheres were in fact multipotential, single tumorspheres were dissociated and plated under adherent conditions in the presence of 1% fetal calf serum and without growth factors (differentiation medium). After 7 days *in vitro*, cultures were processed for immunocytochemistry to detect neuronal and glial cell types. As expected, tumor derived progenitor cells differentiated into neurons, astrocytes and oligodendrocytes indicated by their expression of β -III-Tubulin, GFAP and O4 (Figure 16), respectively, suggesting that they are multipotential. Such multipotentiality was maintained unaltered even after extensive culturing.

Together, these results indicate that oligodendroglioma contain a small subset of progenitor cells with the capability to proliferate and differentiate in a stem-like fashion. Furthermore, tumor derived progenitor cells express characteristic markers for neural stem cells like Nestin, Musashi-1 and CD15/LeX.

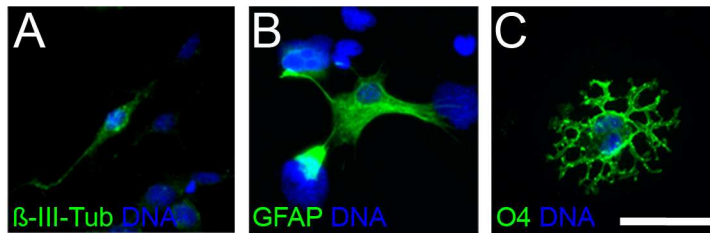


Figure 16: Oligodendrogloma derived stem cells are multipotential. Upon withdrawal of growth factors cancer stem cells differentiate into β -III-tubulin positive neurons (A), GFAP positive astrocytes (B) and O4 positive oligodendrocytes (C). Scale bar represents 30 μ m.

4.1.3 Oligodendrogloma derived cancer stem cells are tumorigenic

Cancer stem cells are rare cells within a tumor which give rise to the diverse tumor cell population to drive tumorigenesis. To determine their malignant potential I intracranially (i.e. under the skull into underlying brain tissue) injected oligodendrogloma derived progenitor cells into the right hemisphere of FvB/N wild type mice. When injected orthotopically (i.e. grafting of tissue or cells in their natural position), as little as 1×10^4 cells reproducibly established large tumors. Transplantation experiments were done with 3 independent tumorsphere lines and 6 animals per group. Usually, mice showed severe neurological symptoms (cycling and/or partially paralyzed animals) within days after the injection and animals developed massive tumors within weeks in the forebrain close to the injection site. In contrast, even at higher cell numbers (1×10^6) normal neural stem cells isolated from the subventricular zone of wild type mice injected as control never developed tumors (n=15) (Figure 17).

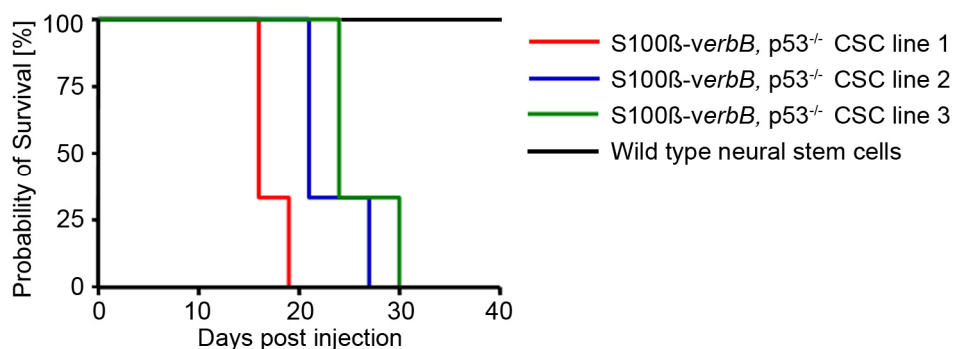


Figure 17: Oligodendrogloma derived stem cells are tumorigenic. After intracranial injection of cancer stem cells into FvB/N mice (1×10^4 cells) orthotopic tumors consistently formed within 3 to 4 weeks indicating their malignancy. Survival of animals (n=6 per group) challenged with independent CSC lines is shown. Normal stem cells from the subventricular zone of wild type mice were injected as controls and never developed tumors.

Brains of symptomatic mice were isolated, fixed and paraffin embedded followed by immunohistochemistry and hematoxylin and eosin staining (H&E, a popular staining method in histology and the most widely used stain in medical diagnosis to identify cancers). Infiltration of human glioma is a key feature that contributes to their poor prognosis and therapeutic response. Remarkably, both spontaneous (Figure 18A-C) and orthotopic murine tumors (Figure 18D-F) were infiltrative evidenced by their easily recognized nuclei invading the surrounding brain tissue. Furthermore, histopathologic analysis of orthotopic tumors demonstrated additional oligodendroglioma-like features such as (1) high cellularity, (2) high mitotic index, (3) subpial infiltration (Figure 18A) and (4) the characteristic “fried egg” appearance of cells due to a clear and swollen cytoplasm forming a perinuclear halo (Figure 18C,F). Occasionally, tumors showed rhythmic palisading of cells (Figure 18E). Intriguingly, the orthotopic tumor (Figure 18D-F). histologically resembled the parental tumor (Figure 18A-C). H&E stainings were analyzed by Dr. Scott Vandenberg from the Neuropathology core at UCSF who confirmed the presence of high grade oligodendroglioma (WHO grade II/III).

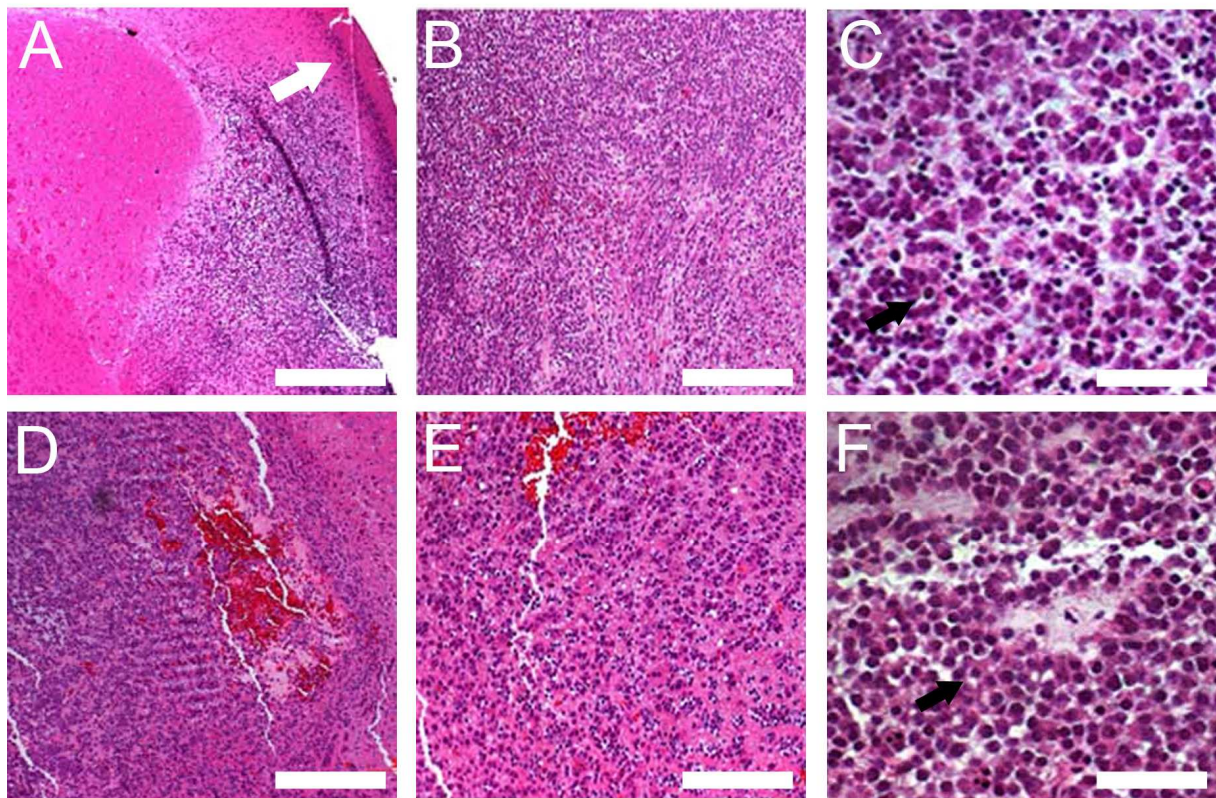


Figure 18: Orthotopic tumors are high grade oligodendroglioma. H&E stained sections of a representative spontaneous oligodendroglioma (A-C) and an orthotopic tumor derived from *S100 β -*verbB*, *p53*^{-/-} cancer stem cells (D-F) after formalin fixation and paraffin embedding. Histopathologic features are characteristic for high grade oligodendroglioma as indicated by a high cellularity, high mitotic index, diffuse invasion, subpial infiltration (arrow in A) and the characteristic “fried egg” appearance of cells, i.e. empty zones around the cell nuclei (black arrows in C, F). Orthotopic tumors showing rhythmic palisading of nuclei, a pattern typical for human oligodendroglioma (E). Scale bars in (A,D) 600 μ m, in (B,E) 300 μ m, in (C,F) 100 μ m.*

To conclusively demonstrate the stemness of oligodendrogloma derived cancer stem cells, I performed sequential transplantation experiments (Figure 19). This was done in analogy to the classical repopulation experiment used to identify true hematopoietic stem cells (Bock et al, 1999). Cultured tumor derived progenitor cells (primary cancer stem cells) were transplanted into FvB/N mice to establish a tumor. At the first sign of neurological impairment animals were sacrificed and the tumor mass was dissected out taking care not to include stem cell enriched regions like the SVZ. The tumor cells were then enzymatically dissociated and cultured under conditions identical to those used to establish tumor stem cell lines from the original oligodendrogloma. This resulted in the establishment of secondary cancer stem cell lines which were intracranially injected into new recipients again developing brain tumors. As before, cancer stem cells were isolated and re-cultured (tertiary cancer stem cells) followed by transplantation into new recipients. CSCs from orthotopic tumors were sequentially transplanted for 4 passages demonstrating their malignant potential and *in vivo* self renewing potential (Figure 20).

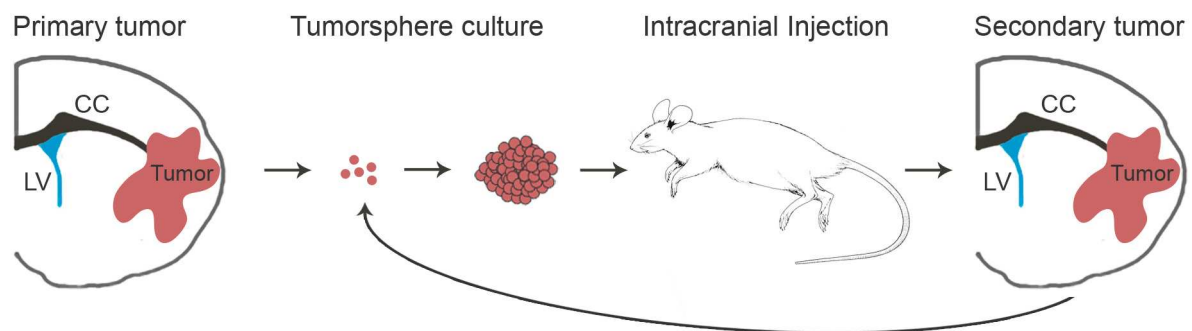


Figure 19: Evaluation of the tumorigenicity of oligodendrogloma derived stem cells. Tumorigenicity was determined by injecting oligodendrogloma-derived neural stem cells in the forebrain of FvB/N mice. Secondary cancer stem cells were isolated and re-cultured from orthotopic tumors and transplanted into new recipients. CSCs were successfully transplanted for several passages demonstrating their malignancy and *in vivo* self-renewing potential.

It is noteworthy that tumors developed even faster (within 2 weeks; Figure 20) with CSCs isolated from tumors of later passages suggesting that these cells became more aggressive maybe due to accumulation of additional mutations during culturing and serial implantation. In addition, particularly aggressive cells could have been selected upon transplantation, tumor growth and culturing. Notably, CSCs from orthotopic tumors cultured under same conditions as their parental cell line retained their self-renewing capacity and multipotentiality after transplantation and re-culturing (data not shown). Together, the successful serial development of oligodendrogloma-like tumors provided evidence that I have indeed isolated cancer stem cells.

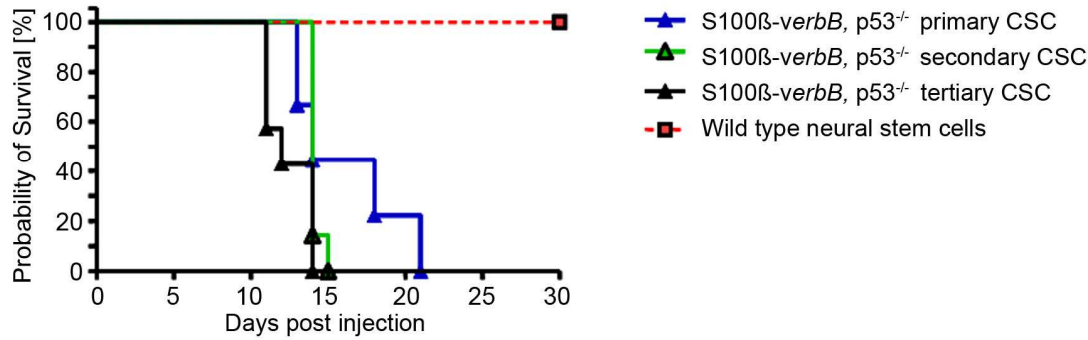


Figure 20: Survival upon sequential intracranial injection of tumor derived stem cells. Animals challenged with cancer stem cells isolated from a parental tumor usually died within 3 weeks (blue line). Secondary tumorspheres were re-cultured from these orthotopic tumors and transplanted into new recipients. Note that tumor formation occurs much faster with cells from the secondary (green line) or tertiary tumor (black line). Normal stem cells from the subventricular zone of wild type mice were injected as controls and never developed tumors.

4.1.4 Spontaneous and orthotopic tumors show similar marker expression

Oligodendroglioma in S100 β -*verbB*, p53^{-/-} transgenic mice mainly consist of oligodendrocyte progenitors marked by the expression of NG2 and Olig2. Thus, I next tested whether CSCs generate orthotopic tumors which resembled the cellular composition of the primary tumor.

Evidently, immunohistochemical analysis have shown that the majority of cells within the tumor are highly positive for the early oligodendrocyte markers NG2 and Olig2 (Figure 21A,B). These cells displayed a round shape without any extensions or branches, a morphology indicative of progenitors rather than mature oligodendrocytes. Importantly, although forming huge and relatively defined tumor masses around the injection site, cells are clearly infiltrating neighboring tissue at the border of the tumor.

Similar to human oligodendroglioma and the parental tumor, the number of astrocytes labeled by GFAP was very low within the tumor (Figure 21C) whereas large quantities of astrocytes were present in the surrounding normal brain tissue. Moreover, hardly any neurons could be detected in orthotopic tumors (Figure 21D).

As shown in Figure 15E, tumors also contain a small number of Nestin-positive stem like precursors and cells within the tumor are highly proliferative as indicated by the expression of phospho-histone-3 (PH3), a marker for mitotic cells (Figure 21F).

In conclusion, tumor-derived progenitor cells satisfy all of the critical criteria to be defined as multipotential neural stem cells, both *in vitro* and *in vivo*. In addition, after orthotopic injections, they generate tumors mimicking the cellular composition and histology of the parental tumor. This is the first demonstration that high grade oligodendroglioma contain tumor-initiating cells with stem-like features or in other words, cancer stem cells.

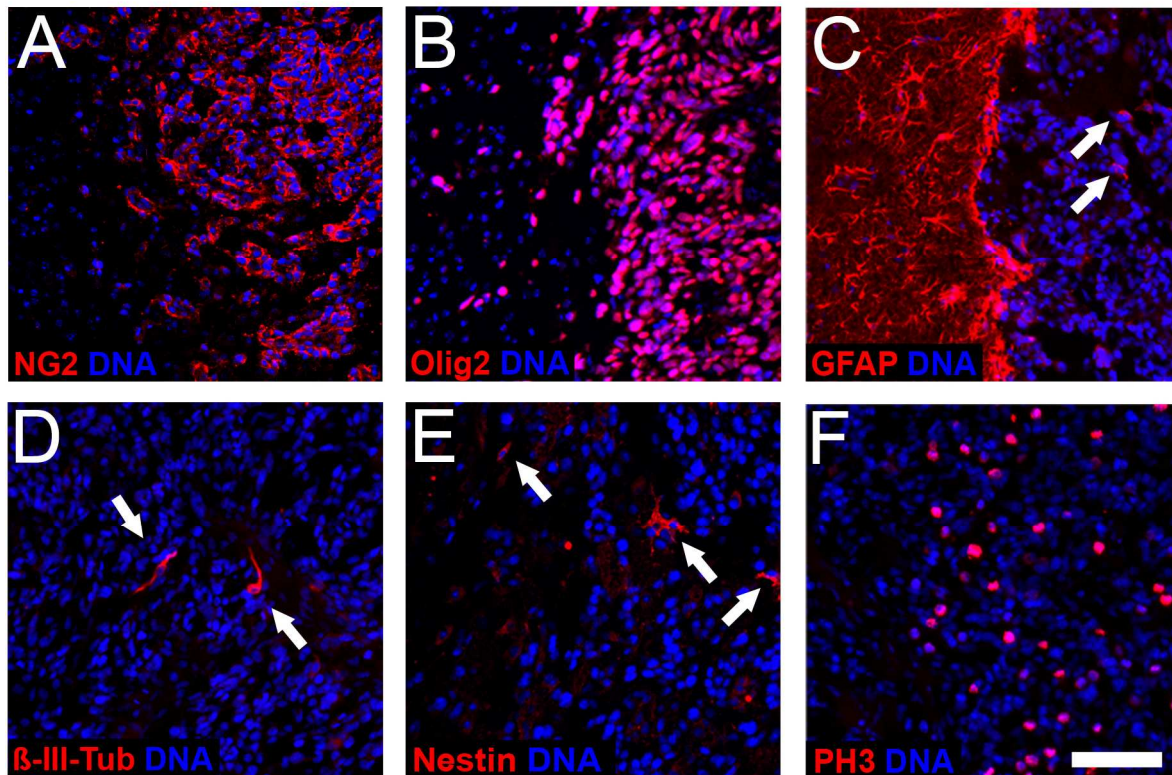


Figure 21: Orthotopic tumors recapitulate characteristics of the parental tumor. Immunohistochemical characteristics of orthotopic tumor samples. Images shown are located at the tumor border (except β -III-tubulin staining in (D)). Normal brain tissue adjacent to the tumor is always on the left hand side. Tumors mainly consisted of oligodendrocyte progenitors as shown by the high expression of NG2 (A) and Olig2 (B). In contrast, the number of GFAP positive astrocytes was very low (see arrows in (C)). Note that the GFAP immunoreactivity was confined outside the tumor mass (C). Only a few β -III-tubulin positive neurons could be detected within the tumor mass (D). Nestin positive stem cell-like tumor cells were present in orthotopic tumors (E). Tumors displayed intense mitotic activity as shown by the expression of PH3 (F). Scale bar represents 100 μ m.

4.1.5 Isolation and characterization of premalignant stem cells from *S100 β -verbB*, *p53*^{+/-} mice

The cancer stem cell hypothesis claims that pathological adult stem cells give rise to a heterogeneous tumor and maintain it by aberrant differentiation and proliferation. My data clearly demonstrate that oligodendroglioma contain a rare population of cells with stem-like features that can reconstitute a new tumor with all cell types represented in the tumor of origin upon serial transplantation. However, it remains to be determined how these CSCs are generated and whether they arise from a mutated stem cell, or a downstream progenitor or differentiated cell that has regained stem cell-like properties because of genetic alterations. I propose that cancer stem cells are generated from defective adult neural stem cells evading normal cell cycle control and differentiation. Over time the accumulation of additional mutations will lead to the formation of an aberrant pool of cancer stem cells which are capable to generate tumor cells. Transgenic *S100 β -verbB* *p53*^{-/-} mice consistently died of

high-grade oligodendroglioma by 2 month providing an excellent model of tumor formation. However, it is less suitable to examine the events which cause the potential progression of normal adult stem cells to cancer stem cells.

In contrast, in *S100 β -verbB* mice heterozygous for p53, tumors developed with a significant delay of 4-6 months. Thus, the *S100 β -verbB* p53^{+/-} model provided an unique opportunity to study stepwise changes leading to the generation of cancer stem cells.

Postembryonic or adult stem cells reside in distinct areas of the brain such as the subventricular zone (SVZ) of the lateral ventricle and are contributing to tissue repair, growth and maintenance (Alvarez-Buylla & Temple, 1998; Lois & Alvarez-Buylla, 1994). In order to determine whether defective stem cells might indeed drive tumorigenesis, I next focused on stem cells from transgenic mice at earlier stages before tumor development and compared typical stem cell properties with them of normal stem cells from wild-type animals. Particularly, changes in proliferation, self-renewing, differentiation and asymmetric cell division were assessed. Already identifying differences at this point would strongly support the idea that normal stem cells progressively develop towards cancer stem cells.

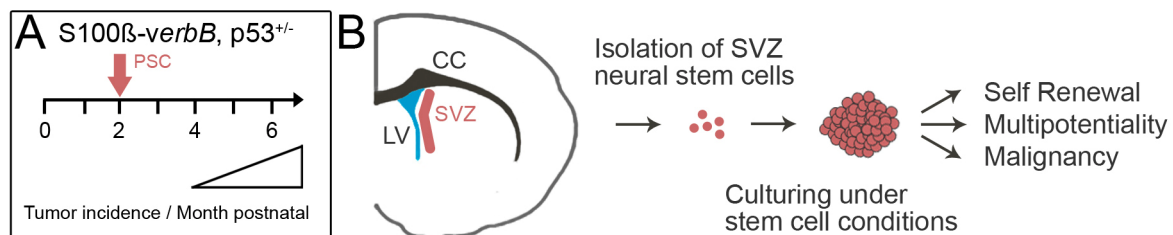


Figure 22: Isolation of premalignant stem cells from tumor prone mice. (A) Illustration of the progression pathway of transgenic *S100 β -verbB*, p53^{+/-} mice. (B) Schematic representation of an adult mouse brain hemisphere showing the subventricular zone (SVZ), a region enriched for neural stem cells. Neural stem cells were isolated from the SVZ of tumor prone mice prior to tumor formation (pre-malignant stem cells). Then, stem-cell properties such as self-renewal capacity, multipotentiality and malignant potential were determined. CC, corpus callosum; LV, lateral ventricle; SVZ, subventricular zone.

Neural stem cells were isolated from the subventricular zone of tumor prone *S100 β -verbB*, p53^{+/-} mice prior to tumor occurrence at 2 months postnatal, which were referred to as pre-malignant stem cells (PSCs). The SVZ was dissected from brain sections, tissues enzymatically dissociated and stem cells were isolated and cultured as described above. Cultures of neural stem cells derived from age-matched wild-type mice and littermates either overexpressing *verbB* alone or mice hetero- or homozygous for p53 only were established as controls.

4.1.6 Stem cells isolated from premalignant *S100 β -verbB*, *p53*^{+/-} mice and from *S100 β -verbB*, *p53*^{-/-} tumorspheres show self-renewal defects

The epidermal growth factor receptor (EGFR) is involved in neural development and regulates proliferation and self-renewing capacities of adult neural stem cells. Moreover, EGFR amplification is observed at high frequency in a variety of brain tumors like glioblastoma multiforme (GBM) or oligodendroglioma (Sibilia et al, 2007). Tumor formation in a mouse model for oligodendroglioma is in part due to upregulation of EGFR thus providing the opportunity to study the direct impact of EGFR on self-renewing properties of adult stem cells.

To investigate whether deregulation of EGFR influences the self-renewing capacity of transgenic stem cells, I performed so called sphere-forming assays and quantified secondary neurosphere formation.

Normal stem cells from wild type mice (NSCs), premalignant (PSCs) as well as cancer stem cells (CSCs) formed neurospheres (Figure 23A-C) which could be passaged over many generations indicating that they have extensive self-renewing capacity. However, when I plated the same amount of cells from either cell line in complete medium, the number of secondary spheres was higher in PSCs and CSCs compared to wild type controls. The number of sphere-forming cells directly correlates with the number of self-renewing cells, i.e. the number of stem cells and transit amplifying cells. It is noteworthy, however, that I could not make a difference between these cells based on the sphere forming assay. Anyway, an overall increase of self-renewing cells in the PSCs ($17.7 \pm 6.5\%$) and CSCs ($25.2 \pm 12.6\%$) could be detected compared to NSCs ($13.8 \pm 7.5\%$) (Figure 23E).

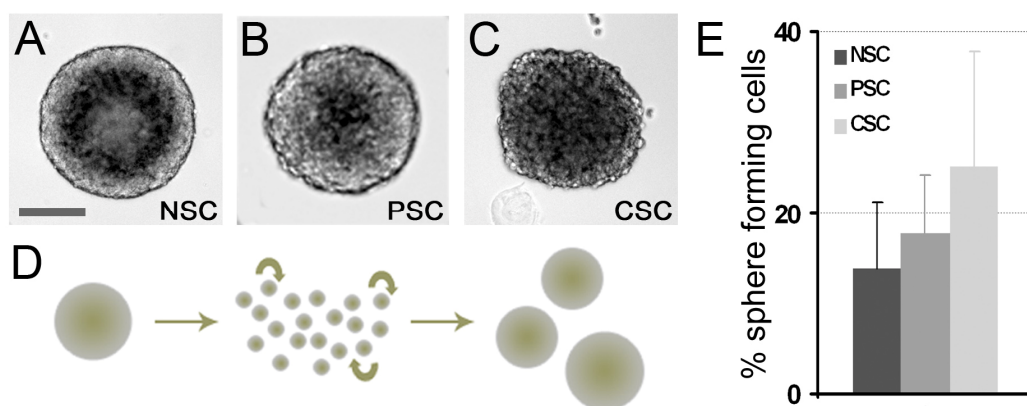


Figure 23: Self-renewing defects in transgenic stem cells. (A-C) Normal stem cells (NSCs), premalignant stem cells (PSCs) and cancer stem cells (CSCs) can be maintained in neurosphere culture for many generations. (D) Illustration of sphere forming assays. Neurospheres were dissociated and the number of secondary spheres, correlating with the number of self-renewing cells within the sphere, was quantified. (E) PSCs ($17.7 \pm 6.5\%$) and CSCs ($25.2 \pm 12.6\%$) have increased numbers of self-renewing cells compared to NSCs ($13.8 \pm 7.5\%$). Scale bar represents 200 μ m.

In an alternative approach to determine the number of self-renewing cells, I performed immunocytochemistry on dissociated neurospheres using CD15/LeX, a marker for stem cells and transit amplifying cells which has been used to identify mouse embryonic neural progenitors as well as adult stem cells (Capela & Temple, 2002). Neurosphere cultures from both NSCs and PSCs grown under proliferative conditions expressed CD15/LeX. Similar to results obtained from sphere forming assays, higher number of CD15/LeX positive cells in PSCs ($38.8 \pm 4.3\%$) compared to normal adult stem cells ($24.8 \pm 5.8\%$) (Figure 24) were observed.

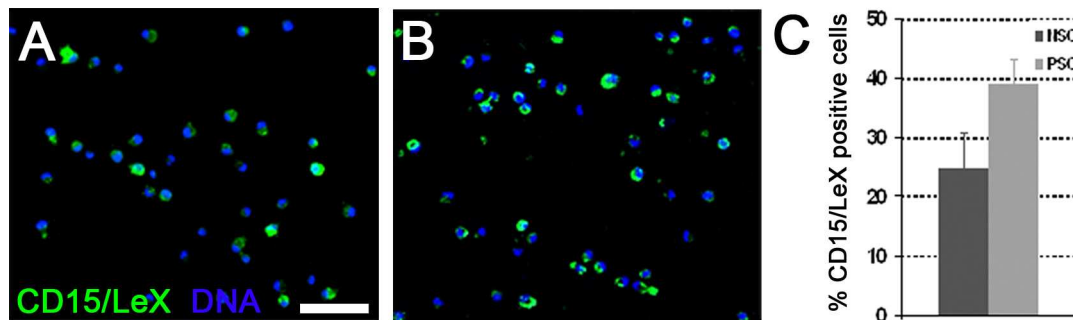


Figure 24: CD15/LeX positive cells are increased in premalignant stem cells. Immunocytochemistry for the stem cell/transit amplifying cell marker CD15/LeX on dissociated cells from NSCs (A) and PSCs (B) grown under proliferative conditions. (C) Quantification of cells revealed that PSCs consist of a higher number of CD15/LeX positive cells ($38.8 \pm 4.3\%$) as compared to NSCs ($24.8 \pm 5.8\%$). Scale bar represents 70 μm .

Together, these data demonstrate that ectopic EGFR expression in this mouse model for oligodendroglioma increased the self-renewing capacity of adult stem cells already at premalignant stages.

4.1.7 Differentiation defects in oligodendroglioma derived cancer stem cells and premalignant stem cells

Adult neural stem cells are multipotential giving rise to neurons, astrocytes and oligodendrocytes (Gage et al, 2000). Brain cancer stem cells, on the other hand, preferentially develop into the cells found in the primary tumor (Vescovi et al, 2006). Before, I assessed the multipotentiality of cancer stem cells and found that oligodendroglioma derived neural cancer stem cells generate all three neural cell types (Figure 16) although the number of astrocytes and neurons was relatively low compared to oligodendrocytes (see below). In addition, I have shown that orthotopically injected CSCs primarily give rise to immature oligodendrocytes (Figure 21A-B) suggesting that these cancer stem cells have lost their normal differentiation potential.

EGFR deregulation in cancer stem cells could directly influence their differentiation potential being responsible for the generation of mainly oligodendrocytes as compared to astrocytes

and neurons. To test this hypothesis I quantitatively compared the differentiation capacity of premalignant and cancer stem cells to that of normal neural stem cells.

In brief, neurospheres from NSCs and PSCs as well as tumorspheres from CSCs were dissociated and cells plated under adherent conditions in the absence of growth factors to induce differentiation. Usually, cells were fixed after 7 days and subjected to immunocytochemistry to detect neuronal and glial cells. Expression of GFAP and β -III-tubulin for astrocytes and neurons, respectively, and the early and later oligodendrocyte markers Olig2, NG2 and O4 were examined.

Since oligodendroglioma mainly consist of oligodendrocyte progenitors I first focused on potential differentiation defects of PSCs and CSCs in the oligodendrocyte lineage. The transcription factor Olig2 is expressed in immature progenitor cells of the developing brain and spinal cord in regions that give rise both to neurons and oligodendrocytes (Lu et al, 2002; Zhou & Anderson, 2002). In the adult subventricular zone Olig2 expression was identified in fast proliferating CD15/Lex positive cells, suggesting a role of Olig2 in transit amplifying type C cells (Aguirre et al, 2004) which presumably are oligodendrocyte precursors. There, Olig2 is maintained to direct transit amplifying cells towards the oligodendrocyte lineage or downregulated to induce neural fate (Hack et al, 2005).

Similar to cells from primary and orthotopic tumors, after 7 days under differentiation conditions a large number of CSCs expressed Olig2 ($80.3 \pm 5.6\%$). In contrast, only $18.4 \pm 2.5\%$ Olig2 positive cells were observed in neural stem cells from control mice. Interestingly, in PSCs isolated from *S100 β -verbB*, *p53*^{+/-} mice long before tumor formation, a considerably increased number of Olig2 positive cells was detected ($29.3 \pm 3.9\%$) (Figure 25).

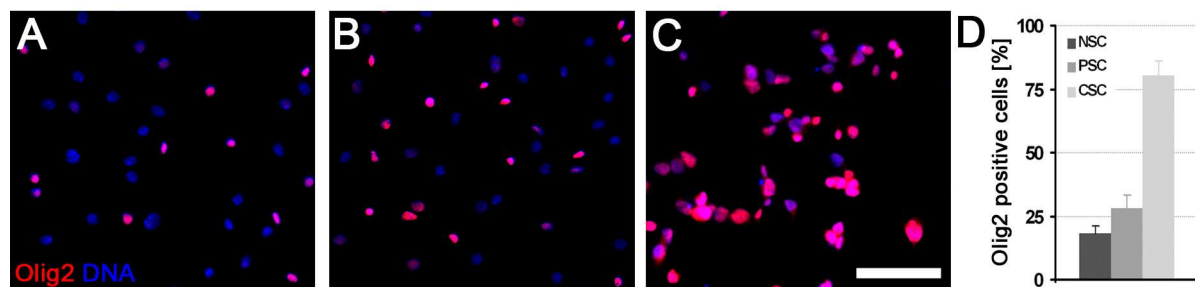


Figure 25: Analysis of Olig2 expression in differentiated stem cells and cancer stem cells. NSCs (A), PSCs (B) and CSCs (C) were dissociated and grown under adherent conditions in the absence of growth factors to induce differentiation and stained for Olig2 (red) and DAPI (blue). (D) Increased numbers of Olig2 positive cells could be detected in PSCs ($29.3 \pm 3.9\%$) compared to neural stem cells from control mice ($18.4 \pm 2.5\%$). Note that the majority of differentiated CSCs express Olig2 ($80.3 \pm 5.6\%$). Scale bar represents 100 μ m.

Next I compared the expression of NG2, another marker for oligodendrocyte progenitors, in PSCs and CSCs with normal neural stem cells and obtained essentially the same results as with Olig2.

In the absence of growth factors, even more premalignant stem cells from *S100 β -verbB, p53^{+/-}* mice ($24.4 \pm 7.9\%$) developed into NG2 positive oligodendrocyte progenitors whereas only $8.8 \pm 2.5\%$ of differentiated control stem cells expressed this marker. Again, a dramatic increase of the early oligodendrocyte marker was observed when cancer stem cells were induced to differentiate ($84.4 \pm 3.5\%$) (Figure 26).

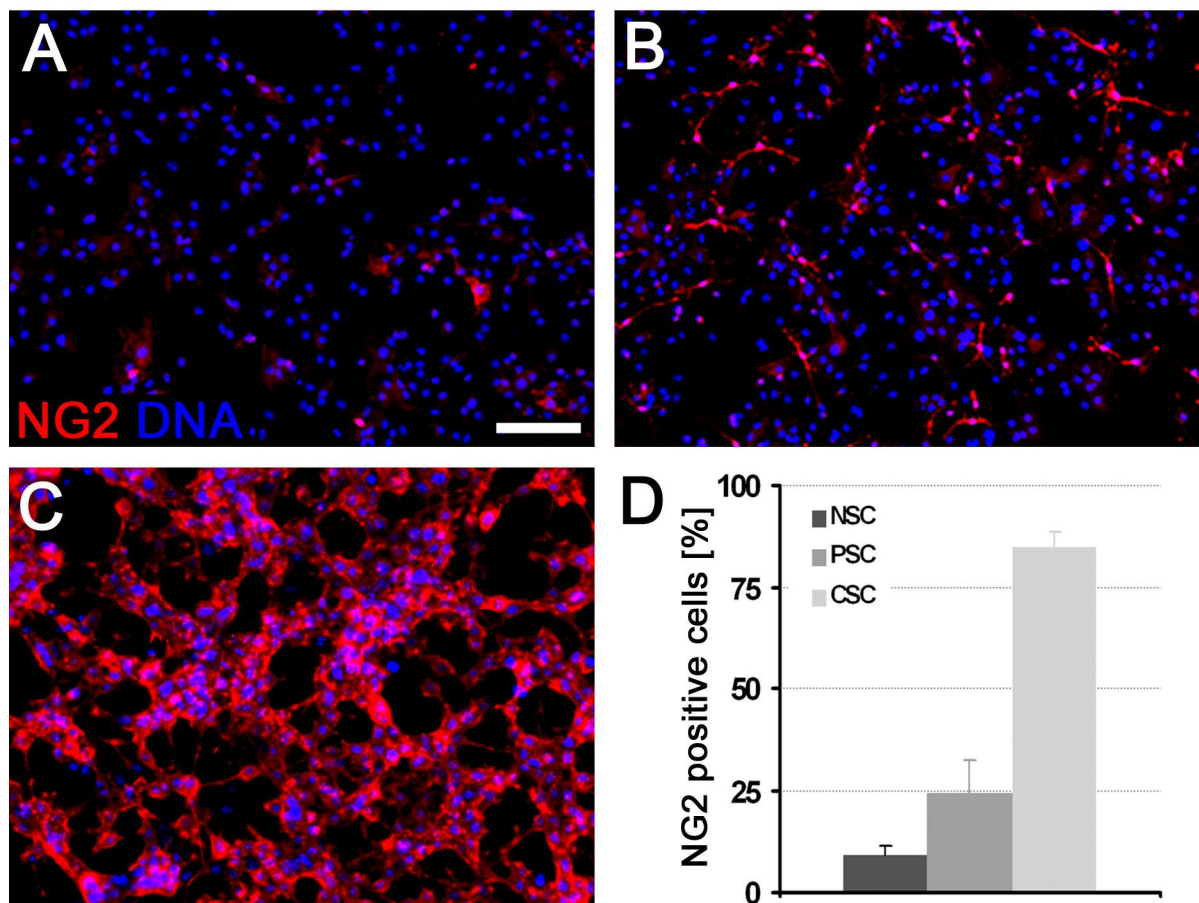


Figure 26: Oligodendrocyte progenitors are generated at higher number by differentiated PSCs and CSCs. Wild type (A), *S100 β -verbB, p53^{+/-}* premalignant (B) and *S100 β -verbB, p53^{-/-}* cancer stem cells (C) were grown under differentiation conditions for 7 days and subjected to immunocytochemistry for the early oligodendrocyte marker NG2 (red). DNA was counterstained in blue. (D) Quantification showing that premalignant ($24.4 \pm 7.9\%$) and especially cancer stem cells ($84.4 \pm 3.5\%$) generate significantly higher numbers of NG2 compared to control adult neural stem cells ($8.8 \pm 2.5\%$). Scale bar represents 100 μ m.

Early progenitor cells eventually give rise to more mature oligodendrocytes and sequentially begin to express the oligodendrocyte antigen O4, galactocerebroside (GalC) and finally mature myelin antigens such as MBP (myelin basic protein) *in vivo* and *in vitro* (Nishiyama, 2007; Dawson et al, 2003).

To evaluate whether the accumulation of Olig2⁺/NG2⁺ positive cells in these differentiation experiments indeed reflected an increased potential of PSCs to differentiate further into the oligodendrocyte lineage I next tested for the oligodendrocyte marker O4.

As for the progenitor cells, I expected an substantial increase of more mature oligodendrocytes. Surprisingly, the number of O4 positive cells was only moderately increased in PSCs ($5.3 \pm 2.8\%$) (Figure 27B) and CSCs ($4.7 \pm 2.1\%$) (Figure 27C) compared to the wild type population ($2.3 \pm 0.7\%$) (Figure 27A)

Oligodendrocyte progenitors (NG2⁺, Figure 27D, arrow) and more mature oligodendrocytes (O4⁺, Figure 27D, arrowhead) differentiated from both wild type and premalignant stem cells show a typical stellate morphology and are highly branched. During the maturation of oligodendrocytes, expression of the NG2 proteoglycan is downregulated whereas more O4 antigen is generated, with intermediate stages where both antigens can be detected (asterisk in Figure 27D). In contrast, cancer stem cells induced to differentiation show a totally different morphology, with cells generated generally of round shape and high expression of NG2. CSC-derived oligodendrocytes immunopositive for the O4 antigen, on the other hand, do have some processes although they were much less branched (arrow in Figure 27E). For differentiation experiments, usually 25000 cells/well in 8 well chamber slides from each cell line were plated, resulting in relatively dense cultures but still giving cells enough space to expand. However, under this conditions, CSCs totally overgrew the slide giving rise to a confluent layer of cells suggesting that, at least a part of these cells, did not respond to the differentiation signals but continue to proliferate. Therefore, the number of cells plated from CSCs was reduced to approximately 10000/well. Still, cells aggregated and formed clusters as shown in Figure 27E and a large number of dividing cells could be detected.

The high number of oligodendrocyte progenitors derived from cancer stem cells under conditions which favor differentiation, together with the morphological abnormalities and continuous proliferation indicate that these cells possessed a block in their differentiation potential which would explain the accumulation of immature oligodendrocytes. Interestingly, when cells acutely isolated from a orthotopic tumor were grown under adherent conditions in the absence of any mitogens, almost all cells were immunopositive for NG2 and O4, respectively, showing a morphology very similar to oligodendrocytes generated from wild type and premalignant stem cells (Figure 27F).

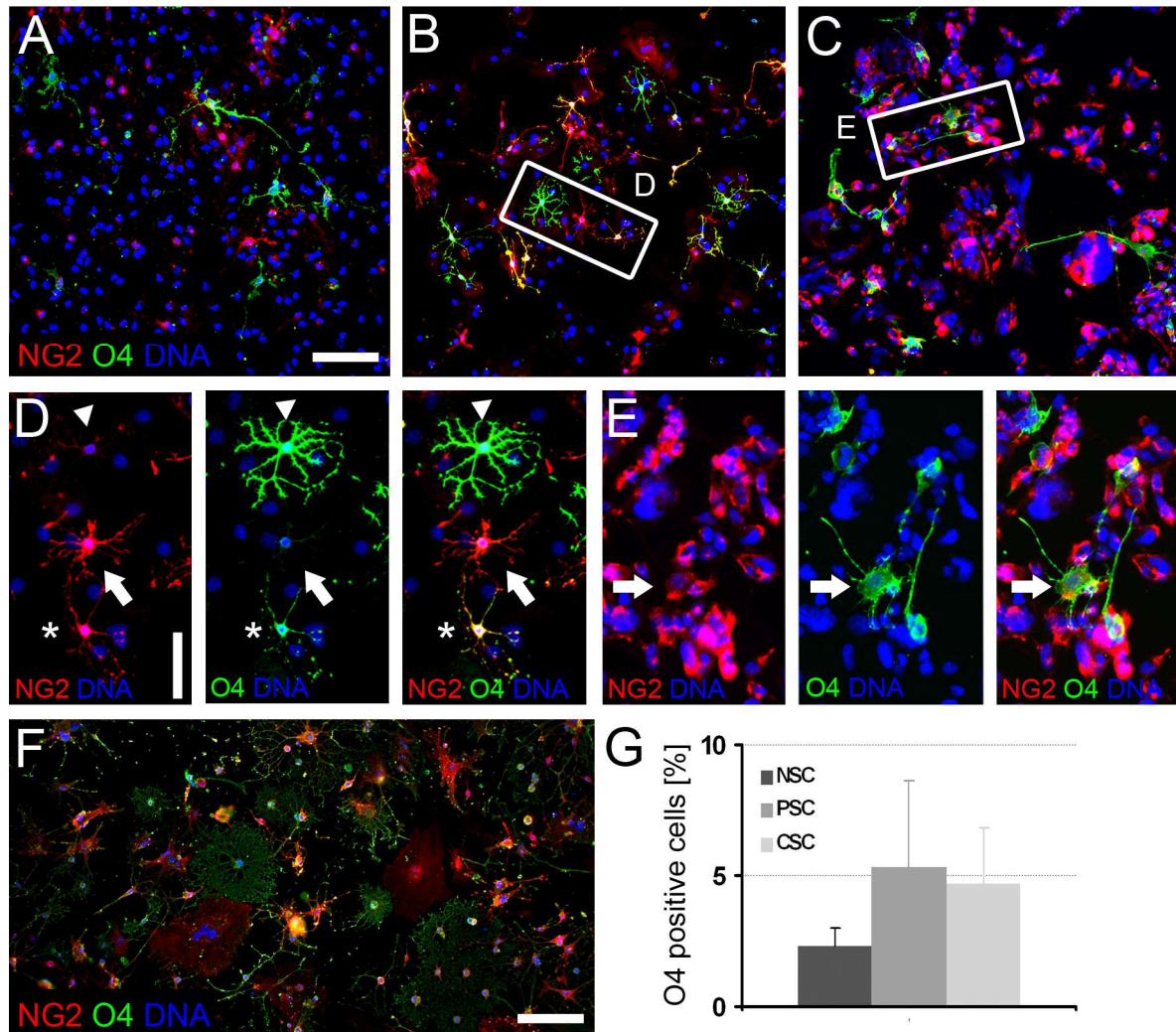


Figure 27: Differentiation block in oligodendrocyte progenitors. NSCs (A), PSCs (B) and CSCs (C) were grown under differentiation conditions for 7 days and stained for the early oligodendrocyte marker NG2 (red) and the more mature oligodendrocyte marker O4 (green), DNA was counterstained in blue. (D) (Inset in B) Immunofluorescence image showing the typical stellate morphology of NG2⁺ oligodendrocyte progenitors (arrow) and O4 oligodendrocytes (arrowheads). The asterisk indicates a NG2⁺/O4⁺ transition state. (E) (Inset in C). In contrast, cells differentiated from CSCs were of round shape and O4 positive oligodendrocytes possessed less processes and branches. (F) Acutely isolated tumor cells essentially generate cells of the oligodendrocytic lineage morphologically similar to controls. (G) Despite the accumulation of progenitor cells, quantification revealed that PSCs ($5.3 \pm 2.8\%$) and CSCs ($4.7 \pm 2.1\%$) generate similar amounts of O4 positive oligodendrocytes as control adult neural stem cells ($2.3 \pm 0.7\%$). Scale bars in (A, F) 100 μm , in (D) 50 μm .

Together, my data suggest that premalignant stem cells already show a defect in the differentiation pattern and preferentially generate cells of the oligodendrocytic lineage including transit amplifying cells. Since oligodendroglioma consist of mainly Olig2⁺ and NG2⁺ cells, early changes observed in premalignant stem cells might reflect their ability to later give rise to CSCs, which in turn generate tumors. Importantly, these tumors contain cells with stem cell properties which almost exclusively develop into early oligodendrocyte progenitors after being induced to differentiation. These cells, however, showed a distinct morphology to oligodendrocytes derived from normal adult stem cells further supporting a defect and/or block of differentiation of stem cells originated from this murine oligodendroglioma model.

Next, I wanted to determine whether cells of the neuronal and astrocytic lineage are also affected in transgenic stem cells. Therefore, dissociated NSCs, PSCs and CSCs were plated under differentiation conditions as described before and stained for the neuronal marker β -III-tubulin and for GFAP to identify astrocytes. Adult neural stem cells induced to differentiate generated around 15% of neuronal cells as indicated by β -III-tubulin positive staining ($14.4 \pm 10.7\%$). However, PSCs ($4.5 \pm 3.1\%$) and CSCs ($6.2 \pm 4.1\%$) generated lower numbers of β -III-tubulin positive cells suggesting that the differentiation within the neuronal lineage is impaired (Figure 28A-D).

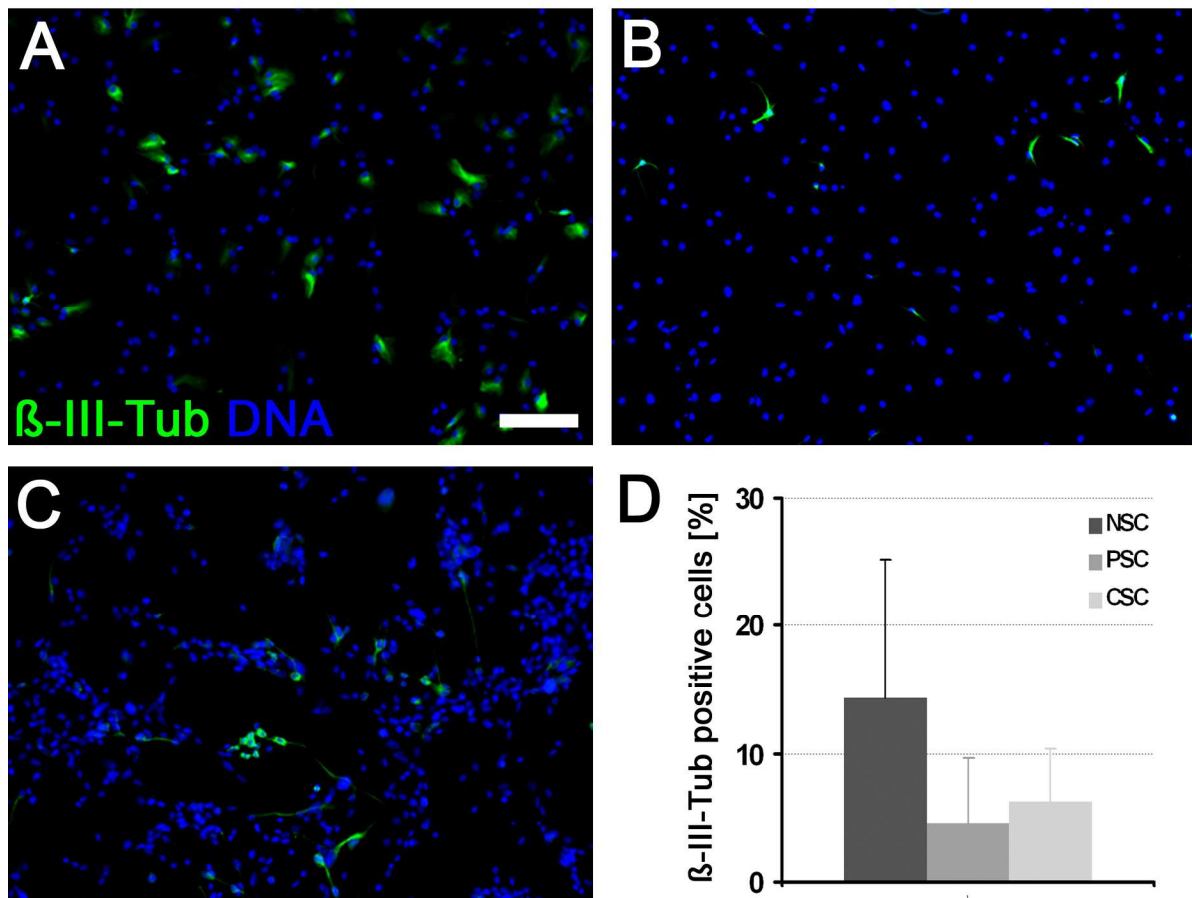


Figure 28: Neurons were generated at lower numbers by differentiated PSCs and CSCs. Wild type (A), *S100 β -verbB*, *p53*^{+/-} premalignant (B) and *S100 β -verbB*, *p53*^{-/-} cancer stem cells (C) were dissociated and grown in the absence of growth factors to induce differentiation. After 7 days, cells were fixed and subjected to immunocytochemistry to detect the neuronal marker β -III-tubulin (green), DNA was counterstained in blue. (D) Quantification of β -III-tubulin expressing cells revealed a decreased number of neurons in PSCs ($4.5 \pm 3.1\%$) and CSCs ($6.2 \pm 4.1\%$) compared to normal neural stem cells ($14.4 \pm 10.7\%$). Scale bar represents 100 μ m.

With $36.0 \pm 3.0\%$ of GFAP-immunoreactive cells, astrocytes represent the majority of differentiated wild type stem cells (Figure 29A). Similar to neuronal cells, the number of GFAP positive cells was considerably reduced to $26.1 \pm 5.4\%$ in premalignant stem cells derived from *S100 β -verbB*, *p53*^{+/-} mice (Figure 29B). An even more dramatic decline could be observed in the number of astrocytes when cancer stem cells were induced to

differentiate. In contrast to NSCs and PSCs, after culturing these cells for 7 days in the absence of mitogens, hardly any astrocytes could be detected by immunocytochemistry ($2.3 \pm 1.1\%$) (Figure 29C).

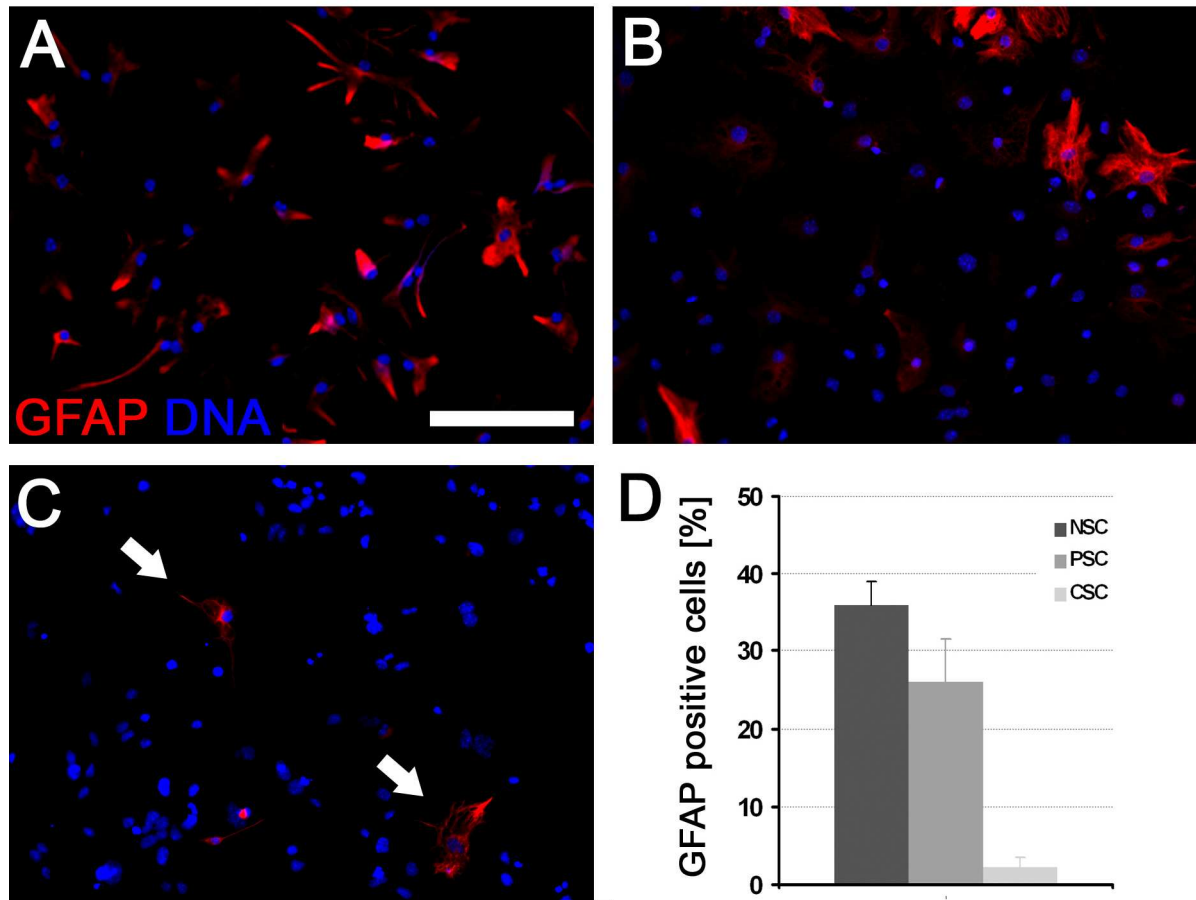


Figure 29: Premalignant and cancer stem cells generate fewer cells of the astrocytic lineage. Immunocytochemical analysis for the astrocyte-marker GFAP (red) in differentiated NSCs (A), PSCs (B) and CSCs (C). Nuclei were counterstained with DAPI (blue). (D) The number of astrocytes was only moderately decreased in PSCs ($26.1 \pm 5.4\%$) compared to NSCs ($36.0 \pm 3.0\%$), however, only a few GFAP positive cells could be detected in differentiated CSCs ($2.3 \pm 1.1\%$). Scale bar represents 100 μm .

In summary, premalignant stem cells derived from *S100 β -verbB*, *p53*^{+/-} mice display significant alterations in their differentiation potential, reminiscent of cancer stem cells, already long before tumor occurrence: they preferentially generate oligodendrocyte progenitors with delayed or impaired maturation at the expense of astrocytic and neuronal cells. My results strengthen the proposition that early changes in neural stem cells induced by e.g. oncogenic mutations lead to premalignant stem cells which, after acquiring additional mutations, transform into cancer stem cells. I have isolated cells from oligodendroglioma with stem-like features which showed a similar differentiation pattern as seen in PSCs, however, the observed defects were even more severe: the vast majority of cells developed into oligodendrocyte progenitors and only a few neurons and astrocytes could be detected after growing cancer stem cells under differentiation conditions.

The following table summarizes the results obtained from the differentiation experiments described in the last chapter. It is important to note, that at the beginning of this study, all differentiation experiments were performed with pooled cell lines, i.e. a mixture of stem cells isolated from several mice (e.g. the initial wild type neurosphere line, which I referred to as wild type “old”, is a pool of stem cells obtained from 3 different FvB/N mice). In addition, some of the results available represent only data from the analysis done with these initial cell lines (e.g. GFAP and O4).

Table 1: Summary of differentiation experiments. The table shows a quantitative analysis of the differentiation capacity of cell lines from wild type neural stem cells, premalignant *S100 β -verbB*, *p53*^{+/-} stem cells and oligodendrogloma derived cancer stem cells with respect to their ability to generate cells of the oligodendrocytic lineage (NG2, Olig2, O4 immunoreactivity), neurons (β -III-tubulin positive) and astrocytes (GFAP positive).

| Marker | NG2 | Olig2 | O4 | β -III-Tub | GFAP |
|---|-------------|-------------|------------|------------------|-------------|
| % marker expression of total cells | | | | | |
| Wild type stem cell lines | | | | | |
| Average | 8.8 | 18.4 | 2.3 | 14.4 | 36.0 |
| ± SEM | 2.5 | 2.5 | 0.7 | 10.7 | 3.0 |
| WT “old” ¹ | 5.2 | 18.1 | 2.3 | 19,8 | 3,0 |
| WT “new” ² | 9.7 | 21.2 | n.d | 21,3 | n.d |
| 108127 | 9.5 | 15.2 | n.d | 2,0 | n.d |
| 108437 | 10.9 | 19.2 | n.d | n.d. | n.d |
| <i>S100β-verbB</i>, <i>p53</i>^{+/-} premalignant stem cell lines | | | | | |
| Average | 24.2 | 29.3 | 5.3 | 4,5 | 26,1 |
| ± SEM | 7.9 | 3.9 | 2.8 | 3,1 | 5.4 |
| PSC “old” ³ | 38.8 | n.d. | 5.3 | 3.2 | 26.1 |
| 108439 | 17.1 | 31.8 | n.d | 3.3 | n.d |
| 11939 | 18.3 | 25.8 | n.d | 9.5 | n.d |
| 11407 | 20.6 | 25.2 | n.d | 3.3 | n.d |
| 11144 | 24.6 | 34.2 | n.d | 5.8 | n.d |
| 9495 | 26.9 | 29.3 | n.d | 2.2 | n.d. |
| <i>S100β-verbB</i>, <i>p53</i>^{-/-} cancer stem cell lines | | | | | |
| Average | 84.9 | 29.3 | 5.3 | 4.5 | 26.1 |
| ± SEM | 3.5 | 3.9 | 2.8 | 3,1 | 5.4 |
| CSC “old” | 88.9 | 85.8 | 6.2 | 3.3 | 1.5 |
| 10110 | 82.9 | 74.5 | 3.2 | 4.4 | 3.1 |
| 9683 | 82.9 | 80.5 | n.d. | 11.0 | n.d. |

¹ WT “old” represents a pool of stem cells isolated from the SVZ of 3 different wild type mice. ² WT “new” is a pool of stem cells isolated from the SVZ of 2 wild type mice (107268 and 107270). ³ PSC “old” is a pool of stem cells isolated from the SVZ of 3 *S100 β -verbB*, *p53*^{+/-} mice (9490, 9492 and 9493). Other stem cell lines were named after the animal number from the mouse which they were isolated from. For each data set, means ± SEM (standard error of the mean) of experiments from independent cell lines are shown. When only one cell line was used for the analysis, results represent the average and standard deviation from several individual experiments. For each data point, > 1000 cells were counted.

4.1.8 Neural stem cells from *S100 β -verbB, p53^{-/-}* but not *S100 β -verbB, p53^{+/-}* are tumorigenic

Although premalignant stem cells already showed self-renewal and differentiation defects they were not yet tumorigenic. Indeed, in contrast to cancer stem cells, premalignant stem cells derived from *S100 β -verbB, p53^{+/-}* mice never gave rise to tumors after intracranial injections. Animals, even when transplanted with high numbers of PSCs (up to 1×10^6), never developed tumors. One group of animals (n=6) was sacrificed 9 months after injection with PSC “old” cells and histopathology on brain sections revealed no signs of tumor formation. Transplantation experiments were repeated with two additional PSC lines to test their tumorigenicity. Animals were nonsymptomatic 2 months after intracranial injection of PSCs and sacrificed to analyze them for hallmarks of oligodendroglioma. Again, no indications for tumor formation were obvious (Figure 30).

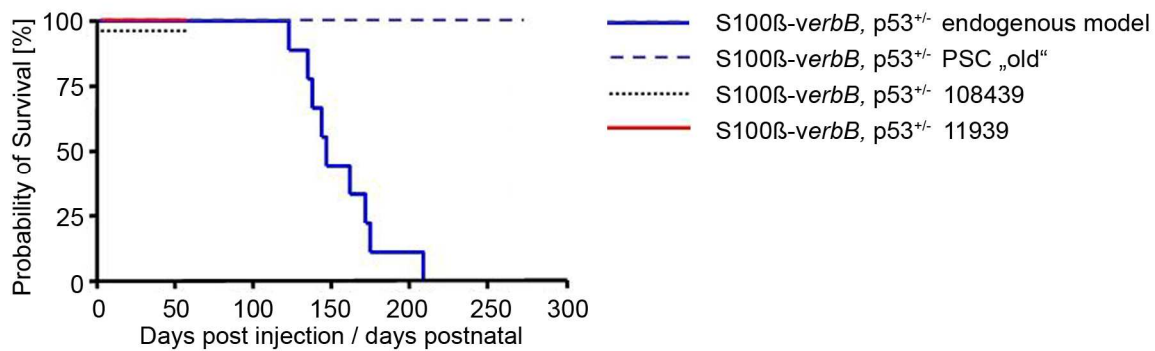


Figure 30: Premalignant stem cells do not form tumors in transplantation experiments. Premalignant stem cells were intracranially injected into FvB/N mice. Animals never developed neurological impairment and histochemical analysis on brain sections showed no signs of tumor formation. 3 groups (n=6) of animals were challenged with independent PSC lines, and sacrificed and analyzed after 2 and 9 month, respectively. For comparison, the survival of *S100 β -verbB, p53^{+/-}* animals (endogenous model) is shown.

Interestingly, when SVZ-derived stem cells from *S100 β -verbB, p53^{-/-}* animals were transplanted into FvB/N mice (n=15), recipients consistently developed tumors within 2-3 weeks (Figure 31E). Moreover, when induced to differentiate, these cells preferentially developed into Olig2⁺ ($64.7 \pm 0.9\%$) and NG2⁺ ($74.6 \pm 3.5\%$) oligodendrocyte progenitors whereas the number of β -III-tubulin positive neurons was very low ($3.9 \pm 3.7\%$) (Figure 31A-D). This differentiation pattern was very similar to that observed in oligodendroglioma-derived cancer stem cells isolated from *S100 β -verbB, p53^{-/-}* mice.

However, at the time when neural stem cells have been isolated from the SVZ of these mice, tumor formation has already been obvious. As mentioned, oligodendroglioma are highly infiltrative, therefore I could not rule out a contamination as tumor cells, including potential CSCs from the tumor site might have migrated to the SVZ. As CSCs displayed higher self renewal capacity, it is possible that these cells overgrew normal neural stem cells during

culturing. Alternatively, as hypothesized in my model, neural stem cells in the SVZ of *S100 β -verbB*, *p53*^{-/-} themselves could have transformed into cancer stem cells being the initiating cause of tumor formation.

This hypothesis would further be supported by the malignant potential of these neural stem cells which, similar to oligodendrogloma derived CSCs but unlike PSCs, gave rise to orthotopic tumors in transplantation experiments.

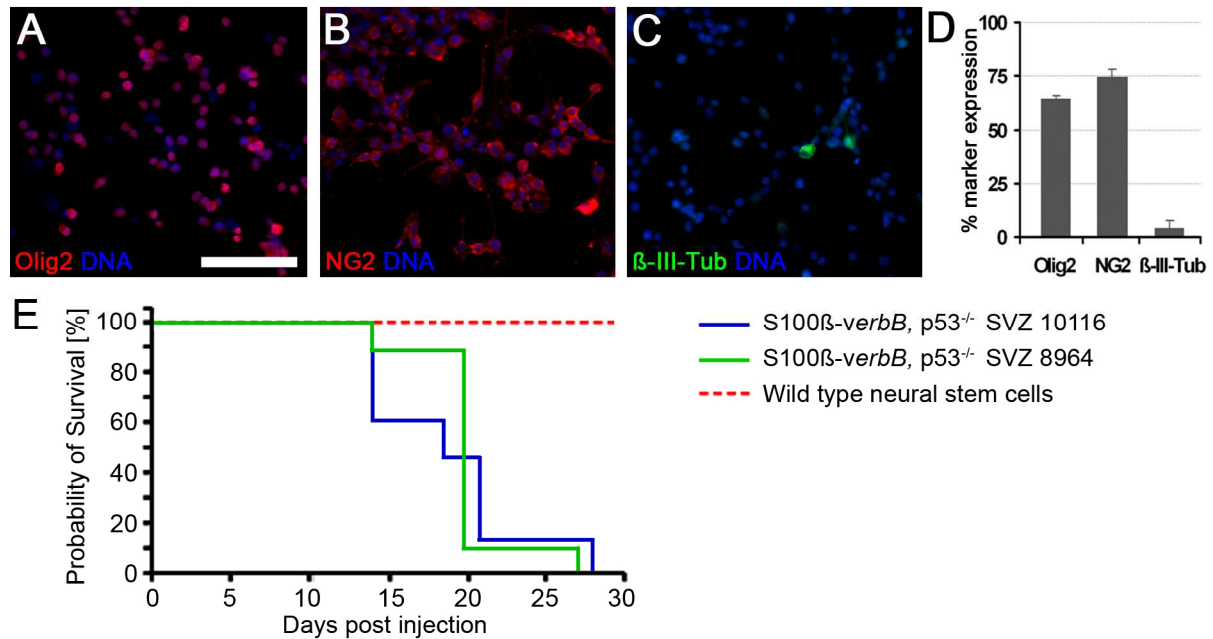


Figure 31: *S100 β -verbB*, *p53*^{-/-} neural stem cells phenocopy cancer stem cells. Neural stem cells were isolated from the subventricular zone of *S100 β -verbB*, *p53*^{-/-} mice and grown in the absence of mitogens. The majority of cells differentiated into Olig2⁺ (64.7 ± 0.9%) (A) and NG2⁺ (74.6 ± 3.5%) (B) oligodendrocyte progenitor cells whereas only a few neurons could be detected (3.9 ± 3.7%) (C). Similar to cancer stem cells, intracranial injection of neural stem cells from *S100 β -verbB*, *p53*^{-/-} consistently resulted in tumor formation (E). Scale bar represents 100 μ m.

4.1.9 Deregulation of EGFR signaling but not loss of p53 influences cell fate decisions

Both, *S100 β -verbB*, *p53*^{+/-} and *S100 β -verbB*, *p53*^{-/-} mice develop high grade oligodendrogloma and I have shown that neural stem cells, isolated long before tumor occurrence, already display differentiation defects giving rise to increased numbers of cells of the oligodendrocytic lineage.

Next I wanted to explore in more detail to what extent ectopic expression of *verbB* and the loss of tumor suppressors, respectively, contribute to the observed differentiation defects.

Transgenic mice exclusively overexpressing *verbB*, the oncogenic version of EGFR, from the S100 β promoter develop low-grade oligodendroglioma (Weiss et al., 2003). I isolated subventricular zone stem cells 2 month postnatally before tumor occurrence as described and evaluated their differentiation potential (n=6 independent lines). Immunocytochemistry revealed that after differentiation for 7 days 27.4 \pm 4.9% of S100 β -*verbB* stem cells developed into Olig2⁺ (data not shown) and 23.3 \pm 7.0% into NG2⁺ oligodendrocyte progenitors. In contrast, only 7.9 \pm 5.0% of differentiated cells expressed the neuronal marker β -III-tubulin (Figure 32A,D). Interestingly, this almost resembled the differentiation pattern of premalignant stem cells from S100 β -*verbB*, p53^{+/-} mice. These data indicate that alterations in EGFR signalling, initiated through the overexpression of *verbB*, directly contributed to differentiation defects observed in transgenic stem cell lines.

In addition, I evaluated the differentiation capabilities of stem cells derived from littermates either hetero- or homozygous for the tumor suppressor p53. Loss of p53 had little effect on the oligodendrocytic lineage as NG2 expression was comparable to that of neural stem cells from wild type controls (11.9 \pm 1.9% in p53^{+/-} stem cells, 12.3 \pm 1.3% in p53^{-/-} stem cells; Figure 32). p53^{-/-} stem cells also generated similar amounts of Olig2⁺ oligodendrocyte progenitors (16.7 \pm 0.9%, data not shown) and neurons (16.2 \pm 3.3%) as compared to wild type controls. Surprisingly however, I detected significantly less β -III-tubulin positive cells in differentiated stem cells from p53^{+/-} mice (Figure 32B-D).

Together, it was observed for the first time that neural stem cells in a transgenic mouse model for oligodendroglioma undergo differentiation changes before the establishment of a tumor. However, after intracranial injection, these cells never gave rise to orthotopic tumors (Figure 32E). Ectopic expression of *verbB* in the stem cell/progenitor cell pool alters EGFR signaling and might probably be the initiating factor which leads to the accumulation of oligodendrocytic progenitor cells. Upon loss of the tumor suppressor p53, transgenic S100 β -*verbB* mice progress to high grade oligodendroglioma and tumors develop with decreased latency and increased penetrance. However, in contrast to *verbB* overexpression, p53 loss only moderately influences the *in vitro* differentiation capabilities of neural stem cells. *In vivo*, the loss of p53 leads to increased proliferation as a result of increased cell division and reduced apoptosis (Symonds et al, 1994) which, together with additional genetic alterations, may explain the progression from low- to high grade oligodendroglioma.

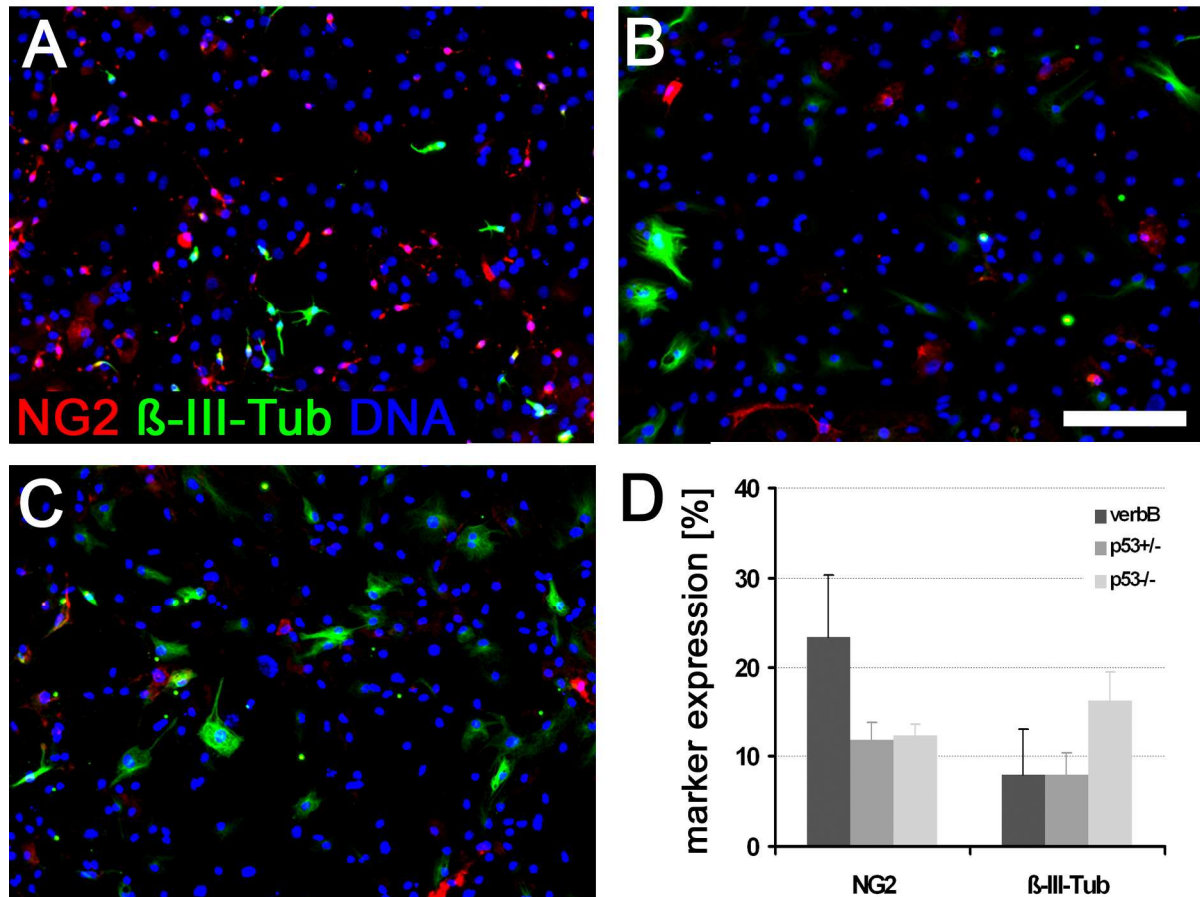


Figure 32: Deregulation of EGFR signaling but not loss of p53 causes differentiation defects. Stem cells isolated from the SVZ of S100 β -*verbB* (A), p53^{+/-} (B) and p53^{-/-} (C) mice were cultured under differentiation conditions and subjected to immunocytochemistry for NG2 (red) and β -III-tubulin (green), nuclei were counterstained with DAPI (blue). (D) Quantification revealed that S100 β -*verbB* stem cells differentiated into higher numbers of NG2⁺ oligodendrocyte progenitors (23.3 \pm 7.0%) compared to stem cells cultured from animals either hetero- or homozygous for the tumor suppressor p53 (11.9 \pm 1.9% and 12.3 \pm 1.3%, respectively). β -III-tubulin expression was similar to wild type controls in differentiated p53^{-/-} stem cells (16.2 \pm 3.3%) whereas stem cells derived from S100 β -*verbB* mice differentiated into lower numbers of neurons (7.9 \pm 5.0%). Interestingly, stem cells heterozygous for p53 generated also a very low number of β -III-tubulin positive cells (7.9 \pm 2.5%). Scale bar represents 100 μ m.

Thus, I next wanted to determine the *in vitro* proliferation rate of transgenic stem cells from the oligodendroglioma model and compare it to neural stem cells of wild type mice. Amplification rates were quantified using the fluorescence-based CyQuant kit (Molecular probes). In brief, spheres were dissociated and same amounts of cells (2500 cells/well) were plated in 96-well plates and cultured in a medium consisting of DMEM/F12 enriched with N2 supplement (Gibco), bovine pituitary extract (BPE, Gibco), EGF, bFGF, glutamine and P/S (referred to as N5 medium) to support growth under adherent conditions (Sun et al, 2005). At the indicated time points, a dye was added to the wells and a fluorescence signal, correlating with the cell number, was measured using a microplate reader and plotted against the time grown under proliferative conditions (Figure 33). Analyses were done in triplicates and data represent the average of experiments with 3 independent cell lines.

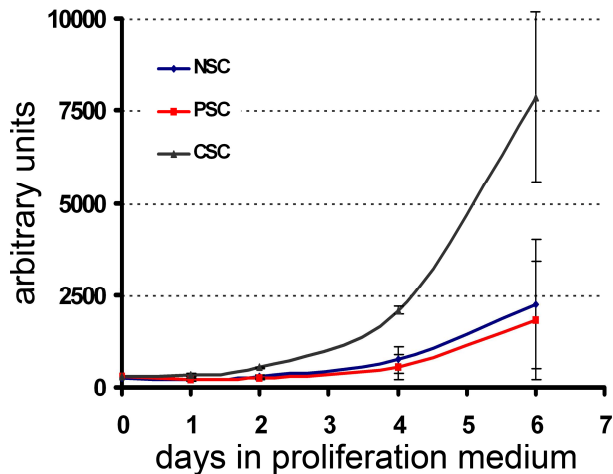


Figure 33: Cancer stem cells but not premalignant stem cells show increased viability. NSCs (blue line), PSCs (red line) and CSCs (black line) were dissociated and same amounts of cells plated in N5 medium under adherent conditions. Whereas NSCs and PSCs showed comparable rates of amplification, proliferation was significantly higher in CSCs. Proliferation was quantified using the CyQuant kit and arbitrary fluorescence units correlating with the cell number are shown.

As expected, growth rates of PSCs were very similar to neural stem cells from wild type controls. However, dissociated spheres represent a heterogeneous pool of cells, consisting not only of stem cells but also transit amplifying cells, glial and neuronal progenitors; the different cell types have different intrinsic proliferation properties which could mask changes in proliferation of a subpopulation of stem cell progeny. In contrast, CSCs displayed a significantly higher amplification rate which was similar to observations *in vivo*. As mentioned earlier, response to differentiation signals was decreased in cancer stem cells as they continued to proliferate even in the absence of mitogens as EGF and bFGF. Together, a differentiation block in combination with a proliferation advantage of cancer stem cells isolated from oligodendroglioma was detected.

The proliferation advantage observed in cancer stem cells could also result from increased survival due to loss of p53. Alternatively, progeny from normal and premalignant stem cells could be reduced in numbers because of higher rates of apoptosis. To evaluate changes in survival, spheres from NSCs, PSCs and CSCs were dissociated and spun down on a chamber slides followed by TUNEL staining (Roche) to detect cells undergoing programmed cell death.

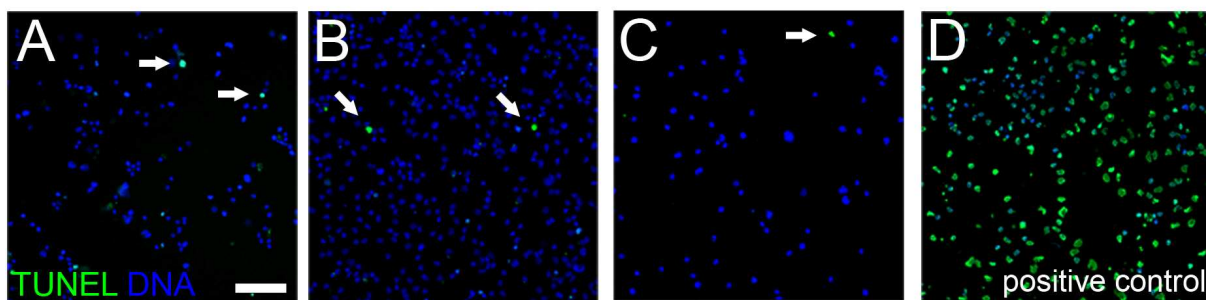


Figure 34: Premalignant and cancer stem cells show no changes in survival. NSCs (A), PSCs (B) and CSCs (C) were dissociated and cultured in differentiation medium for 7 days. TUNEL staining (green, arrows in A-C) revealed that under these conditions only very few cells underwent apoptosis. As a positive control, cells were treated with DNase before TUNEL labeling to induce DNA breaks (D). Scale bar represents 100 μ m.

No differences in the number of apoptotic cells were observed (data not shown). In addition, differentiation defects found in PSCs and CSCs might originate in increased cell death of e.g. astrocytes and neurons whereas cells of the oligodendrocytic lineage are not affected finally leading to the observed accumulation of oligodendrocyte progenitors. Therefore, stem cells derived from either wild type, *S100 β -verbB*, *p53*^{+/-} or *S100 β -verbB*, *p53*^{-/-} mice were cultured under conditions to induce differentiation and subjected to TUNEL labelling after 7 days. Again, the number of TUNEL positive cells was very low (< 0.5%, arrows in Figure 35A-C) and no obvious differences in apoptosis could be detected between the different cell lines. As positive controls, cells were treated with DNase to induce DNA breaks before TUNEL labelling (Figure 35D). In addition, negative controls where fluorescent dyes were omitted were included in my analyses (data not shown).

Together, no differences in the survival of wild type and transgenic stem cells used in this study were found. Moreover, growth rates of premalignant stem cells were indistinguishable from normal stem cells grown under the same conditions. Thus, defects in proliferation and/or survival cannot explain the differentiation defects observed in PSCs. Amplification rates of cancer stem cells, in contrast, were significantly higher compared to wild type stem cells and might be a result of loss of p53. However, my data rule out a direct effect of p53 loss on the differentiation capacity of stem cells.

4.1.10 Premalignant stem cells and cancer stem cells encounter a defect in asymmetric cell division

Proliferation and apoptosis were not significantly altered in premalignant stem cells and thus it is unlikely that these factors contributed to the observed differentiation defects. Alternatively, this might be explained by abnormal asymmetric cell divisions.

The function of asymmetric cell division is to generate cell fate diversity and to maintain the pool of progenitor cells but also to control the balance between stem cells, proliferative progenitor cells and post-mitotic differentiated cells. Interestingly, several findings point dysfunctional asymmetric cell division as a key factor in development of brain tumors (Caussinus & Hirth, 2007; Caussinus & Gonzalez, 2005; Klezovitch et al, 2004).

Thus, I determined whether known regulators of the asymmetric cell division machinery were expressed in adult neural stem cells and premalignant stem cells. Indeed, I could identify the expression of murine *Lgl-1*, *Par3*, *Par6a*, *Par6b* and *Numb* in both, NSCs and PSCs and in whole brain preparations from wild type mice (Figure 35). My data indicate that neural stem cells express asymmetrically localized proteins and therefore might indeed have the potential to divide asymmetrically in culture. Moreover, neurosphere cultures are heterogeneous and do not only consist of stem cells but also transit amplifying cells and their immediate progeny,

the neuronal and glial progenitors. Again, this suggests that cultured stem cells are able to divide asymmetrically to generate the diverse cell types found within neurospheres.

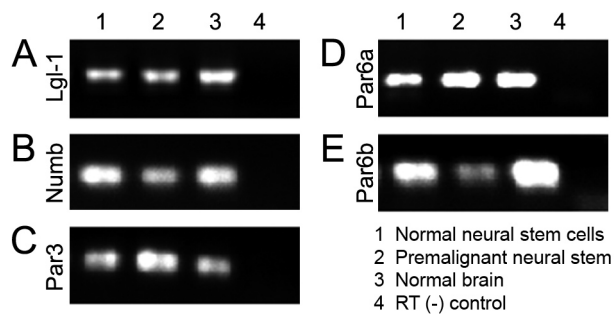


Figure 35: Gene expression of regulators of asymmetric cell division. Expression of *Lgl-1* (A), *Numb* (B), *Par3* (C), *Par6a* (D) and *Par6b* (E) was detected by non-quantitative PCR from wild type neural stem cells (lane 1), premalignant stem cells (lane 2) and normal brain preparations (lane 3). Samples without reverse transcriptase were included as negative controls (lane 4).

As a consequence, I next wanted to identify asymmetrically dividing cells and quantify the frequency of symmetric to asymmetric divisions. To this end, a modified pair cell assay was performed (Shen et al, 2002; Sun et al, 2005). In brief, cells grown in neurosphere cultures were dissociated and plated under adherent and proliferative conditions at clonal densities on Terasaki well plates. To identify asymmetric cell divisions, cells were fixed after one round of cell divisions (~20-24h after plating) and cell pairs were stained for various cell fate markers and regulators of ACD. Asymmetric cell divisions, defined as a scenario where only one daughter cell of a cell pair inherits a cell fate marker, were visualized by fluorescence microscopy and quantified. Note that cell pairs were only counted when at least one daughter was positive for the respective marker; the overall distribution of markers was considerably lower in most cases.

At first, cell pairs from wild type neural stem cells were stained for the stem cell/transit amplifying cell marker CD15/LeX. I found that a proportion of cells segregated CD15/LeX to only one daughter cell which presumably remained a stem cell or transit amplifying cell whereas the other cell acquired different cell fate (Figure 36A, left). In addition to asymmetric cell divisions, also cell pairs were found where both siblings inherited this marker (Figure 36A, right). That kind of symmetric division might be necessary to increase the stem cell and/or progenitor pool within the sphere during proliferative conditions, whereas the former one is important to generate cell diversity. To my knowledge, this is the first demonstration of asymmetric CD15/LeX segregation in neural stem cells.

Murine neural stem cell proliferation can be stimulated by epidermal growth factor and its receptor EGFR can influence progenitor cell fate choice (Burrows et al, 1997). Moreover, EGFR has been shown to be asymmetrically distributed during mitosis of embryonic neural

progenitor cells *in vivo* and *in vitro* (Sun et al, 2005). In agreement with these data, I could also identify cell pairs which segregated the EGFR selectively to one daughter cell (Figure 36B, right) but also pairs where both daughter cells were positive for EGFR (Figure 36B, left). This might suggest that cells inheriting EGFR continue to proliferate or to self-renew, and represent the pool of stem cells and progenitor cells.

In *Drosophila*, Numb is a well-established determinant of cell fate (Rhyu et al, 1994; Knoblich et al, 1995). Similar, mouse Numb shows asymmetric distribution in neural progenitor/stem cell divisions during neurogenesis (Shen et al, 2002; Zhong et al, 1996a) and has a conserved function in cell fate determination (Petersen et al, 2004; Li et al, 2003; Petersen et al, 2002; Shen et al, 2002). Numb was detected in dissociated dividing neural stem cells and also found to be asymmetrically inherited in a fraction of stem cells (Figure 36C, left). Like all other markers, Numb showed heterogeneous expression within the stem cell pool being absent in a proportion of cells but also becoming segregated symmetrically in other cell pairs (Figure 36C, right). Again this points to heterogeneity of cell fates in neurosphere cultures.

In *Drosophila* neuroblasts, the successful asymmetric localization of Numb depends on the assembly of an apical complex consistent of dPar3 (Schober et al, 1999; Wodarz et al, 1999), dPar6 (Petronczki & Knoblich, 2001), atypical protein kinase C (aPKC) (Wodarz et al, 2000), Inscuteable (Insc) (Kraut & Campos-Ortega, 1996), Partner of Inscuteable (Pins) (Parmentier et al, 2002; Schaefer et al, 2000; Yu et al, 2000) and G-proteins (Schaefer et al, 2001). The major function of this protein complex is to establish cell polarity (Ohno, 2001) and allows basal localization of cell fate determinants through a negative interaction with the tumor suppressor Lgl. The Par complex is also very conserved in mammalian cells since homologues of Par3 (Izumi et al, 1998) and Par6 (Joberty et al, 2000) have been identified as regulators of polarity arguing for a functional role in mammalian asymmetric cell division. An interaction of the mammalian Par complex with mammalian atypical PKC and a mammalian Lgl-homologue, Lgl-1 (Plant et al, 2003) has been described.

In cell pair assays, I could detect expression of Par3 in a large proportion of cells. According to the role of Par3 as a regulator of cell polarity, I expected this protein to be asymmetrically inherited during divisions of stem cells. It was surprising though, that asymmetric localization of Par3 was never detected in these assays (Figure 36D).

The expression of other Par-proteins could be identified by PCR analysis. However, with the available antibodies for immunocytochemistry I was unable to detect Par6 protein in my experiments (data not shown). Similar, Lgl-1 was identified by PCR but due to lack of a specific antibody, I could not determine its potential role during asymmetric cell division of neural stem (data not shown).

It is believed that Olig2 promotes oligodendrogenesis and opposes neuronal cell fate (Hack et al, 2005). This might be due to up- or downregulation of this transcription factor in a committed cell, or alternatively, by asymmetric distribution of Olig2 into only one cell during division of a progenitor cell. To distinguish between these possibilities, I performed cell pair assays and detected Olig2 using immunocytochemistry. Olig2 was normally present in the nucleus but became localized to the cytoplasm during cell division and always segregated symmetrically to both daughter cells (Figure 36E). This argues against a role as a classical cell fate determinant that is inherited exclusively by one daughter cell to acquire distinct fate.

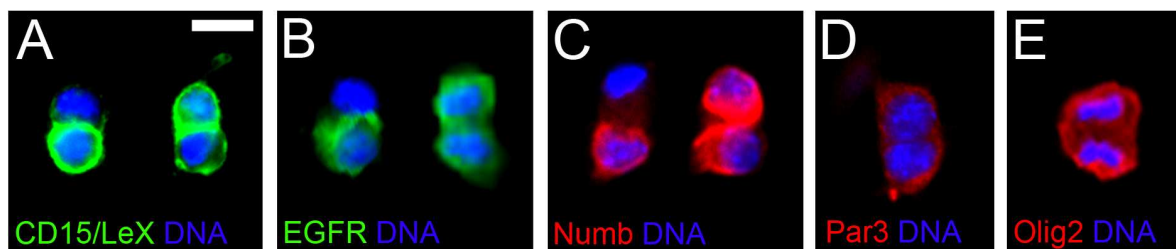


Figure 36: Adult neural stem cells divide asymmetrically and symmetrically *in vitro*. Some neural stem cells localized CD15/LeX asymmetrically (A, green, left) and segregated it exclusively to one daughter cell whereby the CD15/LeX negative cell acquired different fate. NSC also divided symmetrically by distributing CD15/LeX to both daughter cells (A, right). Similar, EGFR (B, green) and the cell fate determinant Numb (C, red) can be either symmetrically (right) or asymmetrically (left) localized during mitosis of neural stem cells. In contrast, asymmetric distribution of Par3 (D, red) and Olig2 (E, red) could never be detected. Scale bar represents 10 μ m.

Next, I concentrated in more detail on the oligodendrocyte marker NG2 since its expression was significantly increased in the premalignant and cancer stem cell pool. Adult wild type neural stem cells from premalignant as well as cancer stem cells showed asymmetric segregation of NG2 as well as symmetric distribution to both daughter cells (Figure 37). Strikingly, the number of asymmetric NG2 divisions was significantly decreased in PSCs ($14.9 \pm 3.2\%$, $n > 200$ pairs from 3 independent experiments) and CSCs ($5.2 \pm 2.1\%$, $n > 200$ pairs from 3 independent experiments) compared to wild type neural cells ($53.8 \pm 15.4\%$, $n > 400$ pairs from 5 independent experiments). It is important to note, that the number of NG2 positive cells of wild type neurosphere cultures grown under proliferative conditions was relatively low (around 5-10%). The majority of these NG2 positive cells divide in an asymmetric fashion. PSCs and CSCs on the other hand contained increased numbers of NG2 positive cells which preferentially divided symmetrically. This observation was very interesting as the reduction in the frequency of asymmetric cell division might explain why I observed that PSCs and CSCs generate significantly more oligodendrocytes when induced to differentiate.

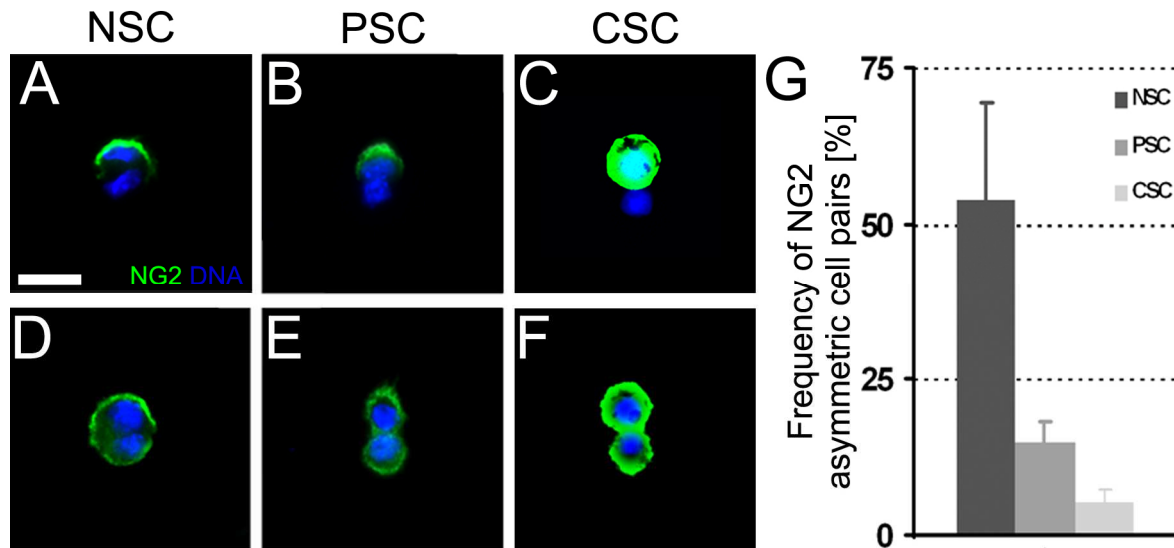


Figure 37: Asymmetric NG2 distribution is impaired in dividing premalignant stem cells and cancer stem cells. Asymmetric (A-C) and symmetric (D-E) NG2 segregation in sibling pairs of NSCs (A, D), PSCs (B, E) and CSCs (C, F). Quantification reveals that the incidence of pairs asymmetric for NG2 decreases in PSCs ($14.9 \pm 3.2\%$) and CSCs ($5.2 \pm 2.1\%$) compared to wild type neural stem cells ($53.8 \pm 15.4\%$) indicative of defects in asymmetric cell divisions in transgenic stem cells (G). Scale bar represents 10 μm .

In summary, my data demonstrate that adult neural stem cells in culture divide asymmetrically into unequal daughter cells by segregating cell fate markers exclusively to one sibling.

To my knowledge, it was shown for the first time that NG2 is asymmetrically localized during divisions of progenitor cells. Importantly, I found defects in the asymmetric cell division of premalignant and cancer stem cells. My data provides a mechanistic insight to defects in adult neural stem cells that might explain the progressive transformation to cancer stem cells: an initial mutation in a multipotential stem cell causes a defect in asymmetric cell division and disturbs the balance of asymmetric versus symmetric divisions. This imbalance directly affects tissue homeostasis, the self-renewing and differentiation capabilities of these stem cells.

4.1.11 Epigenetic changes lead to the progression of premalignant to cancer stem cells

MicroRNAs (miRNAs) are small non-coding RNAs that negatively regulate gene expression at the posttranscriptional level (Bartel, 2004).

Research from several groups has provided evidence that miRNAs act as key regulators of processes as diverse as early development (Reinhart et al, 2000), cell differentiation (Chen et al, 2004), cell proliferation and cell death (Brennecke et al, 2003). Recent studies suggest

possible links between miRNAs, neurodevelopment and cancer (Cheng et al, 2005; Krichevsky et al, 2003).

Differentiation defects seen in premalignant and cancer stem cells could be explained not only by defective protein segregation during asymmetric cell division but also by posttranscriptional mechanisms such as gene regulation by miRNAs. Two important observations prompted us to investigate potential changes in miRNA expression profiles within PSCs and CSCs: At first, regulators of miRNA biogenesis but also individual miRNAs have been shown to be directly or indirectly involved in the formation of certain tumors such as glioblastoma. More importantly, several genes involved in the regulation of asymmetric cell division are predicted targets for miRNAs (Enright et al, 2003), e.g. the cell fate determinant Notch is regulated by miRNA-1 during cardiac differentiation in *Drosophila* (Kwon et al, 2005)

In collaboration with Dr. Graeme Hodgson (Brain Tumor Research Centre, UCSF) I profiled expression of 238 miRNAs in samples of cultured neural stem cells by quantitative RT-PCR using TaqMan 238-plex miRNA assays and detected several differences between NSCs and PSCs.

Interestingly, we found that expression of 35 miRNAs was significantly downregulated in premalignant stem cells. The majority of these miRNAs has so far not been addressed or was not brain specific. However, some miRNAs found to be downregulated in PSCs were enriched in the brain and/or have brain specific functions. I concentrated in more detail at miR137 and miR124a, the latter being involved in neuronal differentiation. The loss of certain miRNAs in transgenic stem cells could either be a cause or a consequence of their differentiation defects. To distinguish between these possibilities, miR137 and miR124a were re-introduced into premalignant stem cells and the effect on their differentiation pattern evaluated.

In brief, wild type and premalignant stem cells were grown under adherent conditions in N5 medium. Synthetic miRNAs (Dharmacon) mimicking endogenous miRNAs were transfected into adherent cells using standard transfection methods (Lipofectamin, Invitrogen). In addition, I transfected cells with scrambled miRNA as controls. The next day, the medium was replaced with differentiation medium (N5 without EGF, FGF but 1% serum) and cells were cultured for additional 3 days, fixed and subjected to immunocytochemistry.

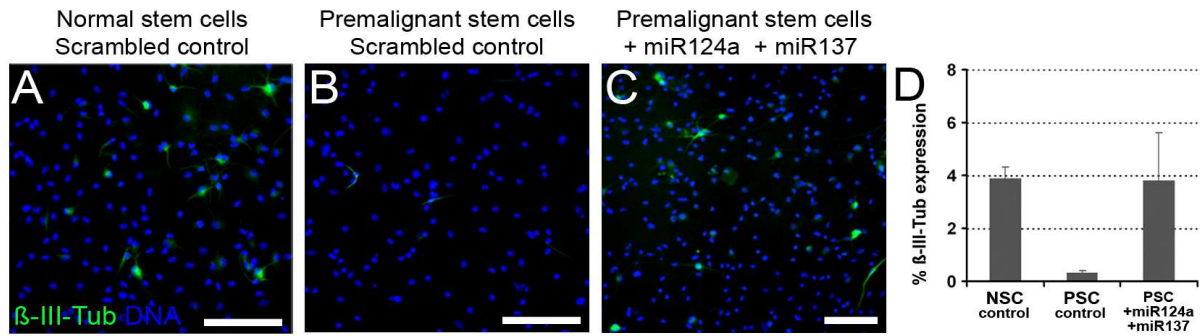


Figure 38: Reintroduction of miRNAs rescues the differentiation defect in premalignant stem cells. NSCs (A) and PSCs (B) were transfected with scrambled miRNAs as controls and grown under differentiation conditions for 3 days. In contrast to NSCs ($3.9 \pm 0.4\%$), only a few neurons could be detected in PSCs ($0.3 \pm 0.1\%$). (C) Transfection of miR-124a and miR-137 into PSCs increased the number of neurons to almost wild type levels ($3.8 \pm 1.8\%$). Scale bars represent 100 μ m.

Control neural stem cells induced to differentiate, generated $3.9 \pm 0.4\%$ neuronal cells as indicated by β -III-tubulin positive staining (Figure 39A,D). In contrast, only very few neurons were detected in the premalignant stem cells pool ($0.3 \pm 0.1\%$) (Figure 39B,D). The introduction of miR124a in combination with miR137 almost completely rescued the differentiation defect in premalignant stem cells as comparable amounts of neurons could be detected ($3.8 \pm 1.8\%$) (Figure 38C,D).

This result suggested that loss of miRNAs in the premalignant stem cell pool might contribute to the altered differentiation capabilities and impaired generation of neurons.

4.2 Discussion

The cancer stem cell theory states that tumors contain a subset of cells with the ability to self-renew and differentiate. Consequently, these are the only cells that can maintain tumor growth indefinitely and are also able to propagate tumor growth in immunodeficient mice. The remaining cells, although actively proliferating and making up the majority of the cells in the tumor lack tumorigenic potential (Ailles & Weissman, 2007; Cho & Clarke, 2008).

Although first demonstrated in human myeloid leukemia (Bonnet & Dick, 1997), evidence for the existence of a cancer stem cell compartment has recently also emerged in solid tumors, such as cancers of breast (Al-Hajj et al, 2003), pancreas (Li et al, 2007), head and neck (Prince et al, 2007), colon (Dalerba et al, 2007; O'Brien et al, 2007; Ricci-Vitiani et al, 2007) and brain (Galli et al, 2004; Singh et al, 2003; Singh et al, 2004; Hemmati et al, 2003; Ignatova et al, 2002).

Here I report on the isolation and characterization of cancer stem cells from a murine mouse model of oligodendroglioma that show all the features of stem cells and, in addition, the ability to generate new tumors following transplantation into immunocompromised mice that faithfully reproduce the phenotype of the primary tumor.

4.2.1 Tumor-derived cells share common characteristics of neural stem cells

Oligodendroglioma are diffusely infiltrating glial brain tumors which have aggressive characteristics and cause high mortality and morbidity (Ligon et al, 2006; Marie et al, 2001). EGFR amplification and loss of the tumor suppressors *ink4a/arf* and/or *p53*, respectively, are mutations frequently found in human oligodendroglioma. Similar, mice expressing an oncogenic version of the EGFR (*verbB*) in neural stem cells and their progeny from the *S100 β* promoter and lacking both copies of the tumor suppressor *p53* develop high grade oligodendroglioma reflecting the pathology of the human disorder (Weiss et al, 2003).

I could successfully isolate cancer stem cells from tumor bearing *S100 β -verbB*, *p53^{-/-}* mice by culturing them in serum-free conditions in the presence of growth factors, similar to those used for amplification and maintenance of normal neural stem cells as neurospheres (Doetsch et al, 1999; Reynolds & Weiss, 1992). Under these conditions, tumor derived cells formed free floating clusters (Figure 15A) and because of their origin, were referred to as tumorspheres. However, the neurosphere assay is only an indirect method to confirm the presence of CSCs in oligodendroglioma as they can only be identified retrospectively.

CD133, a cell surface marker previously shown to be expressed on normal human neural stem cells (Uchida et al, 2001) has also been proven useful to identify CSCs from human glioma (Singh et al, 2004). Unfortunately, I failed in my attempts to directly isolate CSCs from

murine oligodendroglial tumors using cell sorting techniques based on antibodies for prominin-1, the mouse homolog of CD133. Due to a lack of immunoreactivity with neural cells in the adult murine brain, available antibodies for prominin-1 were not suitable for the selection of either neural stem cells or cancer stem cells.

My results show that tumor-derived stem cells have the ability to form tumorspheres and can be propagated for prolonged times in culture. My data also rule out that tumorspheres originate from transit amplifying cells which are also known to undergo a limited number of passages when cultured under these conditions (Doetsch et al, 2002). Among the characteristics in common between oligodendroglioma-derived tumorspheres and normal neural stem cells is the expression of specific genes, including Nestin, Musashi and CD15/LeX (Figure 15), accepted markers for neural stem cells and early progenitors. Unfortunately, due to technical issues with available antibodies I could not include additional stem cell markers in this study, such as CD133/Prominin, Bmi1 and Sox2. Withdrawal of growth factors, presence of serum and culturing under adherent conditions resulted in the differentiation of tumor-derived cells into neurons, astrocytes and oligodendrocytes as indicated by their expression of β -III-tubulin, GFAP and O4 (Figure 16), respectively, suggesting that they are multipotential. Importantly, multipotentiality was maintained unaltered even after prolonged culturing of tumorspheres.

Together, I have demonstrated that tumor-derived stem-like cells and NSCs express many of the same genes and proteins and they share common characteristics, including self-renewal and multipotency. However, as discussed later, differences exist between NSCs and CSCs which undergo aberrant proliferation and differentiation, and to a high extent, recapitulate the properties of their parental tumor.

4.2.2 Oligodendroglioma derived cancer stem cells are tumorigenic and phenocopy the parental tumor in transplantation experiments

Collectively, my studies show that cells endowed with some of the features expected from stem cells can be found in tumors of murine oligodendroglioma. However, it was unknown whether these cells are involved in the establishment, expansion and recurrence of brain tumors, or in other words, whether they are tumorigenic. Alternatively, it is possible that they emerge as a result of the uncontrolled proliferation of the actual tumorigenic cells, which are developmentally disturbed.

The most widely accepted approach to validate a CSC population is xenotransplantation of CSCs in immunocompromised mice followed by serial transplantation (Clarke et al, 2006; Bonnet & Dick, 1997). In a similar approach, oligodendroglioma-derived stem cells were intracranially injected into FvB/N mice to determine their malignant potential. I found that

mice injected with as little as 1×10^4 cells showed severe neurological symptoms within days and reproducibly established large tumors (Figure 17) whereas control NSCs even injected at higher numbers never developed tumors. Next, to conclusively demonstrate the presence of CSCs in these tumors, serial re-transplantation experiments were performed. Primary CSCs cultured from a spontaneous *S100 β -*verbB*, p53^{-/-} tumor were orthotopically injected into FvB/N mice to establish a tumor. Symptomatic animals were sacrificed, the secondary tumor was excised, CSCs were isolated and cultured to establish a secondary CSC line. As before, these cells could initiate new tumors. CSCs could be sequentially transplanted into new recipients for several passages (Figure 20), always resulting in the formation of tumors that recapitulated the phenotype of the original tumor and the primary orthotopic tumor. This provides direct evidence for the *in vivo* self-renewal capacity and malignant potential of this population. Notably, following serial transplantation, CSCs formed more aggressive tumors which also developed faster. This is probably due to the accumulation of additional mutations during culturing *in vivo* and/or the selection of particularly aggressive cells following isolation and short time culture between the individual transplantations. However, even after culturing and serial transplantation, CSCs retained their ability to self-renew and differentiate.*

Orthotopic tumors essentially contained cells expressing typical markers of the oligodendrocytic lineage, mainly Olig2 and NG2 (Figure 21), as in typical human oligodendroglioma (Marie et al, 2001) and parental tumors. In addition, immunohistochemical analyses have shown that the majority of cells within the tumor displayed a morphology indicative of progenitor cells rather than mature oligodendrocytes which are infiltrating neighboring tissue at the border of the tumor (Figure 21). Similar to human oligodendroglioma and the parental tumor, the number of astrocytes and neurons was very low within the tumor whereas large quantities of these cells were present in the surrounding normal brain tissue. Interestingly, tumors also contained small numbers of Nestin positive neural precursor, which, after dissection and culturing of the tumor mass, might be the cells responsible for the formation of tumorspheres (Figure 21).

Furthermore, histopathologic analyses revealed that CSCs have the ability to recapture the pathophysiology of the parental tumor. Orthotopic tumors showed characteristic oligodendroglioma-like features such as high cellularity, high mitotic index, diffuse invasion, subpial infiltration and the characteristic “fried egg” appearance of cells (Figure 18).

In conclusion, tumor-derived progenitor cells satisfy all of the criteria necessary to be classified as brain cancer stem cells: first, they show cancer-initiating abilities upon orthotopic transplantation and phenocopy the tumor of origin. CSCs have extensive self-renewal ability, both *in vitro* and *in vivo* as shown by clonogenic neurosphere forming assays and successful serial orthotopic transplantations, respectively. In addition, they display multilineage differentiation capacity although they essentially recapitulate the phenotype of

the tumor from which they were derived from. Moreover, orthotopic tumors mimic the cellular composition and histology of the parental tumor.

Although there is a lot of empirical evidence for their existence, the origin of brain cancer stem cells is a highly controversial topic (Sakariassen et al, 2007). Brain tumors can be very heterogeneous, consisting of cells expressing markers of more than one neural lineage, implicating a multipotential cell of origin. Indeed, CSCs have been reported to be isolated from various brain tumors, including gliomas, astrocytoma, medulloblastoma and ependymomas (Nakano & Kornblum, 2006). However, it remains to be determined, whether solid tumors arise from the transformation of stem cells, or alternatively, whether tumor cells reactivate the signaling pathways used by stem cells to regulate self-renewal, proliferation and differentiation. In general, stem cells persist the whole lifetime of an organism and have the potential to extensively self-renew and proliferate thus making them a likely target for tumorigenesis (Huntly & Gilliland, 2005). Recent experiments in mice further support the cancer stem cell theory. Many tumors develop near germinal zones of the adult brain, such as the SVZ, and exposure to oncogenes results in the formation of tumors preferentially in this region as opposed to non-proliferative brain areas (Sanai et al, 2005; Hopewell & Wright, 1969).

Transit amplifying cells, the immediate descendants of neural stem cells have been shown to undergo extensive proliferation at the expense of neuroblast formation when exposed to high concentrations of EGF. Prolonged exposure to EGF leads to the conversion of these cells to highly infiltrative cells with glial characteristics and the ability to move along white matter tracts and blood vessels (Doetsch et al, 2002), properties also associated with glioma cells. Interestingly, EGFR amplification is frequently found in human oligodendroglioma (Weiss et al, 2003) and other brain tumors (Mellinghoff et al, 2005; Maher et al, 2001; Wechsler-Reya & Scott, 2001). Thus, activation of signaling pathways that normally regulate stem cells may play an important role in brain tumor formation. Excessive signaling through these pathways in neural stem or progenitor cells might induce transformation of these cells and can also help to explain the formation of oligodendroglioma in a mouse model with activated EGFR signaling. Moreover, EGFR is involved in neural development and regulates proliferation and self-renewing capacities of adult neural stem cells (Sibilia et al, 2007). Indeed, CSCs showed increased self-renewing capacities (Figure 23) and proliferation rates (Figure 33) compared to neural stem cells isolated from the SZV of control mice.

4.2.3 Stem cells undergo changes before tumor occurrence - progression of neural stem cells to premalignant and cancer stem cells

Characterizing in more detail those cells in the brain tumor population that are able to maintain the tumor will give insights into the mechanism of brain tumorigenesis and will allow us to trace back to the cell of origin in the normal brain. One can speculate that CSCs are indeed generated from defective adult neural stem cells evading normal cell cycle control and differentiation. After accumulation of additional mutations, this aberrant pool of stem cells will be able to generate tumors.

The transgenic *S100 β -verbB*, *p53*^{-/-} model provides an excellent and fast model for oligodendroglioma formation. However, to study initial events and the stepwise progression from normal stem cells to cancer stem cells I made use of *S100 β -verbB* mice heterozygous for *p53*, in which tumors developed with a significant delay of 4-6 months. Neural stem cells were isolated from the SVZ of tumor prone *S100 β -verbB*, *p53*^{+/-} mice prior to tumor occurrence and thus referred to as premalignant stem cells. Next, changes in characteristic properties of stem cells such as self-renewing, differentiation or the ability to divide asymmetrically were investigated.

To test whether the self-renewing capacity of stem cells might already be affected at premalignant stages, I performed so called neurosphere forming assays and quantified secondary sphere formation. Interestingly, I found that similar to CSCs, stem cells from *S100 β -verbB*, *p53*^{+/-} mice had higher self-renewing capacities compared to controls although not as severe as in the case of the cancer stem cell pool (Figure 23). The number of sphere-forming cells correlates with the number of stem cells and transit amplifying cells, both able to self-renew, and unfortunately I cannot say which of these cells contribute to what extent to the formation of secondary spheres. Is there really a higher number of stem cells in the premalignant pool? Or is the amount of stem cells unaltered but the generation of transit amplifying cell increased, maybe due to defects in asymmetric cell division? This question is difficult to assess as there are no specific markers which convincingly identify either cell type. However, in an alternative approach, I found higher expression of CD15/Lex, a marker for neural progenitors (Capela & Temple, 2002) in proliferating PSCs supporting the finding that the self-renewing capacity of adult stem cells is increased already at premalignant stages. In contrast, the *in vitro* proliferation rate of PSCs was not significantly altered compared to controls. However, as mentioned before, dissociated spheres are very heterogeneous and consist not only of stem cells but also of transit amplifying and other progenitor cells. Thus, different intrinsic proliferation properties of individual cell types might mask changes in the proliferation of distinct subpopulations. Again, to study the properties of individual cell types

in more detail, techniques to specifically isolate cells based on marker expression would be necessary.

To evaluate changes in survival of transgenic stem cells due to loss of p53, TUNEL assays were performed to detect cells undergoing programmed cell death. Neural stem cells from controls, PSCs and CSCs were grown under proliferative conditions or induced to differentiate but no differences in the number of apoptotic cells were observed (Figure 34 and data not shown). However, it is possible that in the context of the original surrounding (e.g. the stem cell niche), cells would receive various stimuli inducing them to either proliferate or undergo apoptosis which could not be assessed in this *in vitro* system. Thus, it will be necessary to study apoptosis and survival of neural stem and progenitor cells *in vivo* and/or challenge these cells with cytotoxic agents to evaluate their response to apoptotic stimuli.

4.2.4 Differentiation defects in transgenic stem cells

Although tumor-derived progenitor cells share many similarities with NSCs I could already demonstrate that CSCs show increased self-renewing and proliferation capacities. In addition I found that CSCs undergo aberrant differentiation. When induced to differentiation, CSCs generated all three neural cell types, i.e. neurons, astrocytes and oligodendrocytes (Figure 16). However, the number of neurons and astrocytes was relatively low, and the majority of cells (> 80%) expressed markers of early oligodendrocyte progenitors, namely Olig2 and NG2 (Figure 25,26). In addition, when injected orthotopically, CSCs primarily gave rise to immature oligodendrocytes as shown by marker expression (Figure 21). Together, this suggests that CSCs have lost their normal differentiation potential and essentially recapitulate the properties of the tumor they originate from; in the case of oligodendroglioma, this mainly leads to the generation of cells of the oligodendrocyte lineage.

Interestingly, in premalignant stem cells isolated long before tumor formation, an considerable increased number of Olig2 positive cells ($29.3 \pm 3.9\%$) was detected compared to NSCs from wild type controls ($18.4 \pm 2.5\%$) (Figure 25). Essentially the same results were obtained in the expression of NG2 in control NSCs ($8.8 \pm 2.5\%$) and PSCs ($24.4 \pm 7.9\%$) grown in the absence of growth factors (Figure 26). These findings were remarkable as altered stem cell properties at a stage before tumor formation strongly support the idea that normal stem cells progressively develop towards cancer stem cells. However, to conclusively make such a statement, more research is needed to be done. Here, only premalignant stem cells isolated at 2 months postnatal were investigated. The whole timeframe of tumor formation should be covered to evaluate whether the number of oligodendrocytes generated from PSCs indeed increases continuously. I propose that PSCs give rise to CSCs by progressively acquiring additional mutations and should therefore be more sensitive to

transforming mutations than normal stem cells. To prove that, PSCs and NSCs shall be challenged with oncogenes or, alternatively, tumor suppressors shall be knocked out, to become cancer stem cells. In combination with respective imaging techniques developed at UCSF it will be possible to monitor tumor outgrowth after orthotopic injection of these cells into recipient mice and to compare their malignant potential. It could already be demonstrated that unmodified PSCs were not tumorigenic, as even transplanted at higher number, PSCs never induced tumor formation (Figure 30). I hypothesize that these cells have not yet accumulated all the changes necessary to become malignant. The finding that PSCs develop a higher malignant potential when challenged to become CSCs would strongly suggest a stepwise transition to a malignant state.

The accumulation of Olig2⁺/NG2⁺ positive cells observed in differentiation experiment suggests an increased potential of transgenic stem cells to further develop into the oligodendrocyte lineage. Surprisingly, when tested for the more mature oligodendrocyte marker O4, only a moderate increase of O4 positive cells was found in the progeny of PSCs ($5.3 \pm 2.8\%$) and CSCs ($4.7 \pm 2.1\%$) compared to the wild type population ($2.3 \pm 0.7\%$) (Figure 28). Moreover, obvious differences in their morphology were found. Oligodendrocytes generated from NSCs and PSCs show a typical stellate morphology and were highly branched, whereas O4 positive cells derived from CSCs were much less branched. The majority of CSCs differentiated mainly in NG2 positive cells of round shape (Figure 27). In addition, even in the absence of growth factors, conditions which normally favor neural stem cells to differentiate, CSCs continued to proliferate suggesting that these cells, at least to a high extent, did not respond to the differentiation stimulus. It is important to note that even prolonged culturing under differentiation conditions (up to 14 days) did not essentially increase the number of mature oligodendrocytes. The high number of oligodendrocyte progenitor cells derived from CSCs under conditions which induce differentiation, together with the morphological abnormalities and continuous proliferation indicates that these cells possess a block in their differentiation potential which would explain the accumulation of immature oligodendrocytes.

Next, I determined to what extent cells of the neuronal and astrocytic lineage were affected in transgenic stem cells and stained differentiated cultures from NSCs, PSCs and CSCs for the neuronal marker β -III-tubulin and for GFAP to identify astrocytes.

The amount of neurons derived from PSCs ($4.5 \pm 3.1\%$) and CSCs ($6.2 \pm 4.1\%$) was lower compared to wild type controls ($14.4 \pm 10.7\%$) (Figure 28). However, it is noteworthy, that these differences are not statistically significant as one of the described wild type cell lines only expressed very few neurons resulting in a very high standard deviation. Usually, stem cells from wild type animals generated more neurons (around 25%) and I observed a clear

tendency of decreased numbers of β -III-positive cells in PSCs and CSCs. Anyway I would need to establish additional wild type lines to statistically strengthen this observation.

Astrocytes represent the majority of differentiated control stem cells ($36.0 \pm 3\%$). Similar to neurons, the number of GFAP-immunoreactive cells was considerably reduced in PSCs ($26.1 \pm 5.4\%$). More dramatically, I could only detect very few astrocytes ($2.3 \pm 1.1\%$) when CSCs were cultured under differentiation conditions (Figure 29).

Interestingly, SVZ-derived neural stem cells from $S100\beta$ -*verbB*, $p53^{-/-}$ animals showed a very similar differentiation pattern as CSCs. These cells preferentially developed into $Olig2^+$ ($64.7 \pm 0.9\%$) and $NG2^+$ ($74.6 \pm 3.5\%$) oligodendrocyte progenitors whereas the number of β -III-tubulin positive neurons was very low ($3.9 \pm 3.7\%$) (Figure 31). Furthermore, when these cells were transplanted into FvB/N mice, recipients developed tumors that phenocopied CSCs derived orthotopic tumors. This observation was interesting as it may indicate that neural stem cells from $S100\beta$ -*verbB*, $p53^{-/-}$ mice already have transformed and were the initiating cause of oligodendroglioma formation. However, conclusions from this result must be viewed with caution. Oligodendroglioma start developing within 2 month in the $S100\beta$ -*verbB*, $p53^{-/-}$ model and at the time when neural stem cells have been isolated from the SVZ of these animals, tumor formation has already been detected. In addition, oligodendroglioma are highly infiltrative and thus, I cannot rule out a contamination with tumor cells and potential CSCs in my preparation.

Both, $S100\beta$ -*verbB*, $p53^{+/-}$ and $S100\beta$ -*verbB*, $p53^{-/-}$ mice developed high grade oligodendroglioma but it was not known to what extent defective EGFR signaling and loss of the tumor suppressor p53 contribute to the defects observed in PSCs and CSCs. Transgenic mice exclusively overexpressing *verbB* from the $S100\beta$ promotor develop low-grade oligodendroglioma (Weiss et al, 2003). Interestingly, after differentiation, these cells showed very similar marker expression compared to premalignant stem cells. Loss of p53, on the other hand, had little effect on the differentiation pattern and was comparable to wild type neural stem cells (Figure 32). Together, these results indicate that alterations in EGFR signalling but not loss of the tumor suppressor p53 are responsible for the observed differentiation defect.

Together, I observed for the first time that neural stem cells in oligodendroglioma prone mice show significant alterations in their differentiation potential already long before tumor occurrence; they preferentially generate oligodendrocyte progenitors with delayed or impaired maturation at the expense of astrocytic and neuronal cells. However, they never formed orthotopic tumors following intracranial transplantation into recipient mice and thus were referred to as premalignant stem cells. These results strengthen the hypothesis that early defects in neural stem cells, together with additional genetic alterations lead to a

progression to a more malignant stem cell type, the cancer stem cells, which are responsible for tumor growth and maintenance. I was able to isolate stem-like cells from murine oligodendroglioma which show essentially the same differentiation behavior as PSCs although even more severe, again supporting the idea that it is a transformed stem cells rather than a differentiated cell which drives tumorigenesis.

4.2.5 Defects in asymmetric cell division and epigenetic changes influence stem cell differentiation

Proliferation and survival were not significantly altered in premalignant stem cells and thus it is unlikely that these factors contributed to the observed differentiation defects.

miRNAs are small, non-coding RNAs that primarily function as gene regulators (Bartel, 2004). They potentially regulate thousands of genes of which many are involved in transcriptional regulation or other essential cellular functions, such as cell cycle control (Lewis et al, 2003). Therefore, it is not surprising that miRNAs play important roles in diverse biological processes. Importantly, various miRNAs have been shown to regulate cell fate, including lineage differentiation in a number of tissue types. For example, miR181 has been shown to modulate hematopoietic lineage differentiation (Chen et al, 2004), miR223 regulates human granulopoiesis (Fazi et al., 2005), miR1 and miR133 promote myogenesis and myoblast proliferation (Chen et al, 2006). In the brain, miR124a and miR9 affect neural lineage differentiation (Krichevsky et al, 2006; Krichevsky et al, 2003). In addition, miRNAs participate in the control of cell proliferation and apoptosis (Cimmino et al, 2005; Chan et al, 2005; Brennecke et al, 2003). Interestingly, several genes involved in the regulation of asymmetric cell division are predicted targets for miRNAs (Enright et al, 2003). Because of the importance of miRNAs in such essential functions, it is not surprising that abnormalities in miRNA expression are likely to contribute to many pathological processes including the development of cancer (Cheng et al, 2005; Krichevsky et al, 2003).

Indeed, several miRNAs were downregulated in premalignant stem cells which was demonstrated by expression profiling of 238 miRNAs (a collaboration with Dr. Graeme Hodgson, UCSF Brain Tumor Research Centre). Consistent with that, another study reported a decrease of miRNA expression in several types of cancer (colon, kidney, prostate, urinary bladder, lung and breast) when compared to normal tissue (Lu et al, 2005). Analysis of the expression of miRNAs in glioblastoma multiforme cell lines identified nine overexpressed miRNAs and four miRNAs with lower expression levels (Ciafrè et al, 2005). One of the overexpressed miRNAs, miR21 has been suggested to be anti-apoptotic (Chan et al, 2005).

I have to mention that this first expression profiling analysis was performed on PSCs originating from another oligodendroglioma model, the *S100 β -verbB*, *ink4a/arf^{+/-}* model.

PSCs isolated from these transgenic animals essentially showed the same phenotype as the S100 β -*verbB*, p53^{+/-} model, i.e. increased numbers of oligodendrocyte progenitors at the expense of astrocytes and neurons. However, tumor formation in this model was less consistent and thus I decided to continue my study with S100 β -*verbB*, p53^{+/-} transgenic animals. Anyway, in this first screen, two interesting candidates with significantly reduced expression levels were identified - miR137 and miR124a, the latter being involved in neuronal differentiation. When I re-introduced these miRNAs into premalignant stem cells and induced them to differentiate, they essentially generated the same amount of neurons as wild type neural stem cells (Figure 38). In contrast, hardly any neurons could be detected in PSCs transfected with scrambled miRNA as control. These results suggest that loss of these miRNAs in the premalignant stem cell pool might directly contribute to the impaired generation of neurons following differentiation. Even a preliminary experiment as shown here has highlighted that miRNAs are undoubtedly involved in the observed differentiation phenotype. However, more work needs to be done before I can dissect the contribution of miRNAs in the progression of neural stem cells to premalignant stem cells and later tumorigenesis. These experiments need to be repeated including more miRNAs and cell lines. Moreover, it has to be evaluated whether altered miRNA levels also affect other neural cell types, e.g. it would be interesting to find out whether reintroduction of miR137 and miR124a also reduces the high number of NG2 and Olig2 positive oligodendrocyte progenitors. Importantly, in an additional miRNA expression profiling experiment which has only been finished very recently and included various cancer stem cell lines from S100 β -*verbB*, p53^{-/-} mice, the loss of e.g. miR124a has been confirmed.

In addition to epigenetic changes, the reported differentiation phenotype of PSCs and CSCs might also be explained by abnormal asymmetric cell division which normally is required to generate cell fate diversity and to maintain the pool of progenitor cells. Understandably, the balance between symmetric and asymmetric cell divisions must be tightly controlled. Indeed, there is a lot of empirical evidence that dysfunctional ACD is an initiating factor in brain cancer development. Normally, *Drosophila* neuroblasts divide asymmetrically as a result of the asymmetric localization cell fate determinants such as Numb and Prospero. However, when the machinery that regulates ACD is disrupted, these neuroblasts divide symmetrically and form tumors (Caussinus & Hirth, 2007; Lee et al, 2006b; Caussinus & Gonzalez, 2005; Klezovitch et al, 2004). Mutants for the cell fate determinant Numb or Prospero are tumorigenic and can be serially transplanted into new hosts. Moreover, these tumor cells have been shown to be capable of rapid neoplastic transformation (Caussinus & Gonzalez, 2005). Mutants for PINS and Lgl generate neuroblasts that divide symmetrically and essentially self-renew instead of giving rise to more committed progeny (Lee et al, 2006b). Similar, the human homologue of Lgl, Hugel-1, is frequently deleted in cancers (Kuphal et al,

2006; Schimanski et al, 2005) and loss of cell polarity causes severe brain dysplasia in *Lgl* knockout mice (Klezovitch et al, 2004). On the other hand, overexpression of a constitutively active form of aPKC, normally localized to the apical cortex of the *Drosophila* neuroblast as part of the Par complex, causes a large increase in symmetrically dividing neuroblasts (Lee et al, 2006b). In addition, aPKC has been reported to play an important role in human lung cancer (Regala et al, 2005). The observation that some proteins can both induce symmetric cell divisions and function as an oncogene in mammalian cells further supports the evidence for a link between defects in asymmetric cell division and cancer.

The apparatus regulating ACD is very well conserved and indeed, in mammalian stem cells I have identified the expression of murine *Lgl-1*, *Par3*, *Par6a*, *Par6b* and *Numb*, which are known regulators of *Drosophila* neuroblast ACD (Figure 35). These results suggest that cultured stem cells have the potential to divide asymmetrically to generate the heterogeneous cell population found within neurospheres. To verify this assumption and to investigate ACD of neural stem cells in more detail, I performed cell pair assays (Sun et al, 2005; Shen et al, 2002) to visualize asymmetrically dividing cells by immunocytochemistry. Both asymmetric and symmetric distribution of the stem/progenitor cell marker CD15/LeX were detected which suggest that these types of divisions reflect their ability to either increase the stem or progenitor pool or to generate one cell with different cell fate (Figure 36). In agreement with earlier data, I also found EGFR to be asymmetrically segregated during stem cell division (Sun et al, 2005) (Figure 36). Neural stem cells can be stimulated by EGF and its receptor EGFR has been shown to influence progenitor cell fate (Burrows et al, 1997) and it is very likely that cells inheriting EGFR continue to acquire stem cell fate and continue to self-renew whereas the other cell becomes more committed and differentiates into a specific neural cell type. The fact that EGFR signalling is often deregulated in cancers makes a scenario plausible where both daughter cells inherit this receptor which leads to the excessive accumulation of self-renewing progenitor cells instead of a hierarchical generation of different cell types. Similar to *Drosophila*, *Numb* is a well-established regulator of cell fate in mammalian stem cells (Petersen et al, 2004; Petersen et al, 2002; Shen et al, 2002; Zhong et al, 1996a). Indeed, I found *Numb* to be expressed in cultured neural stem cells and could also detect asymmetric as well as symmetric cell division (Figure 36). The asymmetric localization of *Numb* in *Drosophila* neuroblasts requires the assembly of an apical complex consisting of Par proteins and other regulators of ACD (Goldstein & Macara, 2007; Suzuki & Ohno, 2006; Betschinger & Knoblich, 2004). Similar, the Par complex is also conserved in mammalian cells and homologues of *Par3* and *Par6* have been identified as regulators of cell polarity (Joberty et al, 2000; Izumi et al, 1998). Consistent with that data, *Par3* was expressed in a large proportion of cells. However, it was surprising that I never detected asymmetric distribution of this protein in dividing cell pairs which I had expected from a

regulator of cell polarity. It has been demonstrated that epithelial extrinsic signals are required for the timing and positioning of Par proteins in *Drosophila* neuroblasts (Siegrist & Doe, 2006). Thus it is possible, that my assay conditions, i.e. an isolated stem cell dividing in the absence of extrinsic cues, interfere with the establishment of cell polarity and asymmetric localization of Par3. It does not explain, however, why proteins like Numb which have been shown to depend on the formation of an apical polarity complex, at least in *Drosophila*, were still able to asymmetrically localize and become exclusively inherited by one daughter cell only. However, it cannot be ruled out that the ubiquitous Par3 localization detected in immunostainings resulted from unspecific binding of the available antibody. Notably, I never detected Par6 protein in neural stem cells by immunocytochemistry using the available commercial antibodies although Par6 expression was demonstrated by PCR. Similar, Lgl-1 expression was detected by PCR but due to the lack of a functional antibody I could not further investigate its role in the asymmetric cell division of cultured neural stem cells.

Olig2 promotes oligodendrogenesis (Hack et al, 2005) by either up- or downregulation in a committed cell, or alternatively, by asymmetric inheritance by only one daughter cell during cell division. In pair assays, Olig2 was found to be symmetrically distributed in all cell divisions observed which argues against a role for Olig2 as a classical segregating determinant.

In contrast, a high proportion ($53.8 \pm 15.4\%$) of adult neural stem cells showed asymmetric segregation of NG2. Strikingly, this frequency was significantly reduced in premalignant stem cells ($14.9 \pm 3.2\%$) and cancer stem cells ($5.2 \pm 2.1\%$) (Figure 37). This observation was very interesting as the impaired ability to localize NG2 exclusively to one cell and consequently more symmetric divisions might explain such a high number of NG2 positive oligodendrocyte progenitors in differentiating PSC and CSC cultures. Increased numbers of symmetric divisions may not only promote the expansion of this cell type, but might also be permissive for events leading to genetic instability. The machinery controlling asymmetric cell division also controls the orientation of the mitotic spindle (Lee et al, 2006a; Yamanaka et al, 2003; Kaltschmidt et al, 2000), and a defective centrosome presumably might lead to errors in chromosome segregation (Caussinus & Gonzalez, 2005). The tight regulation of centrosome function by tumor suppressors is also important in mammalian cells to avoid genetic instability (McDermott et al, 2006).

Together, my data strongly support the cancer stem cell theory because they provide a mechanistic insight into defects of adult stem cells at a premalignant stage which become more severe at later stages when these cells transform into cancer stem cells. In addition, my results provide a direct link between oncogenic mutations in EGFR signalling and defects in asymmetric cell division. Clearly, further studies are needed to understand whether the increase of symmetric NG2 distribution is a result of the defective localization of known ACD

regulators. To that end, the ratio of asymmetric to symmetric cell divisions has to be quantified also for the other markers identified to be asymmetrically localized during neural stem cell mitosis. In addition, it needs to be evaluated whether the situation is similar *in vivo* by using cell tracing systems based on selective lentiviral infection of stem cells with GFP markers to follow their progeny. Moreover, further studies in additional tumor types from various species are needed to prove that defective ACD is the initiating factor in tumor development.

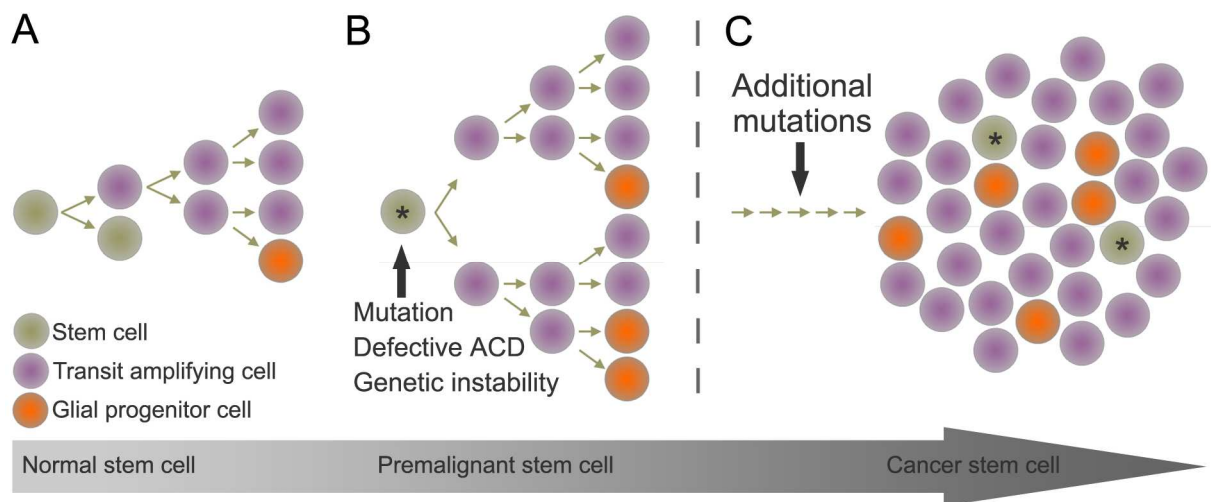


Figure 39: Progressive model for the generation of premalignant stem cells and cancer stem cells from normal adult stem cells. (A) Normal adult stem cells and their immediate progeny divide asymmetrically to self-renew and to generate a more committed cell. They also can divide symmetrically to expand stem cell number. (B) An initiating mutation in an multipotential stem cell (star) causes a defect in asymmetric cell division and a shift to more symmetric cell divisions. (C) Premalignant stem cells generate aberrant progeny, are genetically instable and after acquiring additional mutations, turn into cancer stem cells.

The cancer stem cell model has fundamental implications for the development of new cancer therapeutic agents and identifies a novel cellular target that might be amenable to novel treatments. Stem cells, in general, are relatively quiescent, resistant to cytotoxic agents through the expression of drug efflux pumps and have an active DNA-repair capacity and resistance to apoptosis (Dean et al, 2005). As cancer stem cells share many of the properties of normal stem cells, conventional chemo- and radiation therapies targeting rapidly cycling cells will only lead to the reduction of the tumor by killing the progeny of the CSCs. However, the CSCs themselves will remain unaffected and contribute to tumor occurrence. Moreover, the expression of ATP-binding cassette (ABC) drug transporters will make them even more resistant to these forms of treatment. Only recently, CD133⁺ brain cancer stem cells have been shown to be resistant to radiation, both *in vivo* and *in vitro*, which was contributed to an increase in DNA-repair capacity (Bao et al, 2006a).

Consequently, it is necessary to alter the current paradigm in drug development as eradication of various cancers might require the targeting and elimination of cancer stem cells. However, there is a theoretical concern that normal stem cells could be damaged when targeting CSCs as many pathways are shared by CSCs and their normal counterparts. Self-renewal pathways that are potential targets for disruption can be altered in CSCs allowing for specific targeting and disruption (Yilmaz et al, 2006). Thus, a promising way to eliminate CSCs without damaging normal stem cells would be to target an oncogenic mutation only present in CSCs that affect their ability to self-renew. Indeed, there is some evidence from studies in leukemia that cancer stem cells can be targeted separately from normal hematopoietic stem cells (Gage, 2000; Guzman et al, 2007; Guzman et al, 2005). In the future, selective targeting and elimination of the cancer stem cell population may result in improved clinical outcome for patients with even advanced cancers.

5 Material and Methods

5.1 Animals

5.1.1 Transgenic mice

Transgenic mice used in this study that express *verbB* under the control of the $S100\beta$ promoter and either heterozygous ($S100\beta$ -*verbB*, $p53^{+/-}$ mice) or homozygous ($S100\beta$ -*verbB*, $p53^{-/-}$) for the tumor suppressor p53 have been described previously (Weiss et al, 2003). $S100\beta$ -*verbB* mice develop low-grade oligodendroglioma by overexpressing the avian oncogene *verbB* in postnatal neural stem cells and their progeny in the subventricular zone. Loss of p53 leads to the development of high-grade oligodendroglioma in $S100\beta$ -*verbB*, $p53^{+/-}$ and $S100\beta$ -*verbB*, $p53^{-/-}$ mice although tumor development in animals heterozygous for p53 is significantly delayed.

Wild type mice used in this study were FvB/N mice. Mouse colonies were maintained at the University of California, San Francisco and all animal procedures were performed in accordance with National Institutes of Health and UCSF guidelines.

5.1.2 *Drosophila* strains

For live imaging full length Miranda-GFP was expressed with the UAS/GAL4 system (Brand & Perrimon, 1993) using *scabrous*-Gal4 (Nakao & Campos-Ortega, 1996), *neuralized*-Gal4 (Bellaïche et al, 2001) or *v32*-Gal4 (Petritsch et al, 2003) driver lines. To generate a fusion of GFP and the N-terminus of Miranda, a fragment encoding eGFP generated by PCR using eGFP-vector (Clontech) as template was fused to full-length Miranda amplified by PCR from Miranda-bluescript-SK (Petritsch et al, 2003) with a small linker region and cloned into the pUAST vector. Several independent transgenic lines were generated as described (Petritsch et al, 2003). UAS-Miranda-GFP was combined with red fluorescent histoneH2AvD-mRFP (Schuh et al, 2007) or with UAS-Lgl^{3A} (Betschinger et al, 2003b). Live imaging for PON was performed with UAS-PON-GFP ; *sca*-Gal4 (Roegiers et al, 2001). FRAP experiments of free eGFP were performed using UAS-eGFP (Bloomington stock center).

5.2 Tissue culture

5.2.1 Adult neurosphere culture

Neural stem cells were isolated from the subventricular zone of adult mice (8 weeks postnatal, if not otherwise indicated) essentially as described previously (Doetsch et al, 1999). In brief, mice were anesthetized with 2,2,2-tribromoethanol and killed by cervical dislocation and their brains were removed and placed in $\text{Ca}^{2+}/\text{Mg}^{2+}$ free Hanks' buffer (HBSS) supplemented with penicillin and streptomycin (P/S, UCSF cell culture facility). The lateral walls of the lateral ventricle were dissected, collected in HBSS and incubated for 40 min at 37°C in an activated papain solution. Papain was activated 30 min in advance by incubating 300 μL papain suspension (Worthington) in 1 mL activation solution (1.1 mM EDTA and 5.5 mM L-cystein in H_2O) and further diluted with 4 mL HBSS. Cells were collected by centrifugation (1000 rpm, 10 min, 4°C) and resuspended in cold Neurobasal -A medium (Gibco) without any growth factors or antibiotics. Cells were dissociated by carefully triturating with a P1000 pipette until no clumps were visible and collected by centrifugation (1000 rpm, 10 min, 4°C). The cellular pellet was re suspended in Neurobasal -A medium and centrifuged again. After a final washing step cells were filtered through a 40 μm cell strainer, plated in ultra low adherent 6-well plates (Corning) in neurosphere complete medium (Neurobasal -A medium (Gibco) containing B27 supplement (Gibco), 20 ng/mL epidermal growth factor (EGF, Sigma), 20 ng/mL basic fibroblast growth factor (bFGF, Peprotech), glutamine and P/S) and maintained at 37°C and 5% CO_2 . The culture medium was replaced every 3-4 days.

5.2.2 Isolation of cancer stem cells from oligodendroglioma

For the isolation of cancer stem cells, tumor tissue was dissected from oligodendroglioma, enzymatically dissociated as described above (see 5.2.1) and cultured under the same conditions as neural stem cells (tumorsphere culture).

5.2.3 Passaging of neuro- and tumorspheres

Neurospheres were usually passaged once a week by harvesting them by centrifugation (1000 rpm, 5 min, room temperature), incubating them with Accumax (Innovative Cell Technologies) for 10 min and carefully triturating them. Usually, single cells were then plated at a density of 40000 cells/mL medium in ultra low adherent plates.

5.2.4 Sphere forming- and cell proliferation assays

The self-renewing capacity of isolated neural stem cells and cancer stem cells was estimated using a sphere-forming assay. For neurosphere formation, a single cell (in a 96-well plate) or higher number of cells (200 cells/24 well plate) were maintained in complete medium and the number of secondary spheres was counted after 7-10 days. Proliferation assays were performed using the CyQuant kit (Molecular Probes) according to manufacturers instructions. For these assays, cells were cultured under adherent conditions in DMEM/F12 medium enriched with N2 supplement (Gibco), 35 µg/mL bovine pituitary extract (BPE, Gibco), 20 ng/mL EGF, 20 ng/mL bFGF, glutamine and P/S (N5 medium). Cells were plated at a density of 2500 cells/96 well plate, and cell numbers were measured at the days indicated using a micro plate reader.

5.2.5 Differentiation of neurosphere cultures

Differentiation of early passage spheres was induced by plating dissociated cells at a density of 25000 cells/well in CC2 coated Lab Tek II 8 well chamber slides (Nunc) in Neurobasal -A medium containing 1% FCS (Hyclone), B27 supplement, glutamine and P/S in the absence of growth factors (differentiation medium). Chamber slides were processed 7 days later using immunocytochemistry (see 5.3.3).

5.2.6 Cell pair assays

To study the asymmetric distribution of cell fate markers cell pair assays were performed essentially as described previously (Shen et al., 2002). In brief, spheres were dissociated and single cells were plated at clonal densities (30-40 cells) in Terasaki well plates (Nunc) in complete medium. After 20-24 hours cells were fixed and subjected to immunocytochemistry.

5.2.7 Transfection of miRNAs into neural stem cells

Cells maintained in N5 medium under adherent conditions were incubated with 1 mL 0,05% trypsin for 2 minutes, transferred to a Falcon tube using 5 mL N5 medium and washed two times with PBS. Then, cells were plated at 25000 cells/well in 8 well chamber slides and cultured under proliferative conditions in N5 medium

After 2 days, the medium was replaced with 250 µL N5 transfection medium, i.e. N5 medium without P/S. Lipofectamin transfection reagents (Invitrogen) were prepared according to the manufacturers instructions. In brief, 0,75 µL Lipofectamin was mixed together with 24,25 µL Optimem medium and incubated for 5 min at room temperature. Then, miRNAs (miR124a, miR137; Dharmacon) diluted in Optimem medium were added to get a final concentration of

100 nM and a total volume of 50µL. After a 20 min incubation at room temperature, the transfection reagent was pipetted dropwise on the cells. In addition, negative controls using scrambled RNA were performed.

The next day, the medium was changed to N5 differentiation medium and cells were subjected to immunocytochemistry after another 3 days.

5.3 Immunostaining and histology

5.3.1 Immunofluorescence on *Drosophila* embryos

Embryos were washed with embryo wash (0,7% NaCl, 0,03% Triton X-100) and dechorionated in 5% sodium-hypochlorite for 2 minutes. Embryos were fixed in 500 µL heptane and 500 µL formaldehyde (37%) for 4 min on the Multireax shaker (Heidolph Instruments). For devitalisation, the lower phase was removed and replaced by 500 µL methanol and embryos were vortexed hard for 30 s. After embryos settled down, the supernatant was removed followed by two short washing steps with methanol. Then, embryos were quickly washed twice with PBT and then twice for 5 min.

After blocking in 5% normal goat serum for 1 hour at room temperature, embryos were incubated over night at 4°C in primary antibodies diluted in blocking solution. Next day, the antibody solution was removed and embryos were washed 6 x 5 min in PBT and incubated with secondary antibodies coupled to Cy3 and Cy5 (Jackson), respectively, at 1:200 for 1 h at room temperature. Embryos were again washed 6 x 5 min in PBT, nuclei stained with TOTO3 (1:1000; Molecular probes) followed by 2 additional washing steps. Finally, embryos were mounted in Vectashield mounting medium. Samples were stored at -20°C or directly analyzed by confocal microscopy (Leica TCS SP2).

5.3.2 Whole-mount *in situ* hybridization of *Drosophila* embryos

Whole mount *in situ* hybridization was done according to (Tautz & Pfeifle, 1989) using an antisense RNA probe derived from *miranda* cDNA labelled with digoxigenin-UTP (Roche). Embryos were hybridized at 65°C o/n in hybridization solution, followed by incubation with mouse anti-DIG 1:2000 (Roche) and rabbit anti-Miranda (1:100) and detection of *Miranda* RNA and protein using secondary antibodies coupled to Alexa⁴⁸⁸ and Cy3 at 1:200. Images were taken on a Leica TCS SP2 confocal microscope.

5.3.3 Immunocytochemistry

For immunostaining of cultured cells, cells were washed twice with PBS, fixed for 15 min with 4% Paraformaldehyde (PFA, Sigma) at room temperature, rinsed twice in PBS and blocked in 5% normal serum with or without 0.1% Triton X-100 (Sigma) for 60 min. Cells were incubated overnight with primary antibodies at 4°C (for a complete list of antibodies and conditions used in this study see Table 2). After repeated washing steps, cells were incubated with the appropriate secondary antibody coupled to Alexa⁴⁸⁸ and Alexa⁵⁹⁴ (Invitrogen) at a dilution of 1:1000 for 1 h at room temperature. For nuclei staining, cells were incubated for 10 min in 4,6-diamino-2-phenylindole (DAPI, Sigma) and washed with PBS. Slides were finally mounted with Moeviol and cells were observed by conventional fluorescence microscopy (Zeiss, Axioplan). Negative controls were performed by omitting the incubation with the primary antibody and/or incubation with the appropriate isotype controls.

5.3.4 Immunohistochemistry

For immunohistochemistry on primary and orthotopic tumor tissue, brains were removed and fixed overnight in 4% PFA, cryoprotected in 30% sucrose and sectioned at 12-16 µM on a cryostat. Sections were air dried in the fume hood, postfixed in 4% PFA at room temperature for 10 min and washed twice in PBT for 5 min. Sections were blocked in 5% normal serum for 60 min and incubated overnight with primary antibodies at 4°C in a humid chamber. An additional 45 min blocking step with MOM reagent (Vector Laboratories) followed by two washing steps for 2 min was performed if the primary antibody was produced in mouse. Sections were washed with PBT, 3 times of 5 min each and stained with the appropriate secondary antibody for 60 min. Nuclei were counterstained with DAPI, slides mounted in Moeviol and observed by conventional or confocal microscopy (Zeiss, LSM 510).

5.3.5 Haematoxylin and Eosin staining

Haematoxylin and Eosin stainings were done according to standard procedures and tumor sections were analyzed by a pathologist of the Neuropathology core at UCSF confirming the presence of high grade oligodendroglioma in primary and orthotopic tumors.

5.3.6 Tunel staining

Tunel staining was carried out using the in situ cell death kit (Roche) according to the manufacturers instructions. In brief, fixed cells were incubated for 2 min in 0.1% Triton X-100, 0.1% sodium citrate on ice. Cells were washed twice with PBS and incubated with the Tunel reaction mix for 60 min at 37°C in a humid chamber. After several washing steps in PBS

slides were mounted in Moeviol and apoptotic cells were detected by fluorescence microscopy. As a positive control, cells were treated with 3000 U/mL DNase before incubating with TUNEL reaction mix, fluorescently labeled nucleotides were omitted in negative controls.

5.4 Live Imaging

To visualize GFP fusion proteins in living embryos, embryos were collected on apple agar plates and aged to stage 9 and 10 (4-6h at 29°C). After dechorionation embryos were immobilized on a cover slip (Lu et al, 1999), covered with Halocarbon 95 oil (Halocarbon Products Corp.) and visualized by confocal microscopy (Leica TCS SP2; Objective: HCL PL APO lbd.BL 63.0x1.40 Oil; numerical aperture: 1,4) using 6,5 s time intervals. Neuroblasts were identified by the following criteria: delamination from the symmetrically dividing neuroectodermal cells, asymmetric cell division, giving rise to two differently sized daughter cells and asymmetric localization of proteins such as Miranda (Kaltschmidt et al, 2000). Images were imported into Adobe Photoshop, assembled in Adobe Imageready and converted to QuickTime movies.

5.4.1 Fluorescence recovery after photobleaching (FRAP)

All photobleaching experiments were done by point bleaching of 1 second with maximum laser intensity using the advanced time lapse tool. Recovery period was measured at lower laser intensity in time intervals of 3.25 seconds. For calculating the half time of recovery, images were imported into image J and subtracted for background. The resulting curves were fitted to a single exponential function $y=A(1-e^{-kt})$ with Origin 5.0 (Originlab) from which the FRAP half time $t_{1/2} = \ln(2)/k$ was calculated.

5.5 RNA interference and drug treatment of *Drosophila* embryos

5.5.1 Myosin VI RNA interference

For knocking down Myosin VI activity, 1-2 h old embryos were injected with RNA complementary to Myosin VI RNA (Petritsch et al, 2003) using a microinjection system (air pressure injecting device: Femtojet, Eppendorf; micromanipulator: Leica). Double-stranded DNA was produced by *in vitro* transcription from PCR-generated templates tagged with T7 RNA polymerase promoter sequence and injected into embryos expressing Miranda-GFP and Histone-RFP or PON-GFP. Embryos were aged for 3 h at 29°C and live imaging was performed by confocal microscopy as described.

5.5.2 Injection of Rho kinase inhibitor to impair Myosin II activity

Myosin II activity was downregulated by injection of the Rho-kinase inhibitor (RKI) Y-27632 (17 mg/ml in water; TOCRIS Bioscience) (Barros et al., 2003) into stage 9 embryos expressing Miranda-GFP and Histone-RFP or PON GFP and followed using time lapse confocal microscopy.

5.5.3 Downregulation of proteasome activity

To inhibit proteasome activity, embryos were treated with 50 μ M MG132 (Sigma) or DMSO as a vehicle control in a 1:1 mixture of Schneider's medium and heptane for 15 or 30 minutes. Then, embryos were fixed and subjected to immunohistochemistry as described.

5.6 Stereotactic injections and serial transplantation of cancer stem cells

To evaluate the *in vivo* tumorigenicity of cancer stem cells, 1×10^4 cells were stereotactically implanted into the right brain hemisphere of FvB/N mice (coordinates: anterior-posterior, +2; medial-lateral, +2; dorsal-ventral, 3 mm from the bregma). Animals were kept under observation and sacrificed upon developing neurological symptoms. Tissue was prepared for immunohistochemistry as described. In addition, secondary tumorsphere cultures were established, their capacity for self-renewing and differentiation was evaluated and cells were re-injected in FvB/N mice. Cancer stem cells from orthotopic tumors were serially transplanted for 4 passages demonstrating their malignant potential.

5.7 SDS Page and immunoblotting

Miranda-GFP/scabrous-Gal4, Miranda-GFP and scabrous-Gal4 embryos, respectively, were homogenized in extraction buffer (25 mM Hepes (pH 7), 50 mM KCl, 150 mM NaCl, 1 mM $MgCl_2$, 250 mM sucrose, 1 mM DTT, 1% Triton X-100 and protease inhibitor cocktail (Roche)), lysates were mixed with the same volume of 2X Laemmli buffer (100 mM Tris-HCl pH 6.8, 4% SDS, 2% 2-Mercaptoethanol, 20% glycerol, 0,002% bromophenol blue) and boiled for 5 min to denature the proteins before loading on the SDS gel.

SDS-PAGE was performed according to standard procedures (Laemmli, 1970) in a Tris/glycine buffer system by aligning proteins in a 5% stacking gel (1.4 ml H_2O , 330 μ L Acrylamid/Bisacrylamid (29:1), 250 μ L 1.0 M Tris (pH 6.8), 20 μ L SDS (10%), 20 μ L APS (10%); 2 μ L TEMED) and separating them in a 8% resolving gel (4.6 ml H_2O , 2.7 mL Acrylamid/Bisacrylamid (29:1), 2.5 mL 1.5 M Tris (pH 8.8), 100 μ L SDS (10%), 100 μ L APS (10%); 6 μ L TEMED). Electrophoresis was conducted at 30 mA in a Mini Trans Blot

electrophoresis tank (Biorad) in 1X running buffer (25 mM Tris, 0.19 M Glycin, 0.1% SDS) under denaturing and reducing conditions.

Following electrophoresis, proteins were transferred to a PVDF membrane (Hybond P; Amersham) using a wet blot apparatus (Biorad) according to the manufacturers instructions. Before, the membrane was activated by methanol and equilibrated in transfer buffer (3.03g Tris, 14.41g Glycine, 1 ml 20% SDS, 100 mL methanol, ad 1l H₂O). Protein transfer occurred at 70 V for 80 min.

Blocking of non-specific binding is achieved by incubating the membrane 60 min in washing buffer (1X PBS, 0,05% Tween, pH7,4) containing 0.05% Tween and 5% non-fat dry milk. After blocking, the membrane was incubated over night at 4°C with the primary antibody diluted in washing buffer. The membrane was washed 5 times for 5 min in washing buffer and subsequently incubated with the respective secondary antibody coupled to horseradish peroxidase for 1 h at room temperature and washed again 5 times for 5 min. Secondary antibodies were visualized on autoradiography film (Amersham) using the enhanced chemoluminescent kit (ECL, Amersham) according to the manufacturers instructions.

Table 2: Antibody list. The following table contains information about the antibodies used in this study including ordering information and conditions for incubation, washing and use of secondary antibodies. All incubation and washing steps were performed in PBS with or without detergent /serum as indicated.

| Species | Antigen | Company (Order number) | Dilution | Blocking /Incubation | Washing | 2 nd antibody |
|------------|----------------------|---------------------------|----------|----------------------|-------------------|---|
| Rabbit-IgG | aPKC | Santa Cruz (SC-216) | 1:200 | 10% NGS, 0.1% Triton | PBS, 0.1% Triton | gt- α -rb-Cy5 |
| Mouse-IgM | CD15/LeX | BD Pharmingen (559045) | 1:500 | 5% NGS | PBS | gt- α -m-IgM-Alexa ⁴⁸⁸ |
| Rabbit-IgG | Cyclin A | Gift from O'Farrell | 1:200 | 10% NGS, 0.1% Triton | PBS, 0.1% Triton | gt- α -rb-Cy5 |
| Sheep-IgG | EGFR | Upstate (06-129) | 1:50 | 5% NGS | PBS | dk- α -shp-Alexa ⁴⁸⁸ |
| Rabbit-IgG | GFAP | DAKO (Z0334) | 1:1000 | 5% NGS, 0.1% Triton | PBS, 0.05% Triton | gt- α -rb-Alexa ⁵⁹⁴ |
| Rat-IgG2a | GFAP | Zymed (13-0300) | 1:500 | 5% NGS, 0.1% Triton | PBS, 0.05% Triton | gt- α -rat-Alexa ⁵⁹⁴ |
| Mouse-IgG | GFP | Santa Cruz (SC-9996) | 1:200 | 10% NGS, 0.1% Triton | PBS, 0.1% Triton | gt- α -m-Cy3 |
| Rabbit-IgG | Miranda | Davids Biotechnology | 1:200 | 10% NGS, 0.1% Triton | PBS, 0.1% Triton | gt- α -rb-Cy5 |
| Mouse-IgG | Miranda | Gift from Matzuzaki | 1:20 | 10% NGS, 0.1% Triton | PBS, 0.1% Triton | gt- α -m-Cy3 |
| Mouse-IgG | Nestin | Chemicon (MAB353) | 1:500 | 5% NGS, 0.1% Triton | PBS, 0.05% Triton | gt- α -m-IgM-Alexa ⁴⁸⁸ |
| Rabbit-IgG | NG2 | Chemicon (AB5320) | 1:200 | 5% NGS, 0.1% Triton | PBS, 0.05% Triton | gt- α -rb-Alexa ^{488/594} |
| Rabbit-IgG | NG2 | Gift from Stallcup | 1:250 | 5% NGS, 0.1% Triton | PBS, 0.05% Triton | gt- α -rb-Alexa ^{488/594} |
| Goat-IgG | Numb | Everest Biotech (EB05296) | 1:100 | 5% BSA, 0.1% Triton | PBS, 0.05% Triton | dk- α -gt-Alexa ⁴⁸⁸ |
| Mouse-IgM | O4 * | Chemicon (MAB345) | 1:500 | 5% NGS | PBS | gt- α -m-IgM-Alexa ⁴⁸⁸ |
| Rabbit-IgG | Olig2 | Chemicon (AB9610) | 1:500 | 5% NGS, 0.1% Triton | PBS, 0.05% Triton | gt- α -rb-Alexa ⁵⁹⁴ |
| Rabbit-IgG | Par-3 | Gift from Macara | 1:200 | 5% NGS, 0.1% Triton | PBS, 0.05% Triton | gt- α -rb-Alexa ⁵⁹⁴ |
| Rabbit-IgG | Phospho-Histone H3 | Upstate (06-570) | 1:200 | 5% NGS, 0.1% Triton | PBS, 0.05% Triton | gt- α -rb-Alexa ⁵⁹⁴ |
| Mouse-IgG | PON | DSHB | 1:5 | 10% NGS, 0.1% Triton | PBS, 0.1% Triton | gt- α -m-Cy35 |
| Rabbit-IgG | β -III-Tubulin | Covance (MRP-435P) | 1:500 | 5% NGS, 0.1% Triton | PBS, 0.05% Triton | gt- α -rb-Alexa ⁵⁹⁴ |
| Mouse-IgG | β -III-Tubulin | Covance (MMS-435P) | 1:1000 | 5% NGS, 0.1% Triton | PBS, 0.05% Triton | gt- α -m-Alexa ⁴⁸⁸ |
| Mouse-IgG | α -Tubulin | Accurate (YSRTMCA77S) | 1:10 | 10% NGS, 0.1% Triton | PBS, 0.1% Triton | gt- α -m-Cy3 |
| Rabbit-IgG | γ -Tubulin | Sigma (T3559) | 1:500 | 10% NGS, 0.1% Triton | PBS, 0.1% Triton | gt- α -rb-Cy5 |

* Note: alternatively, cells were incubated for 30 min with the O4 antibody at a 1:500 dilution in Neurobasal medium, then fixed and stained according to the regular IHC protocol omitting detergents in any further washing or incubation step.

6 References

- Aguirre AA, Chittajallu R, Belachew S & Gallo V (2004) NG2-expressing cells in the subventricular zone are type C-like cells and contribute to interneuron generation in the postnatal hippocampus. *J Cell Biol* 165: 575–589
- Ailles LE & Weissman IL (2007) Cancer stem cells in solid tumors. *Curr Opin Biotechnol* 18: 460–466
- Al-Hajj M, Wicha MS, Benito-Hernandez A, Morrison SJ & Clarke MF (2003) Prospective identification of tumorigenic breast cancer cells. *Proc Natl Acad Sci U S A* 100: 3983–3988
- Altman J (1963) Autoradiographic investigation of cell proliferation in the brains of rats and cats. *Anat Rec* 145: 573–591
- Altman J (1970) Autoradiographic and histological studies of postnatal neurogenesis. IV. Cell proliferation and migration in the anterior forebrain, with special reference to persisting neurogenesis in the olfactory bulb. *J Comp Neurol* 137: 433–457
- Altman J & Das GD (1966a) Autoradiographic and histological evidence of postnatal hippocampal neurogenesis in rats. *J Comp Neurol* 124: 319–335
- Altman J & Das GD (1966b) Autoradiographic and histological evidence of postnatal hippocampal neurogenesis in rats. *J Comp Neurol* 124: 319–335
- Alvarez-Buylla A & Temple S (1998) Stem cells in the developing and adult nervous system. *J Neurobiol* 36: 105–110
- Alvarez-Buylla A & Lim DA (2004) For the long run: maintaining germinal niches in the adult brain. *Neuron* 41: 683–686
- Alvi AJ, Clayton H, Joshi C, Enver T, Ashworth A, Vivanco Md, Dale TC & Smalley MJ (2003) Functional and molecular characterisation of mammary side population cells. *Breast Cancer Res* 5: R1-8
- Asakura A, Seale P, Girgis-Gabardo A & Rudnicki MA (2002) Myogenic specification of side population cells in skeletal muscle. *J Cell Biol* 159: 123–134
- Atwood SX, Chabu C, Penkert RR, Doe CQ & Prehoda KE (2007) Cdc42 acts downstream of Bazooka to regulate neuroblast polarity through Par-6 aPKC. *J Cell Sci* 120: 3200–3206
- Bachoo RM, Maher EA, Ligon KL, Sharpless NE, Chan SS, You MJ, Tang Y, DeFrances J, Stover E, Weissleder R, Rowitch DH, Louis DN & DePinho RA (2002) Epidermal growth factor receptor and Ink4a/Arf: convergent mechanisms governing terminal differentiation and transformation along the neural stem cell to astrocyte axis. *Cancer Cell* 1: 269–277
- Bao S, Wu Q, McLendon RE, Hao Y, Shi Q, Hjelmeland AB, Dewhirst MW, Bigner DD & Rich JN (2006a) Glioma stem cells promote radioresistance by preferential activation of the DNA damage response. *Nature* 444: 756–760
- Bao S, Wu Q, Sathornsumetee S, Hao Y, Li Z, Hjelmeland AB, Shi Q, McLendon RE, Bigner DD & Rich JN (2006b) Stem cell-like glioma cells promote tumor angiogenesis through vascular endothelial growth factor. *Cancer Res* 66: 7843–7848
- Barr FA, Silljé HHW & Nigg EA (2004) Polo-like kinases and the orchestration of cell division. *Nat Rev Mol Cell Biol* 5: 429–440
- Barros CS, Phelps CB & Brand AH (2003) Drosophila nonmuscle myosin II promotes the asymmetric segregation of cell fate determinants by cortical exclusion rather than active transport. *Dev Cell* 5: 829–840
- Bartel DP (2004) MicroRNAs: genomics, biogenesis, mechanism, and function. *Cell* 116: 281–297
- Beaucher M, Goodliffe J, Hersperger E, Trunova S, Frydman H & Shearn A (2007) Drosophila brain tumor metastases express both neuronal and glial cell type markers. *Dev Biol* 301: 287–297
- Bellaïche Y, Gho M, Kaltschmidt JA, Brand AH & Schweisguth F (2001) Frizzled regulates localization of cell-fate determinants and mitotic spindle rotation during asymmetric cell division. *Nat Cell Biol* 3: 50–57
- Bello B, Reichert H & Hirth F (2006) The brain tumor gene negatively regulates neural progenitor cell proliferation in the larval central brain of Drosophila. *Development* 133: 2639–2648
- Beltrami AP, Urbanek K, Kajstura J, Yan SM, Finato N, Bussani R, Nadal-Ginard B, Silvestri F, Leri A, Beltrami CA & Anversa P (2001) Evidence that human cardiac myocytes divide after myocardial infarction. *N Engl J Med* 344: 1750–1757
- Berdnik D, Török T, González-Gaitán M & Knoblich JA (2002) The endocytic protein alpha-Adaptin is required for numb-mediated asymmetric cell division in Drosophila. *Dev Cell* 3: 221–231

- Berger F, Gay E, Pelletier L, Tropel P & Wion D (2004) Development of gliomas: potential role of asymmetrical cell division of neural stem cells. *Lancet Oncol* 5: 511–514
- Betschinger J, Eisenhaber F & Knoblich JA (2005) Phosphorylation-induced autoinhibition regulates the cytoskeletal protein Lethal (2) giant larvae. *Curr Biol* 15: 276–282
- Betschinger J, Mechtler K & Knoblich JA (2006a) Asymmetric segregation of the tumor suppressor brat regulates self-renewal in Drosophila neural stem cells. *Cell* 124: 1241–1253
- Betschinger J, Mechtler K & Knoblich JA (2006b) Asymmetric segregation of the tumor suppressor brat regulates self-renewal in Drosophila neural stem cells. *Cell* 124: 1241–1253
- Betschinger J & Knoblich JA (2004) Dare to be different: asymmetric cell division in Drosophila, C. elegans and vertebrates. *Curr Biol* 14: R674–85
- Betschinger J, Mechtler K & Knoblich JA (2003a) The Par complex directs asymmetric cell division by phosphorylating the cytoskeletal protein Lgl. *Nature* 422: 326–330
- Betschinger J, Mechtler K & Knoblich JA (2003b) The Par complex directs asymmetric cell division by phosphorylating the cytoskeletal protein Lgl. *Nature* 422: 326–330
- Bock TA, Ziegler BL, Bühring HJ, Scheduling S, Brugger W & Kanz L (1999) Characterization of purified and ex vivo manipulated human hematopoietic progenitor and stem cells in xenograft recipients. *Ann N Y Acad Sci* 872: 200–7; discussion 207–10
- Bonnet D & Dick JE (1997) Human acute myeloid leukemia is organized as a hierarchy that originates from a primitive hematopoietic cell. *Nat Med* 3: 730–737
- Brand AH & Perrimon N (1993) Targeted gene expression as a means of altering cell fates and generating dominant phenotypes. *Development* 118: 401–415
- Brennecke J, Hipfner DR, Stark A, Russell RB & Cohen SM (2003) bantam encodes a developmentally regulated microRNA that controls cell proliferation and regulates the proapoptotic gene hid in Drosophila. *Cell* 113: 25–36
- Bresnick AR (1999) Molecular mechanisms of nonmuscle myosin-II regulation. *Curr Opin Cell Biol* 11: 26–33
- Broadus J & Doe CQ (1998) Extrinsic cues, intrinsic cues and microfilaments regulate asymmetric protein localization in Drosophila neuroblasts. *Curr Biol* 7: 827–835
- Broadus J, Fuerstenberg S & Doe CQ (1998) Staufer-dependent localization of prospero mRNA contributes to neuroblast daughter-cell fate. *Nature* 391: 792–795
- Brown J, Cooper-Kuhn CM, Kempermann G, van Praag H, Winkler J, Gage FH & Kuhn HG (2003) Enriched environment and physical activity stimulate hippocampal but not olfactory bulb neurogenesis. *Eur J Neurosci* 17: 2042–2046
- Burrows RC, Wancio D, Levitt P & Lillien L (1997) Response diversity and the timing of progenitor cell maturation are regulated by developmental changes in EGFR expression in the cortex. *Neuron* 19: 251–267
- Calabrese C, Poppleton H, Kocak M, Hogg TL, Fuller C, Hamner B, Oh EY, Gaber MW, Finklestein D, Allen M, Frank A, Bayazitov IT, Zakharenko SS, Gajjar A, Davidoff A & Gilbertson RJ (2007) A perivascular niche for brain tumor stem cells. *Cancer Cell* 11: 69–82
- Capela A & Temple S (2002) LeX/ssea-1 is expressed by adult mouse CNS stem cells, identifying them as nonependymal. *Neuron* 35: 865–875
- Carmena M, Riparbelli MG, Minestrini G, Tavares AM, Adams R, Callaini G & Glover DM (1998) Drosophila polo kinase is required for cytokinesis. *J Cell Biol* 143: 659–671
- Caussinus E & Gonzalez C (2005) Induction of tumor growth by altered stem-cell asymmetric division in Drosophila melanogaster. *Nat Genet* 37: 1125–1129
- Caussinus E & Hirth F (2007) Asymmetric stem cell division in development and cancer. *Prog Mol Subcell Biol* 45: 205–225
- Cayouette M & Raff M (2002) Asymmetric segregation of Numb: a mechanism for neural specification from Drosophila to mammals. *Nat Neurosci* 5: 1265–1269
- Chan JA, Krichevsky AM & Kosik KS (2005) MicroRNA-21 is an antiapoptotic factor in human glioblastoma cells. *Cancer Res* 65: 6029–6033
- Cheeks RJ, Canman JC, Gabriel WN, Meyer N, Strome S & Goldstein B (2004) C. elegans PAR proteins function by mobilizing and stabilizing asymmetrically localized protein complexes. *Curr Biol* 14: 851–862
- Chen C, Li L, Lodish HF & Bartel DP (2004) MicroRNAs modulate hematopoietic lineage differentiation. *Science* 303: 83–86

- Chen J, Mandel EM, Thomson JM, Wu Q, Callis TE, Hammond SM, Conlon FL & Wang D (2006) The role of microRNA-1 and microRNA-133 in skeletal muscle proliferation and differentiation. *Nat Genet* 38: 228–233
- Cheng L, Tavazoie M & Doetsch F (2005) Stem cells: from epigenetics to microRNAs. *Neuron* 46: 363–367
- Chenn A & McConnell SK (1995) Cleavage orientation and the asymmetric inheritance of Notch1 immunoreactivity in mammalian neurogenesis. *Cell* 82: 631–641
- Chia W, Somers WG & Wang H (2008) Drosophila neuroblast asymmetric divisions: cell cycle regulators, asymmetric protein localization, and tumorigenesis. *J Cell Biol* 180: 267–272
- Cho RW & Clarke MF (2008) Recent advances in cancer stem cells. *Curr Opin Genet Dev*
- Choksi SP, Southall TD, Bossing T, Edoff K, de Wit E, Fischer BE, van Steensel B, Micklem G & Brand AH (2006) Prospero acts as a binary switch between self-renewal and differentiation in Drosophila neural stem cells. *Dev Cell* 11: 775–789
- Ciafrè SA, Galardi S, Mangiola A, Ferracin M, Liu C, Sabatino G, Negrini M, Maira G, Croce CM & Farace MG (2005) Extensive modulation of a set of microRNAs in primary glioblastoma. *Biochem Biophys Res Commun* 334: 1351–1358
- Cimmino A, Calin GA, Fabbri M, Iorio MV, Ferracin M, Shimizu M, Wojcik SE, Aqeilan RI, Zupo S, Dono M, Rassenti L, Alder H, Volinia S, Liu C, Kipps TJ, Negrini M & Croce CM (2005) miR-15 and miR-16 induce apoptosis by targeting BCL2. *Proc Natl Acad Sci U S A* 102: 13944–13949
- Clarke MF, Dick JE, Dirks PB, Eaves CJ, Jamieson CHM, Jones DL, Visvader J, Weissman IL & Wahl GM (2006) Cancer stem cells—perspectives on current status and future directions: AACR Workshop on cancer stem cells. *Cancer Res* 66: 9339–9344
- Clevers H (2005) Stem cells, asymmetric division and cancer. *Nat Genet* 37: 1027–1028
- Corotto FS, Henegar JA & Maruniak JA (1993) Neurogenesis persists in the subependymal layer of the adult mouse brain. *Neurosci Lett* 149: 111–114
- Dahlstrand J, Collins VP & Lendahl U (1992) Expression of the class VI intermediate filament nestin in human central nervous system tumors. *Cancer Res* 52: 5334–5341
- Dalerba P, Dylla SJ, Park I, Liu R, Wang X, Cho RW, Hoey T, Gurney A, Huang EH, Simeone DM, Shelton AA, Parmiani G, Castelli C & Clarke MF (2007) Phenotypic characterization of human colorectal cancer stem cells. *Proc Natl Acad Sci U S A* 104: 10158–10163
- Dawson MR, Polito A, Levine JM & Reynolds R (2003) NG2-expressing glial progenitor cells: an abundant and widespread population of cycling cells in the adult rat CNS. *Mol Cell Neurosci* 24: 476–488
- Dean M, Fojo T & Bates S (2005) Tumour stem cells and drug resistance. *Nat Rev Cancer* 5: 275–284
- Doe CQ & Bowerman B (2001) Asymmetric cell division: fly neuroblast meets worm zygote. *Curr Opin Cell Biol* 13: 68–75
- Doe CQ, Chu-LaGriff Q, Wright DM & Scott MP (1991) The prospero gene specifies cell fates in the Drosophila central nervous system. *Cell* 65: 451–464
- Doetsch F, Caillé I, Lim DA, García-Verdugo JM & Alvarez-Buylla A (1999) Subventricular zone astrocytes are neural stem cells in the adult mammalian brain. *Cell* 97: 703–716
- Doetsch F, García-Verdugo JM & Alvarez-Buylla A (1997) Cellular composition and three-dimensional organization of the subventricular germinal zone in the adult mammalian brain. *J Neurosci* 17: 5046–5061
- Doetsch F & Alvarez-Buylla A (1996) Network of tangential pathways for neuronal migration in adult mammalian brain. *Proc Natl Acad Sci U S A* 93: 14895–14900
- Doetsch F, Petreanu L, Caille I, Garcia-Verdugo JM & Alvarez-Buylla A (2002) EGF converts transit-amplifying neurogenic precursors in the adult brain into multipotent stem cells. *Neuron* 36: 1021–1034
- Dontu G, Abdallah WM, Foley JM, Jackson KW, Clarke MF, Kawamura MJ & Wicha MS (2003) In vitro propagation and transcriptional profiling of human mammary stem/progenitor cells. *Genes Dev* 17: 1253–1270
- Dyer MA, Livesey FJ, Cepko CL & Oliver G (2003) Prox1 function controls progenitor cell proliferation and horizontal cell genesis in the mammalian retina. *Nat Genet* 34: 53–58
- Enright AJ, John B, Gaul U, Tuschl T, Sander C & Marks DS (2003) MicroRNA targets in Drosophila. *Genome Biol* 5: R1
- Erben V, Waldhuber M, Langer D, Fetka I, Jansen RP & Petritsch C (2008) Asymmetric localization of the adaptor protein Miranda in neuroblasts is achieved by diffusion and sequential interaction of Myosin II and VI. *J Cell Sci* 121: 1403–1414

- Eriksson PS, Perfilieva E, Björk-Eriksson T, Alborn AM, Nordborg C, Peterson DA & Gage FH (1998) Neurogenesis in the adult human hippocampus. *Nat Med* 4: 1313–1317
- Fields AP & Regala RP (2007) Protein kinase C iota: human oncogene, prognostic marker and therapeutic target. *Pharmacol Res* 55: 487–497
- Filippov V, Kronenberg G, Pivneva T, Reuter K, Steiner B, Wang LP, Yamaguchi M, Kettenmann H & Kempermann G (2003) Subpopulation of nestin-expressing progenitor cells in the adult murine hippocampus shows electrophysiological and morphological characteristics of astrocytes. *Mol Cell Neurosci* 23: 373–382
- Frank DJ, Edgar BA & Roth MB (2002) The *Drosophila melanogaster* gene brain tumor negatively regulates cell growth and ribosomal RNA synthesis. *Development* 129: 399–407
- Frederiksen K & McKay RD (1988) Proliferation and differentiation of rat neuroepithelial precursor cells in vivo. *J Neurosci* 8: 1144–1151
- Fuerstenberg S, Peng CY, Alvarez-Ortiz P, Hor T & Doe CQ (1999) Identification of Miranda protein domains regulating asymmetric cortical localization, cargo binding, and cortical release. *Mol Cell Neurosci* 12: 325–339
- Fukuda S, Kato F, Tozuka Y, Yamaguchi M, Miyamoto Y & Hisatsune T (2003) Two distinct subpopulations of nestin-positive cells in adult mouse dentate gyrus. *J Neurosci* 23: 9357–9366
- Gage FH (2000) Mammalian neural stem cells. *Science* 287: 1433–1438
- Gage FH, Kempermann G, Palmer TD, Peterson DA & Ray J (1998) Multipotent progenitor cells in the adult dentate gyrus. *J Neurobiol* 36: 249–266
- Gage FH, Coates PW, Palmer TD, Kuhn HG, Fisher LJ, Suhonen JO, Peterson DA, Suhr ST & Ray J (1995) Survival and differentiation of adult neuronal progenitor cells transplanted to the adult brain. *Proc Natl Acad Sci U S A* 92: 11879–11883
- Gaiano N, Nye JS & Fishell G (2000) Radial glial identity is promoted by Notch1 signaling in the murine forebrain. *Neuron* 26: 395–404
- Gaiano N & Fishell G (2002) The role of notch in promoting glial and neural stem cell fates. *Annu Rev Neurosci* 25: 471–490
- Galli R, Binda E, Orfanelli U, Cipelletti B, Gritti A, De Vitis S, Fiocco R, Foroni C, Dimeco F & Vescovi A (2004) Isolation and characterization of tumorigenic, stem-like neural precursors from human glioblastoma. *Cancer Res* 64: 7011–7021
- Gimble J & Guilak F (2003) Adipose-derived adult stem cells: isolation, characterization, and differentiation potential. *Cytotherapy* 5: 362–369
- Globus JH & Kuhlenbeck H (1944) The subependymal cell plate (matrix) and its relationship to brain tumors of the ependymal type. *J Neuropathol Exp Neurol* 3: 1–35
- Glover DM, Leibowitz MH, McLean DA & Parry H (1995) Mutations in aurora prevent centrosome separation leading to the formation of monopolar spindles. *Cell* 81: 95–105
- Gmyr V, Kerr-Conte J, Belaich S, Vandewalle B, Leteurtre E, Vantyghem MC, Lecomte-Houcke M, Proye C, Lefebvre J & Pattou F (2000) Adult human cytokeratin 19-positive cells reexpress insulin promoter factor 1 in vitro: further evidence for pluripotent pancreatic stem cells in humans. *Diabetes* 49: 1671–1680
- Goldstein B & Macara IG (2007) The PAR proteins: fundamental players in animal cell polarization. *Dev Cell* 13: 609–622
- Gönczy P & Rose LS (2007) Asymmetric cell division and axis formation in the embryo. *WormBook*: 1–20
- Götz M & Huttner WB (2005) The cell biology of neurogenesis. *Nat Rev Mol Cell Biol* 6: 777–788
- Gould E, Beylin A, Tanapat P, Reeves A & Shors TJ (1999) Learning enhances adult neurogenesis in the hippocampal formation. *Nat Neurosci* 2: 260–265
- Gritti A, Parati EA, Cova L, Frolichsthal P, Galli R, Wanke E, Faravelli L, Morassutti DJ, Roisen F, Nickel DD & Vescovi AL (1996) Multipotential stem cells from the adult mouse brain proliferate and self-renew in response to basic fibroblast growth factor. *J Neurosci* 16: 1091–1100
- Guo W, Lasky JL, 3rd & Wu H (2006) Cancer stem cells. *Pediatr Res* 59: 59R–64R
- Guzman ML, Li X, Corbett CA, Rossi RM, Bushnell T, Liesveld JL, Hébert J, Young F & Jordan CT (2007) Rapid and selective death of leukemia stem and progenitor cells induced by the compound 4-benzyl, 2-methyl, 1,2,4-thiadiazolidine, 3,5 dione (TDZD-8). *Blood* 110: 4436–4444
- Guzman ML, Rossi RM, Karnischky L, Li X, Peterson DR, Howard DS & Jordan CT (2005) The sesquiterpene lactone parthenolide induces apoptosis of human acute myelogenous leukemia stem and progenitor cells. *Blood* 105: 4163–4169

- Guzman-Marin R, Suntsova N, Methippara M, Greiffenstein R, Szymusiak R & McGinty D (2005) Sleep deprivation suppresses neurogenesis in the adult hippocampus of rats. *Eur J Neurosci* 22: 2111–2116
- Hack MA, Saghatelian A, de Chevigny A, Pfeifer A, Ashery-Padan R, Lledo P & Götz M (2005) Neuronal fate determinants of adult olfactory bulb neurogenesis. *Nat Neurosci* 8: 865–872
- Haydar TF, Ang E, Jr & Rakic P (2003) Mitotic spindle rotation and mode of cell division in the developing telencephalon. *Proc Natl Acad Sci U S A* 100: 2890–2895
- Hemmati HD, Nakano I, Lazareff JA, Masterman-Smith M, Geschwind DH, Bronner-Fraser M & Kornblum HI (2003) Cancerous stem cells can arise from pediatric brain tumors. *Proc Natl Acad Sci U S A* 100: 15178–15183
- Holland EC (2000) Glioblastoma multiforme: the terminator. *Proc Natl Acad Sci U S A* 97: 6242–6244
- Hopewell JW & Wright EA (1969) The importance of implantation site in cerebral carcinogenesis in rats. *Cancer Res* 29: 1927–1931
- Horb ME, Shen CN, Tosh D & Slack JM (2003) Experimental conversion of liver to pancreas. *Curr Biol* 13: 105–115
- Horvitz HR & Herskowitz I (1992) Mechanisms of asymmetric cell division: two Bs or not two Bs, that is the question. *Cell* 68: 237–255
- Hughes JR, Bullock SL & Ish-Horowicz D (2004) Inscuteable mRNA localization is dynein-dependent and regulates apicobasal polarity and spindle length in *Drosophila* neuroblasts. *Curr Biol* 14: 1950–1956
- Huntly BJ & Gilliland DG (2005) Leukaemia stem cells and the evolution of cancer-stem-cell research. *Nat Rev Cancer* 5: 311–321
- Ignatova TN, Kukekov VG, Laywell ED, Suslov ON, Vrionis FD & Steindler DA (2002) Human cortical glial tumors contain neural stem-like cells expressing astroglial and neuronal markers in vitro. *Glia* 39: 193–206
- Ikeshima-Kataoka H, Skeath JB, Nabeshima Y, Doe CQ & Matsuzaki F (1997) Miranda directs Prospero to a daughter cell during *Drosophila* asymmetric divisions. *Nature* 390: 625–629
- Izumi Y, Hirose T, Tamai Y, Hirai S, Nagashima Y, Fujimoto T, Tabuse Y, Kemphues KJ & Ohno S (1998) An atypical PKC directly associates and colocalizes at the epithelial tight junction with ASIP, a mammalian homologue of *Caenorhabditis elegans* polarity protein PAR-3. *J Cell Biol* 143: 95–106
- Izumi Y, Ohta N, Hisata K, Raabe T & Matsuzaki F (2006) *Drosophila* Pins-binding protein Mud regulates spindle-polarity coupling and centrosome organization. *Nat Cell Biol* 8: 586–593
- Jan YN & Jan LY (1998) Asymmetric cell division. *Nature* 392: 775–778
- Jessberger S, Zhao C, Toni N, Clemenson GD, Jr, Li Y & Gage FH (2007) Seizure-associated, aberrant neurogenesis in adult rats characterized with retrovirus-mediated cell labeling. *J Neurosci* 27: 9400–9407
- Jiang Y, Jahagirdar BN, Reinhardt RL, Schwartz RE, Keene CD, Ortiz-Gonzalez XR, Reyes M, Lenvik T, Lund T, Blackstad M, Du J, Aldrich S, Lisberg A, Low WC, Largaespada DA & Verfaillie CM (2002) Pluripotency of mesenchymal stem cells derived from adult marrow. *Nature* 418: 41–49
- Joberty G, Petersen C, Gao L & Macara IG (2000) The cell-polarity protein Par6 links Par3 and atypical protein kinase C to Cdc42. *Nat Cell Biol* 2: 531–539
- Justice N, Roegiers F, Jan LY & Jan YN (2003) Lethal giant larvae acts together with numb in notch inhibition and cell fate specification in the *Drosophila* adult sensory organ precursor lineage. *Curr Biol* 13: 778–783
- Kaltschmidt JA, Davidson CM, Brown NH & Brand AH (2000) Rotation and asymmetry of the mitotic spindle direct asymmetric cell division in the developing central nervous system. *Nat Cell Biol* 2: 7–12
- Kaltschmidt JA & Brand AH (2002) Asymmetric cell division: microtubule dynamics and spindle asymmetry. *J Cell Sci* 115: 2257–2264
- Karcavich RE (2005) Generating neuronal diversity in the *Drosophila* central nervous system: a view from the ganglion mother cells. *Dev Dyn* 232: 609–616
- Kessinger A & Sharp JG (2003) The whys and hows of hematopoietic progenitor and stem cell mobilization. *Bone Marrow Transplant* 31: 319–329
- Kim JK, Gabel HW, Kamath RS, Tewari M, Pasquinelli A, Rual J, Kennedy S, Dybbs M, Bertin N, Kaplan JM, Vidal M & Ruvkun G (2005) Functional genomic analysis of RNA interference in *C. elegans*. *Science* 308: 1164–1167
- Klezovitch O, Fernandez TE, Tapscott SJ & Vasioukhin V (2004) Loss of cell polarity causes severe brain dysplasia in Lgl1 knockout mice. *Genes Dev* 18: 559–571
- Knoblich JA (1998) Mechanisms of asymmetric cell division during animal development. *Curr Opin Cell Biol* 9: 833–841

- Knoblich JA, Jan LY & Jan YN (1995) Asymmetric segregation of Numb and Prospero during cell division. *Nature* 377: 624–627
- Knoblich JA (2008) Mechanisms of asymmetric stem cell division. *Cell* 132: 583–597
- Konno D, Shioi G, Shitamukai A, Mori A, Kiyonari H, Miyata T & Matsuzaki F (2008) Neuroepithelial progenitors undergo LGN-dependent planar divisions to maintain self-renewability during mammalian neurogenesis. *Nat Cell Biol* 10: 93–101
- Kornack DR & Rakic P (1999) Continuation of neurogenesis in the hippocampus of the adult macaque monkey. *Proc Natl Acad Sci U S A* 96: 5768–5773
- Kornack DR & Rakic P (2001) The generation, migration, and differentiation of olfactory neurons in the adult primate brain. *Proc Natl Acad Sci U S A* 98: 4752–4757
- Kosodo Y, Röper K, Haubensak W, Marzesco A, Corbeil D & Huttner WB (2004) Asymmetric distribution of the apical plasma membrane during neurogenic divisions of mammalian neuroepithelial cells. *EMBO J* 23: 2314–2324
- Kraut R & Campos-Ortega JA (1996) *inscuteable*, a neural precursor gene of *Drosophila*, encodes a candidate for a cytoskeleton adaptor protein. *Dev Biol* 174: 65–81
- Kraut R, Chia W, Jan LY, Jan YN & Knoblich JA (1996) Role of *inscuteable* in orienting asymmetric cell divisions in *Drosophila*. *Nature* 383: 50–55
- Krichevsky AM, King KS, Donahue CP, Khrapko K & Kosik KS (2003) A microRNA array reveals extensive regulation of microRNAs during brain development. *RNA* 9: 1274–1281
- Krichevsky AM, Sonntag K, Isacson O & Kosik KS (2006) Specific microRNAs modulate embryonic stem cell-derived neurogenesis. *Stem Cells* 24: 857–864
- Kuchinke U, Grawe F & Knust E (1999) Control of spindle orientation in *Drosophila* by the Par-3-related PDZ-domain protein Bazooka. *Curr Biol* 8: 1357–1365
- Kuhn HG, Dickinson-Anson H & Gage FH (1996) Neurogenesis in the dentate gyrus of the adult rat: age-related decrease of neuronal progenitor proliferation. *J Neurosci* 16: 2027–2033
- Kuo CT, Mirzadeh Z, Soriano-Navarro M, Rasin M, Wang D, Shen J, Sestan N, Garcia-Verdugo J, Alvarez-Buylla A, Jan LY & Jan Y (2006) Postnatal deletion of Numb/Numbl-like reveals repair and remodeling capacity in the subventricular neurogenic niche. *Cell* 127: 1253–1264
- Kuphal S, Wallner S, Schimanski CC, Bataille F, Hofer P, Strand S, Strand D & Bosserhoff AK (2006) Expression of HUGL-1 is strongly reduced in malignant melanoma. *Oncogene* 25: 103–110
- Kwon C, Han Z, Olson EN & Srivastava D (2005) MicroRNA1 influences cardiac differentiation in *Drosophila* and regulates Notch signaling. *Proc Natl Acad Sci U S A* 102: 18986–18991
- Laemmli UK (1970) Cleavage of structural proteins during the assembly of the head of bacteriophage T4. *Nature* 227: 680–685
- Le Borgne R, Bardin A & Schweisguth F (2005) The roles of receptor and ligand endocytosis in regulating Notch signaling. *Development* 132: 1751–1762
- Lee C, Andersen RO, Cabernard C, Manning L, Tran KD, Lanskey MJ, Bashirullah A & Doe CQ (2006a) *Drosophila* Aurora-A kinase inhibits neuroblast self-renewal by regulating aPKC/Numb cortical polarity and spindle orientation. *Genes Dev* 20: 3464–3474
- Lee C, Robinson KJ & Doe CQ (2006b) Lgl, Pins and aPKC regulate neuroblast self-renewal versus differentiation. *Nature* 439: 594–598
- Lee C, Wilkinson B, Siegrist S, Wharton R, & Doe C (2006c) Brat is a Miranda cargo protein that promotes neuronal differentiation and inhibits neuroblast self-renewal. *Dev Cell* 10: 441–449
- Leismann O & Lehner CF (2003) *Drosophila* securin destruction involves a D-box and a KEN-box and promotes anaphase in parallel with Cyclin A degradation. *J Cell Sci* 116: 2453–2460
- Lendahl U, Zimmerman LB & McKay RD (1990) CNS stem cells express a new class of intermediate filament protein. *Cell* 60: 585–595
- Lewis BP, Shih I, Jones-Rhoades MW, Bartel DP & Burge CB (2003) Prediction of mammalian microRNA targets. *Cell* 115: 787–798
- Lewis PD (1968) Mitotic activity in the primate subependymal layer and the genesis of gliomas. *Nature* 217: 974–975
- Li C, Heidt DG, Dalerba P, Burant CF, Zhang L, Adsay V, Wicha M, Clarke MF & Simeone DM (2007) Identification of pancreatic cancer stem cells. *Cancer Res* 67: 1030–1037

- Li HS, Wang D, Shen Q, Schonemann MD, Gorski JA, Jones KR, Temple S, Jan LY & Jan YN (2003) Inactivation of Numb and Numbl like in embryonic dorsal forebrain impairs neurogenesis and disrupts cortical morphogenesis. *Neuron* 40: 1105–1118
- Li L & Xie T (2005) Stem cell niche: structure and function. *Annu Rev Cell Dev Biol* 21: 605–631
- Li P, Yang X, Wasser M, Cai Y & Chia W (1997) Inscuteable and Staufen mediate asymmetric localization and segregation of prospero RNA during Drosophila neuroblast cell divisions. *Cell* 90: 437–447
- Ligon KL, Fancy SP, Franklin RJ & Rowitch DH (2006) Olig gene function in CNS development and disease. *Glia* 54: 1–10
- Llamazares S, Moreira A, Tavares A, Girdham C, Spruce BA, Gonzalez C, Karess RE, Glover DM & Sunkel CE (1992) polo encodes a protein kinase homolog required for mitosis in Drosophila. *Genes Dev* 5: 2153–2165
- Lois C & Alvarez-Buylla A (1993) Proliferating subventricular zone cells in the adult mammalian forebrain can differentiate into neurons and glia. *Proc Natl Acad Sci U S A* 90: 2074–2077
- Lois C & Alvarez-Buylla A (1994) Long-distance neuronal migration in the adult mammalian brain. *Science* 264: 1145–1148
- Lu B, Rothenberg M, Jan LY & Jan YN (1998) Partner of Numb colocalizes with Numb during mitosis and directs Numb asymmetric localization in Drosophila neural and muscle progenitors. *Cell* 95: 225–235
- Lu B, Ackerman L, Jan LY & Jan YN (1999) Modes of protein movement that lead to the asymmetric localization of partner of Numb during Drosophila neuroblast division. *Mol Cell* 4: 883–891
- Lu J, Getz G, Miska EA, Alvarez-Saavedra E, Lamb J, Peck D, Sweet-Cordero A, Ebert BL, Mak RH, Ferrando AA, Downing JR, Jacks T, Horvitz HR & Golub TR (2005) MicroRNA expression profiles classify human cancers. *Nature* 435: 834–838
- Lu L, Bao G, Chen H, Xia P, Fan X, Zhang J, Pei G & Ma L (2003) Modification of hippocampal neurogenesis and neuroplasticity by social environments. *Exp Neurol* 183: 600–609
- Lu QR, Sun T, Zhu Z, Ma N, Garcia M, Stiles CD & Rowitch DH (2002) Common developmental requirement for Olig function indicates a motor neuron/oligodendrocyte connection. *Cell* 109: 75–86
- Luskin MB (1993) Restricted proliferation and migration of postnatally generated neurons derived from the forebrain subventricular zone. *Neuron* 11: 173–189
- Maher EA, Furnari FB, Bachoo RM, Rowitch DH, Louis DN, Cavenee WK & DePinho RA (2001) Malignant glioma: genetics and biology of a grave matter. *Genes Dev* 15: 1311–1333
- Malatesta P, Hartfuss E & Götz M (2000) Isolation of radial glial cells by fluorescent-activated cell sorting reveals a neuronal lineage. *Development* 127: 5253–5263
- Malberg JE & Duman RS (2003) Cell proliferation in adult hippocampus is decreased by inescapable stress: reversal by fluoxetine treatment. *Neuropsychopharmacology* 28: 1562–1571
- Manabe N, Hirai S, Imai F, Nakanishi H, Takai Y & Ohno S (2002) Association of ASIP/mPAR-3 with adherens junctions of mouse neuroepithelial cells. *Dev Dyn* 225: 61–69
- Marie Y, Sanson M, Mokhtari K, Leuraud P, Kujas M, Delattre JY, Poirier J, Zalc B & Hoang-Xuan K (2001) OLIG2 as a specific marker of oligodendroglial tumour cells. *Lancet* 358: 298–300
- Markakis EA & Gage FH (1999) Adult-generated neurons in the dentate gyrus send axonal projections to field CA3 and are surrounded by synaptic vesicles. *J Comp Neurol* 406: 449–460
- Matsuzaki F, Ohshiro T, Ikeshima-Kataoka H & Izumi H (1998) miranda localizes staufen and prospero asymmetrically in mitotic neuroblasts and epithelial cells in early Drosophila embryogenesis. *Development* 125: 4089–4098
- Mayer B, Emery G, Berdnik D, Wirtz-Peitz F & Knoblich JA (2005) Quantitative analysis of protein dynamics during asymmetric cell division. *Curr Biol* 15: 1847–1854
- Mazurier F, Doedens M, Gan OI & Dick JE (2003) Rapid myeloerythroid repopulation after intrafemoral transplantation of NOD-SCID mice reveals a new class of human stem cells. *Nat Med* 9: 959–963
- McDermott KM, Zhang J, Holst CR, Kozakiewicz BK, Singla V & Tlsty TD (2006) p16(INK4a) prevents centrosome dysfunction and genomic instability in primary cells. *PLoS Biol* 4: e51
- Meller D, Pires RT & Tseng SC (2002) Ex vivo preservation and expansion of human limbal epithelial stem cells on amniotic membrane cultures. *Br J Ophthalmol* 86: 463–471
- Mellinghoff IK, Wang MY, Vivanco I, Haas-Kogan DA, Zhu S, Dia EQ, Lu KV, Yoshimoto K, Huang JH, Chute DJ, Riggs BL, Horvath S, Liau LM, Cavenee WK, Rao PN, Beroukhir R, Peck TC, Lee JC, Sellers WR & Stokoe D et al (2005) Molecular determinants of the response of glioblastomas to EGFR kinase inhibitors. *N Engl J Med* 353: 2012–2024

- Menn B, Garcia-Verdugo JM, Yaschine C, Gonzalez-Perez O, Rowitch D & Alvarez-Buylla A (2006) Origin of oligodendrocytes in the subventricular zone of the adult brain. *J Neurosci* 26: 7907–7918
- Meraldi P, Honda R & Nigg EA (2004) Aurora kinases link chromosome segregation and cell division to cancer susceptibility. *Curr Opin Genet Dev* 14: 29–36
- Mercier F, Kitasako JT & Hatton GI (2002) Anatomy of the brain neurogenic zones revisited: fractones and the fibroblast/macrophage network. *J Comp Neurol* 451: 170–188
- Merkle FT, Tramontin AD, García-Verdugo JM & Alvarez-Buylla A (2004) Radial glia give rise to adult neural stem cells in the subventricular zone. *Proc Natl Acad Sci U S A* 101: 17528–17532
- Miyata T, Kawaguchi A, Okano H & Ogawa M (2001) Asymmetric inheritance of radial glial fibers by cortical neurons. *Neuron* 31: 727–741
- Mori T, Buffo A & Götz M (2005) The novel roles of glial cells revisited: the contribution of radial glia and astrocytes to neurogenesis. *Curr Top Dev Biol* 69: 67–99
- Morrison SJ & Kimble J (2006) Asymmetric and symmetric stem-cell divisions in development and cancer. *Nature* 441: 1068–1074
- Morrison SJ & Spradling AC (2008) Stem cells and niches: mechanisms that promote stem cell maintenance throughout life. *Cell* 132: 598–611
- Muro I, Hay BA & Clem RJ (2002) The Drosophila DIAP1 protein is required to prevent accumulation of a continuously generated, processed form of the apical caspase DRONC. *J Biol Chem* 277: 49644–49650
- Nakano I & Kornblum HI (2006) Brain tumor stem cells. *Pediatr Res* 59: 54R–8R
- Nakao K & Campos-Ortega JA (1996) Persistent expression of genes of the enhancer of split complex suppresses neural development in Drosophila. *Neuron* 16: 275–286
- Nishiyama A (2007) Polydendrocytes: NG2 cells with many roles in development and repair of the CNS. *Neuroscientist* 13: 62–76
- Noctor SC, Flint AC, Weissman TA, Dammerman RS & Kriegstein AR (2001) Neurons derived from radial glial cells establish radial units in neocortex. *Nature* 409: 714–720
- Noctor SC, Martínez-Cerdeño V, Ivic L & Kriegstein AR (2004) Cortical neurons arise in symmetric and asymmetric division zones and migrate through specific phases. *Nat Neurosci* 7: 136–144
- O'Brien CA, Pollett A, Gallinger S & Dick JE (2007) A human colon cancer cell capable of initiating tumour growth in immunodeficient mice. *Nature* 445: 106–110
- Ohno S (2001) Intercellular junctions and cellular polarity: the PAR-aPKC complex, a conserved core cassette playing fundamental roles in cell polarity. *Curr Opin Cell Biol* 13: 641–648
- Ohshiro T, Yagami T, Zhang C & Matsuzaki F (2000) Role of cortical tumour-suppressor proteins in asymmetric division of Drosophila neuroblast. *Nature* 408: 593–596
- Oshima H, Rochat A, Kedzia C, Kobayashi K & Barrandon Y (2001) Morphogenesis and renewal of hair follicles from adult multipotent stem cells. *Cell* 104: 233–245
- Ostap EM (2002) 2,3-Butanedione monoxime (BDM) as a myosin inhibitor. *J Muscle Res Cell Motil* 23: 305–308
- Palmer TD, Takahashi J & Gage FH (1997) The adult rat hippocampus contains primordial neural stem cells. *Mol Cell Neurosci* 8: 389–404
- Parmentier ML, Woods D, Greig S, Phan PG, Radovic A, Bryant P & O'Kane CJ (2002) Rapsynoid/partner of inscuteable controls asymmetric division of larval neuroblasts in Drosophila. *J Neurosci* 20: RC84
- Passegué E, Jamieson CH, Ailles LE & Weissman IL (2003) Normal and leukemic hematopoiesis: are leukemias a stem cell disorder or a reacquisition of stem cell characteristics? *Proc Natl Acad Sci U S A* 100 Suppl 1: 11842–11849
- Peng CY, Manning L, Albertson R & Doe CQ (2000) The tumour-suppressor genes *lgl* and *dlg* regulate basal protein targeting in Drosophila neuroblasts. *Nature* 408: 596–600
- Peters J (2006) The anaphase promoting complex/cyclosome: a machine designed to destroy. *Nat Rev Mol Cell Biol* 7: 644–656
- Petersen PH, Zou K, Krauss S & Zhong W (2004) Continuing role for mouse Numb and Numb1 in maintaining progenitor cells during cortical neurogenesis. *Nat Neurosci* 7: 803–811
- Petersen PH, Zou K, Hwang JK, Jan YN & Zhong W (2002) Progenitor cell maintenance requires numb and numlike during mouse neurogenesis. *Nature* 419: 929–934
- Petritsch C, Tivosanis G, Turck CW, Jan LY & Jan YN (2003) The Drosophila myosin VI Jaguar is required for basal protein targeting and correct spindle orientation in mitotic neuroblasts. *Dev Cell* 4: 273–281

- Petronczki M & Knoblich JA (2001) DmPAR-6 directs epithelial polarity and asymmetric cell division of neuroblasts in *Drosophila*. *Nat Cell Biol* 3: 43–49
- Plant PJ, Fawcett JP, Lin DCC, Holdorf AD, Binns K, Kulkarni S & Pawson T (2003) A polarity complex of mPar-6 and atypical PKC binds, phosphorylates and regulates mammalian Lgl. *Nat Cell Biol* 5: 301–308
- Prince ME, Sivanandan R, Kaczorowski A, Wolf GT, Kaplan MJ, Dalerba P, Weissman IL, Clarke MF & Ailles LE (2007) Identification of a subpopulation of cells with cancer stem cell properties in head and neck squamous cell carcinoma. *Proc Natl Acad Sci U S A* 104: 973–978
- Ra SM, Kim H, Jang MH, Shin MC, Lee TH, Lim BV, Kim CJ, Kim EH, Kim KM & Kim SS (2002) Treadmill running and swimming increase cell proliferation in the hippocampal dentate gyrus of rats. *Neurosci Lett* 333: 123–126
- Rakic P (1985) Limits of neurogenesis in primates. *Science* 227: 1054–1056
- Ramírez-Castillejo C, Sánchez-Sánchez F, Andreu-Agulló C, Ferrón SR, Aroca-Aguilar JD, Sánchez P, Mira H, Escribano J & Fariñas I (2006) Pigment epithelium-derived factor is a niche signal for neural stem cell renewal. *Nat Neurosci* 9: 331–339
- Rani SB, Mahadevan A, Anilkumar SR, Raju TR & Shankar SK (2006) Expression of nestin--a stem cell associated intermediate filament in human CNS tumours. *Indian J Med Res* 124: 269–280
- Rasin M, Gazula V, Breunig JJ, Kwan KY, Johnson MB, Liu-Chen S, Li H, Jan LY, Jan Y, Rakic P & Sestan N (2007) Numb and Numb1 are required for maintenance of cadherin-based adhesion and polarity of neural progenitors. *Nat Neurosci* 10: 819–827
- Regala RP, Weems C, Jamieson L, Copland JA, Thompson EA & Fields AP (2005) Atypical protein kinase Ciota plays a critical role in human lung cancer cell growth and tumorigenicity. *J Biol Chem* 280: 31109–31115
- Reinhart BJ, Slack FJ, Basson M, Pasquinelli AE, Bettinger JC, Rougvie AE, Horvitz HR & Ruvkun G (2000) The 21-nucleotide let-7 RNA regulates developmental timing in *Caenorhabditis elegans*. *Nature* 403: 901–906
- Reya T, Morrison SJ, Clarke MF & Weissman IL (2001) Stem cells, cancer, and cancer stem cells. *Nature* 414: 105–111
- Reynolds BA & Weiss S (1992) Generation of neurons and astrocytes from isolated cells of the adult mammalian central nervous system. *Science* 255: 1707–1710
- Reynolds BA & Rietze RL (2005) Neural stem cells and neurospheres--re-evaluating the relationship. *Nat Methods* 2: 333–336
- Rhyu MS, Jan LY & Jan YN (1994) Asymmetric distribution of numb protein during division of the sensory organ precursor cell confers distinct fates to daughter cells. *Cell* 76: 477–491
- Ricci-Vitiani L, Lombardi DG, Pilozzi E, Biffoni M, Todaro M, Peschle C & De Maria R (2007) Identification and expansion of human colon-cancer-initiating cells. *Nature* 445: 111–115
- Rodríguez LV, Alfonso Z, Zhang R, Leung J, Wu B & Ignarro LJ (2006) Clonogenic multipotent stem cells in human adipose tissue differentiate into functional smooth muscle cells. *Proc Natl Acad Sci U S A* 103: 12167–12172
- Roegiers F, Younger-Shepherd S, Jan LY & Jan YN (2001) Bazooka is required for localization of determinants and controlling proliferation in the sensory organ precursor cell lineage in *Drosophila*. *Proc Natl Acad Sci U S A* 98: 14469–14474
- Russell DS & Rubinstein L (1989) Pathology of Tumours of the Central Nervous System. *Arnold, London*
- Sakakibara S, Nakamura Y, Yoshida T, Shibata S, Koike M, Takano H, Ueda S, Uchiyama Y, Noda T & Okano H (2002) RNA-binding protein Musashi family: roles for CNS stem cells and a subpopulation of ependymal cells revealed by targeted disruption and antisense ablation. *Proc Natl Acad Sci U S A* 99: 15194–15199
- Sakariassen PØ, Immervoll H & Chekenya M (2007) Cancer stem cells as mediators of treatment resistance in brain tumors: status and controversies. *Neoplasia* 9: 882–892
- Sanada K & Tsai L (2005) G protein betagamma subunits and AGS3 control spindle orientation and asymmetric cell fate of cerebral cortical progenitors. *Cell* 122: 119–131
- Sanai N, Alvarez-Buylla A & Berger MS (2005) Neural stem cells and the origin of gliomas. *N Engl J Med* 353: 811–822
- Schaefer M, Petronczki M, Dorner D, Forte M & Knoblich JA (2001) Heterotrimeric G proteins direct two modes of asymmetric cell division in the *Drosophila* nervous system. *Cell* 107: 183–194
- Schaefer M, Shevchenko A, Shevchenko A & Knoblich JA (2000) A protein complex containing Inscuteable and the Alpha-binding protein Pins orients asymmetric cell divisions in *Drosophila*. *Curr Biol* 10: 353–362

- Schimanski CC, Schmitz G, Kashyap A, Bosserhoff AK, Bataille F, Schäfer SC, Lehr HA, Berger MR, Galle PR, Strand S & Strand D (2005) Reduced expression of Hugel-1, the human homologue of *Drosophila* tumour suppressor gene *lgl*, contributes to progression of colorectal cancer. *Oncogene* 24: 3100–3109
- Schmechel DE & Rakic P (1979) A Golgi study of radial glial cells in developing monkey telencephalon: morphogenesis and transformation into astrocytes. *Anat Embryol (Berl)* 156: 115–152
- Schober M, Schaefer M & Knoblich JA (1999) Bazooka recruits Inscuteable to orient asymmetric cell divisions in *Drosophila* neuroblasts. *Nature* 402: 548–551
- Schuh M, Lehner CF & Heidmann S (2007) Incorporation of *Drosophila* CID/CENP-A and CENP-C into centromeres during early embryonic anaphase. *Curr Biol* 17: 237–243
- Schuldt AJ, Adams JH, Davidson CM, Micklem DR, Haseloff J, St Johnston D & Brand AH (1998) Miranda mediates asymmetric protein and RNA localization in the developing nervous system. *Genes Dev* 12: 1847–1857
- Schweisguth F (1999) Dominant-negative mutation in the beta2 and beta6 proteasome subunit genes affect alternative cell fate decisions in the *Drosophila* sense organ lineage. *Proc Natl Acad Sci U S A* 96: 11382–11386
- Schweisguth F (2004) Regulation of notch signaling activity. *Curr Biol* 14: R129–38
- Seki T & Arai Y (1993) Highly polysialylated NCAM expression in the developing and adult rat spinal cord. *Brain Res Dev Brain Res* 73: 141–145
- Seri B, García-Verdugo JM, McEwen BS & Alvarez-Buylla A (2001) Astrocytes give rise to new neurons in the adult mammalian hippocampus. *J Neurosci* 21: 7153–7160
- Shen CP, Jan LY & Jan YN (1997) Miranda is required for the asymmetric localization of Prospero during mitosis in *Drosophila*. *Cell* 90: 449–458
- Shen CP, Knoblich JA, Chan YM, Jiang MM, Jan LY & Jan YN (1998) Miranda as a multidomain adapter linking apically localized Inscuteable and basally localized Staufin and Prospero during asymmetric cell division in *Drosophila*. *Genes Dev* 12: 1837–1846
- Shen Q, Zhong W, Jan YN & Temple S (2002) Asymmetric Numb distribution is critical for asymmetric cell division of mouse cerebral cortical stem cells and neuroblasts. *Development* 129: 4843–4853
- Sibilia M, Kroismayr R, Lichtenberger BM, Natarajan A, Hecking M & Holcman M (2007) The epidermal growth factor receptor: from development to tumorigenesis. *Differentiation* 75: 770–787
- Siegrist SE & Doe CQ (2006) Extrinsic cues orient the cell division axis in *Drosophila* embryonic neuroblasts. *Development* 133: 529–536
- Sigrist S, Jacobs H, Stratmann R & Lehner CF (1995) Exit from mitosis is regulated by *Drosophila* fizzy and the sequential destruction of cyclins A, B and B3. *EMBO J* 14: 4827–4838
- Singh SK, Clarke ID, Terasaki M, Bonn VE, Hawkins C, Squire J & Dirks PB (2003) Identification of a cancer stem cell in human brain tumors. *Cancer Res* 63: 5821–5828
- Singh SK, Hawkins C, Clarke ID, Squire JA, Bayani J, Hide T, Henkelman RM, Cusimano MD & Dirks PB (2004) Identification of human brain tumour initiating cells. *Nature* 432: 396–401
- Slack C, Overton PM, Tuxworth RI & Chia W (2007) Asymmetric localisation of Miranda and its cargo proteins during neuroblast division requires the anaphase-promoting complex/cyclosome. *Development* 134: 3781–3787
- Steiner B, Klempin F, Wang L, Kott M, Kettenmann H & Kempermann G (2006) Type-2 cells as link between glial and neuronal lineage in adult hippocampal neurogenesis. *Glia* 54: 805–814
- Steinert PM, Chou YH, Prahlad V, Parry DA, Marekov LN, Wu KC, Jang SI & Goldman RD (1999) A high molecular weight intermediate filament-associated protein in BHK-21 cells is nestin, a type VI intermediate filament protein. Limited co-assembly in vitro to form heteropolymers with type III vimentin and type IV alpha-internexin. *J Biol Chem* 274: 9881–9890
- Strand D, Jakobs R, Merdes G, Neumann B, Kalmes A, Heid HW, Husmann I & Mechler BM (1994) The *Drosophila* lethal(2)giant larvae tumor suppressor protein forms homo-oligomers and is associated with nonmuscle myosin II heavy chain. *J Cell Biol* 127: 1361–1373
- Stricker SH, Meiri K & Götz M (2006) P-GAP-43 is enriched in horizontal cell divisions throughout rat cortical development. *Cereb Cortex* 16 Suppl 1: i121–31
- Stupp R, Mason WP, van den Bent MJ, Weller M, Fisher B, Taphoorn MJ, Belanger K, Brandes AA, Marosi C, Bogdahn U, Curschmann J, Janzer RC, Ludwin SK, Gorlia T, Allgeier A, Lacombe D, Cairncross JG, Eisenhauer E, Mirimanoff RO & European Organisation for Research and Treatment of Cancer Brain Tumor and Radiotherapy Groups et al (2005) Radiotherapy plus concomitant and adjuvant temozolomide for glioblastoma. *N Engl J Med* 352: 987–996

- Sun Y, Goderie SK & Temple S (2005) Asymmetric distribution of EGFR receptor during mitosis generates diverse CNS progenitor cells. *Neuron* 45: 873–886
- Suzuki A & Ohno S (2006) The PAR-aPKC system: lessons in polarity. *J Cell Sci* 119: 979–987
- Sweeney HL & Houdusse A (2007) What can myosin VI do in cells? *Curr Opin Cell Biol* 19: 57–66
- Symonds H, Krall L, Remington L, Saenz-Robles M, Lowe S, Jacks T & Van Dyke T (1994) p53-dependent apoptosis suppresses tumor growth and progression in vivo. *Cell* 78: 703–711
- Tamamaki N, Nakamura K, Okamoto K & Kaneko T (2001) Radial glia is a progenitor of neocortical neurons in the developing cerebral cortex. *Neurosci Res* 41: 51–60
- Tang C, Ang BT & Pervaiz S (2007) Cancer stem cell: target for anti-cancer therapy. *FASEB J* 21: 3777–3785
- Taupin P (2007) Adult neural stem cells, neurogenic niches, and cellular therapy. *Stem Cell Rev* 2: 213–219
- Tautz D & Pfeifle C (1989) A non-radioactive in situ hybridization method for the localization of specific RNAs in *Drosophila* embryos reveals translational control of the segmentation gene hunchback. *Chromosoma* 98: 81–85
- Taylor G, Lehrer MS, Jensen PJ, Sun TT & Lavker RM (2000) Involvement of follicular stem cells in forming not only the follicle but also the epidermis. *Cell* 102: 451–461
- Till JE & McCulloch EA (1961) A direct measurement of the radiation sensitivity of normal mouse bone marrow cells. *Radiat Res* 14: 213–222
- Tio M, Udolph G, Yang X & Chia W (2001) cdc2 links the *Drosophila* cell cycle and asymmetric division machineries. *Nature* 409: 1063–1067
- Toma JG, Akhavan M, Fernandes KJ, Barnabé-Heider F, Sadikot A, Kaplan DR & Miller FD (2001) Isolation of multipotent adult stem cells from the dermis of mammalian skin. *Nat Cell Biol* 3: 778–784
- Uchida N, Buck DW, He D, Reitsma MJ, Masek M, Phan TV, Tsukamoto AS, Gage FH & Weissman IL (2001) Direct isolation of human central nervous system stem cells. *Proc Natl Acad Sci U S A* 97: 14720–14725
- van Praag H, Schinder AF, Christie BR, Toni N, Palmer TD & Gage FH (2002) Functional neurogenesis in the adult hippocampus. *Nature* 415: 1030–1034
- Vescovi AL, Galli R & Reynolds BA (2006) Brain tumour stem cells. *Nat Rev Cancer* 6: 425–436
- Vick NA, Lin MJ & Bigner DD (1977) The role of the subependymal plate in glial tumorigenesis. *Acta Neuropathol* 40: 63–71
- Voigt T (1989) Development of glial cells in the cerebral wall of ferrets: direct tracing of their transformation from radial glia into astrocytes. *J Comp Neurol* 289: 74–88
- Wakamatsu Y, Maynard TM, Jones SU & Weston JA (1999) NUMB localizes in the basal cortex of mitotic avian neuroepithelial cells and modulates neuronal differentiation by binding to NOTCH-1. *Neuron* 23: 71–81
- Wang H, Ouyang Y, Somers WG, Chia W & Lu B (2007) Polo inhibits progenitor self-renewal and regulates Numb asymmetry by phosphorylating Pon. *Nature* 449: 96–100
- Wang H, Somers GW, Bashirullah A, Heberlein U, Yu F & Chia W (2006) Aurora-A acts as a tumor suppressor and regulates self-renewal of *Drosophila* neuroblasts. *Genes Dev* 20: 3453–3463
- Wechsler-Reya R & Scott MP (2001) The developmental biology of brain tumors. *Annu Rev Neurosci* 24: 385–428
- Weiss WA, Burns MJ, Hackett C, Aldape K, Hill JR, Kuriyama H, Kuriyama N, Milshteyn N, Roberts T, Wendland MF, DePinho R & Israel MA (2003) Genetic determinants of malignancy in a mouse model for oligodendroglioma. *Cancer Res* 63: 1589–1595
- Weissman IL (2000a) Stem cells: units of development, units of regeneration, and units in evolution. *Cell* 100: 157–168
- Weissman IL (2000b) Translating stem and progenitor cell biology to the clinic: barriers and opportunities. *Science* 287: 1442–1446
- Wodarz A, Ramrath A, Grimm A & Knust E (2000) *Drosophila* atypical protein kinase C associates with Bazooka and controls polarity of epithelia and neuroblasts. *J Cell Biol* 150: 1361–1374
- Wodarz A, Ramrath A, Kuchinke U & Knust E (1999) Bazooka provides an apical cue for Inscuteable localization in *Drosophila* neuroblasts. *Nature* 402: 544–547
- Wodarz A (2005) Molecular control of cell polarity and asymmetric cell division in *Drosophila* neuroblasts. *Curr Opin Cell Biol* 17: 475–481
- Wodarz A & Huttner WB (2003) Asymmetric cell division during neurogenesis in *Drosophila* and vertebrates. *Mech Dev* 120: 1297–1309

- Yamanaka T, Horikoshi Y, Sugiyama Y, Ishiyama C, Suzuki A, Hirose T, Iwamatsu A, Shinohara A & Ohno S (2003) Mammalian Lgl forms a protein complex with PAR-6 and aPKC independently of PAR-3 to regulate epithelial cell polarity. *Curr Biol* 13: 734–743
- Yamashita YM, Fuller MT & Jones DL (2005) Signaling in stem cell niches: lessons from the *Drosophila* germline. *J Cell Sci* 118: 665–672
- Yilmaz OH, Valdez R, Theisen BK, Guo W, Ferguson DO, Wu H & Morrison SJ (2006) Pten dependence distinguishes haematopoietic stem cells from leukaemia-initiating cells. *Nature* 441: 475–482
- Yu F, Morin X, Cai Y, Yang X & Chia W (2000) Analysis of partner of inscuteable, a novel player of *Drosophila* asymmetric divisions, reveals two distinct steps in inscuteable apical localization. *Cell* 100: 399–409
- Yu F, Kuo CT & Jan YN (2006) *Drosophila* neuroblast asymmetric cell division: recent advances and implications for stem cell biology. *Neuron* 51: 13–20
- Zhao C, Deng W & Gage FH (2008) Mechanisms and functional implications of adult neurogenesis. *Cell* 132: 645–660
- Zhong W, Feder JN, Jiang MM, Jan LY & Jan YN (1996a) Asymmetric localization of a mammalian numb homolog during mouse cortical neurogenesis. *Neuron* 17: 43–53
- Zhong W, Feder JN, Jiang MM, Jan LY & Jan YN (1996b) Asymmetric localization of a mammalian numb homolog during mouse cortical neurogenesis. *Neuron* 17: 43–53
- Zhou Q & Anderson DJ (2002) The bHLH transcription factors OLIG2 and OLIG1 couple neuronal and glial subtype specification. *Cell* 109: 61–73
- Zigman M, Cayouette M, Charalambous C, Schleiffer A, Hoeller O, Dunican D, McCudden CR, Firnberg N, Barres BA, Siderovski DP & Knoblich JA (2005) Mammalian inscuteable regulates spindle orientation and cell fate in the developing retina. *Neuron* 48: 539–545
- Zuk PA, Zhu M, Ashjian P, De Ugarte DA, Huang JI, Mizuno H, Alfonso ZC, Fraser JK, Benhaim P & Hedrick MH (2002) Human adipose tissue is a source of multipotent stem cells. *Mol Biol Cell* 13: 4279–4295
- Zur A & Brandeis M (2001) Securin degradation is mediated by fzy and fzr, and is required for complete chromatid separation but not for cytokinesis. *EMBO J* 20: 792–801

7 Abbreviations

| | |
|---------|--|
| µg | Microgramm |
| µl | Microliter |
| α | anti |
| ACD | Asymmetric cell division |
| APC/C | Anaphase promoting complex/cyclosome |
| aPKC | Atypical protein kinase C |
| Ara-C | Cytosin-β-D-arabinofuranoside |
| BDM | 2,3-butanedione monoxime |
| bFGF | Basic fibroblast growth factor |
| BPE | Bovine pituitary extract |
| CC | Corpus callosum |
| CNS | Central nervous system |
| CSC | Cancer stem cell |
| DAPI | Diamidino-2-phenylindol dihydrochloride |
| DMEM | Dulbecco's Modified Eagle's Medium |
| DNase | Desoxyribonuclease |
| DTT | Dithiotreitol |
| ECL | Enhanced chemoluminescence |
| EDTA | Ethylenediaminetetraacetic acid |
| EGF | Epidermal growth factor |
| EGFR | Epidermal growth factor receptor |
| ES cell | Embryonic stem cell |
| et al. | et alii (from Latin, "and others") |
| FRAP | Fluorescent recovery after photobleaching |
| g | Gramm |
| GalC | Galactocerebroside |
| GBM | Glioblastoma multiforme |
| GFAP | Glial fibrillary acidic protein |
| GFP | Green fluorescent protein |
| GMC | Ganglion mother cell |
| h | Hour |
| HBSS | Hanks' buffer, Ca ²⁺ /Mg ²⁺ free |
| HCL | Hydrochloric acid |
| H&E | Haematoxylin and eosin |
| HEPES | 4-(2-hydroxyethyl)-1-piperazineethanesulfonic acid |
| kb | Kilo bases |

| | |
|-------------------|---|
| KCl | Potassium chloride |
| Lgl | Lethal giant larvae |
| MBP | Myelin basic protein |
| MgCl ₂ | Magnesium chloride |
| min | Minute |
| miRNA | Microribonucleic acid |
| ml | Milliliter |
| mM | Millimolar |
| mRNA | Messenger ribonucleic acid |
| NaCl | Sodium chloride |
| NGS | Normal goat serum |
| NSC | Neural stem cell |
| NumbI | Numb-like protein |
| P/S | Penicillin and streptomycin |
| PAGE | Polyacrylamide gel electrophoresis |
| PBS | Phosphate buffered saline |
| PFA | Paraformaldehyde |
| PH3 | Phospho-Histone 3 |
| Pins | Partner of Inscuteable |
| PON | Partner of Numb |
| PSC | Premalignant stem cell |
| RFP | Red fluorescent protein |
| RGC | Radial glial cell |
| RNA | Ribonucleic acid |
| ROI | Region of interest |
| rpm | Rounds per minute |
| s | Second |
| SDS | Sodium dodecyl sulfate |
| SGZ | Subgranular zone |
| SVZ | Subventricular zone |
| TEMED | N, N, N', N'-Tetramethylethylenediamine |
| Tris | Trishydroxymethylaminomethane |
| TUNEL | Terminal |
| UAS | Upstream activating sequence |

8 Curriculum vitae

Personal Information

| | |
|----------------|------------------|
| Name | Markus Waldhuber |
| Nationality | Austria |
| Date of birth | 31.07.1979 |
| Place of birth | Leoben, Austria |
| Marital status | Married |

Education and Research Experience

| | |
|-------------------|---|
| Since 10/2004 | Ludwig-Maximilians University Munich, Germany Department of Molecular Biology - Genecenter Graduate Student in the research group of Dr. Claudia Petritsch <ul style="list-style-type: none">- Function of the <i>Drosophila</i> caspase DRONC and programmed cell death during development and neurogenesis- Asymmetric cell divisions and cell fate determination of neuronal stem cell-like neuroblasts |
| 10/2006 - 12/2007 | University of California San Francisco, USA Department of Neurological Surgery Lab of Dr. Gabriele Bergers / Dr. Claudia Petritsch <ul style="list-style-type: none">- The origin of cancer stem cells and role of asymmetric cell division in mammalian stem cells and tumorigenesis |
| 09/2003 - 07/2004 | University of Technology Graz, Austria Department of Biochemistry Undergraduate student in the Lab of Prof. Albin Hermetter. Diploma Thesis: "Functional proteomic screening for lipolytic enzymes in mouse adipose tissue" Degree: Dipl.-Ing. (with excellence) |
| 06/2002 - 08/2002 | Biochemie GmbH, Kundl, Austria (rebranded as Sandoz Austria) Research and Development Scientific assistant in fermentation analytics |
| 09/2001- 08/2003 | University of Technology Graz, Austria Undergraduate studies - Advanced study period Biochemistry, Biotechnology and Food Chemistry |
| 10/1998 - 08/2001 | University of Technology Graz, Austria Undergraduate studies, Chemical Engineering |
| 10/1997 - 08/1998 | Military service , Landwehrkaserne St. Michael, Austria |
| 09/1989 - 06/1997 | Bundesgymnasium Leoben, Austria Matura (High School Diploma) |

Publications

Erben V*, **Waldhuber M***, Langer D., Fetka I, Jansen RP. and Petritsch C.: "Asymmetric localization of the adaptor protein Miranda in neuroblasts is achieved by diffusion and sequential interaction of Myosin II and VI." J. Cell Sci. (2008), Epub ahead of print (*authors contributed equally).

Waldhuber M., Emoto K. and Petritsch C.: "The Drosophila caspase DRONC is required for metamorphosis and cell death in response to irradiation and developmental signals." Mech. Dev. 122 (7-8), 914-27 (2005)

Birner-Gruenberger R., Susani-Etzerodt H., **Waldhuber M.**, Riesenhuber G., Schmidinger H., Rechberger G., Kollroser M., Strauss JG., Lass A., Zimmermann R., Haemmerle G., Zechner R. and Hermetter A.: "The lipolytic proteome of mouse adipose tissue." Mol. Cell Proteomics 4 (11), 1710-7 (2005)